



# Experimental overview on light (anti)(hyper)nuclei production at the LHC

Chiara Pinto  
(CERN)

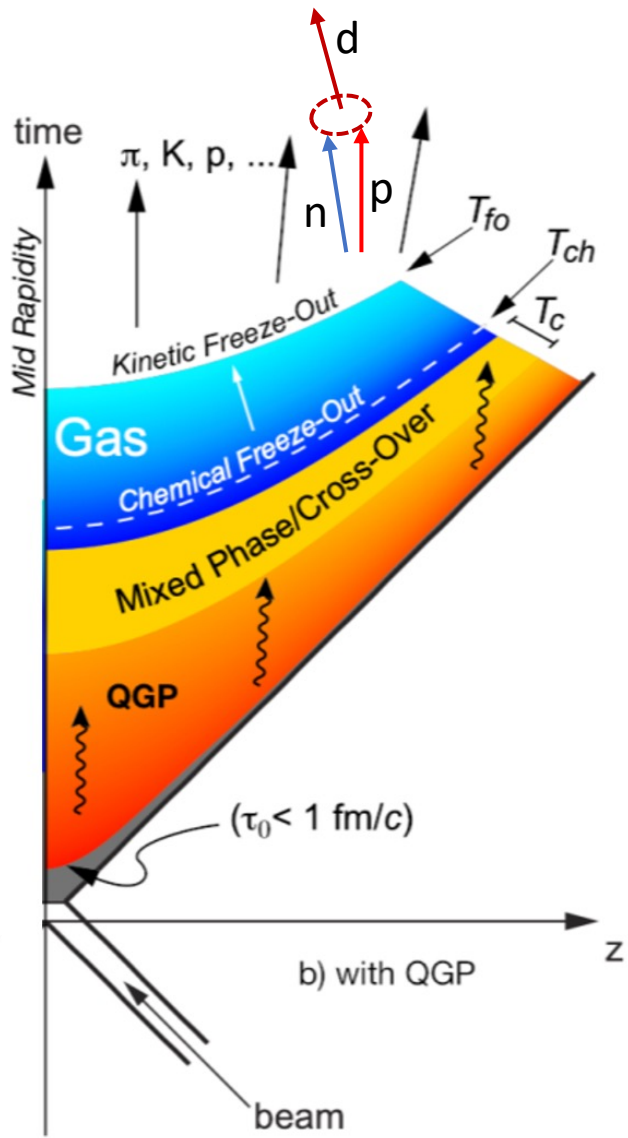
---

6 June 2024





# Production of (anti)nuclei at the LHC



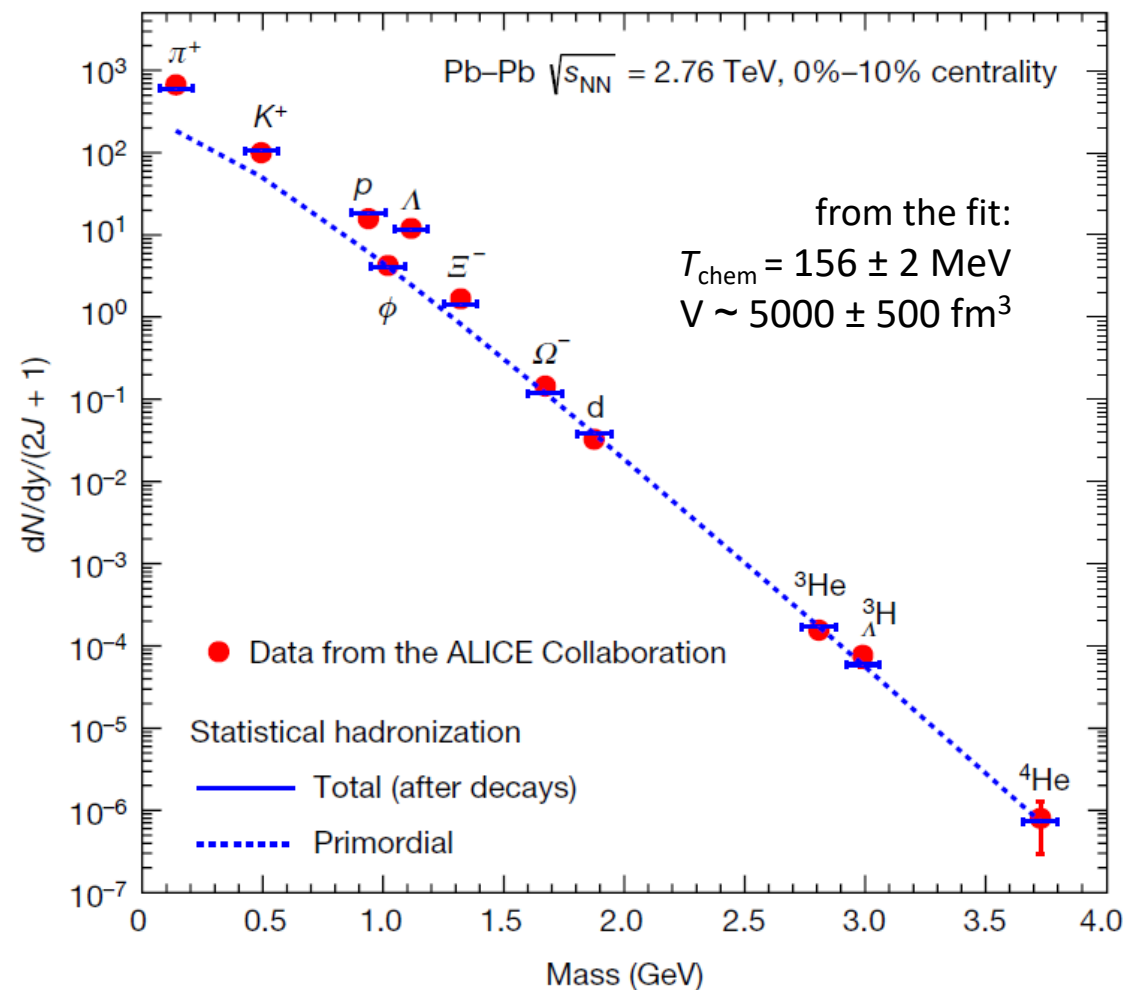
- At LHC energies ( $\sqrt{s} \sim 1\text{--}13 \text{ TeV}$ ) same amount of matter and anti-matter is measured<sup>1</sup> ( $\mu_B \sim 0$ )
- Production measurements useful to investigate the **hadronization mechanism**
- Three classes of phenomenological models available:
  - **statistical hadronization**  $\rightarrow$  works very well for integrated yields (even for nuclei!)
  - **coalescence**  $\rightarrow$  describes fairly well the ratio to protons of integrated yields
  - relativistic **hydrodynamics** + coalescence afterburner  $\rightarrow$  survival of bound states in hadron gas phase with intense rescattering
- Interesting also for astrophysics applications
  - **Cosmic ray** fluxes of antinuclei  $\rightarrow$  dark matter searches
  - **Particle interactions**  $\rightarrow$  neutron stars and equation of state

<sup>1</sup> ALICE Collaboration, arXiv:2311.13332

# Modelling the production of (anti)nuclei

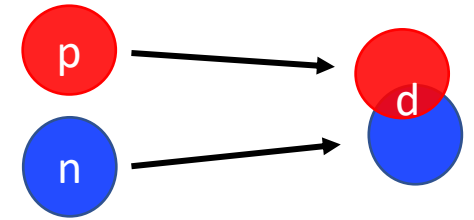
## Statistical models (SHMs)



- Hadrons emitted from a system in statistical and chemical equilibrium
- 3 free parameters:  $V$ ,  $T_{\text{chem}}$ ,  $\mu_B$ 
  - Particle ratios  $\rightarrow$  volume  $V$  cancels
  - Baryochemical potential  $\mu_B$  fixed by  $\bar{p}/p$  ratio  $\rightarrow$  one remaining parameter  $T_{\text{chem}}$
- $dN/dy \propto \exp(-m/T_{\text{chem}})$ 
  - $\Rightarrow$  Nuclei (large  $m$ ): large sensitivity to  $T_{\text{chem}}$
- Typically used in Pb—Pb, for small systems the canonical ensemble is needed (CSM)  $\rightarrow$  exact conservation of B, Q and S is required only in the correlation volume ( $V_c$ )



## Coalescence models

- State-of-the-art models use the *Wigner function formalism*  $\rightarrow$  (anti)nuclei arise from the overlap of the (anti)nucleons phase-space distributions with the Wigner density of the bound state



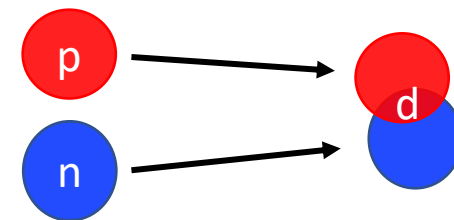
-  Butler et al., Phys. Rev. 129 (1963) 836
-  Mahlein et al., EPJC 83 (2023) 9, 804





# Modelling the production of (anti)nuclei

## Coalescence models

- State-of-the-art models use the *Wigner function formalism*  $\rightarrow$  (anti)nuclei arise from the overlap of the (anti)nucleons phase-space distributions with the Wigner density of the bound state
- Microscopic description
- Key observable is the coalescence parameter  $B_A \rightarrow$  experimental observable tightly connected to the coalescence probability: **Larger  $B_A \Leftrightarrow$  Larger coalescence probability**



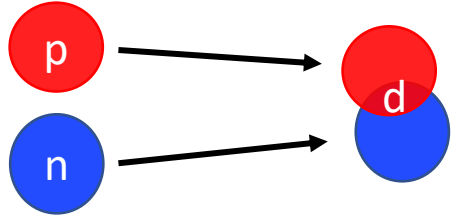
 Butler et al., Phys. Rev. 129 (1963) 836  
 Mahlein et al., EPJC 83 (2023) 9, 804

$$B_A(p_T^p) = E_A \frac{d^3 N_A}{d p_A^3} \bigg/ \left( E_p \frac{d^3 N_p}{d p_p^3} \right)^A \bigg|_{p_T^p = p_T^A / A}$$

# Modelling the production of (anti)nuclei

## Coalescence models

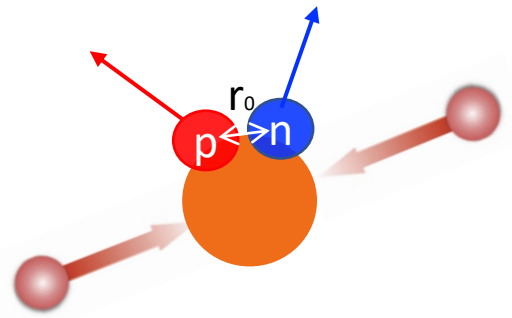
- State-of-the-art models use the *Wigner function formalism* → (anti)nuclei arise from the overlap of the (anti)nucleons phase-space distributions with the Wigner density of the bound state
- Microscopic description
- Key observable is the coalescence parameter  $B_A$  → experimental observable tightly connected to the coalescence probability: **Larger  $B_A$  ⇔ Larger coalescence probability**



Butler et al., Phys. Rev. 129 (1963) 836  
 Mahlein et al., EPJC 83 (2023) 9, 804

<sup>1</sup> PRC 99 (2019) 024001  
<sup>2</sup> PRL 123 (2019) 112002  
<sup>3</sup> PRC 96 (2017) 064613

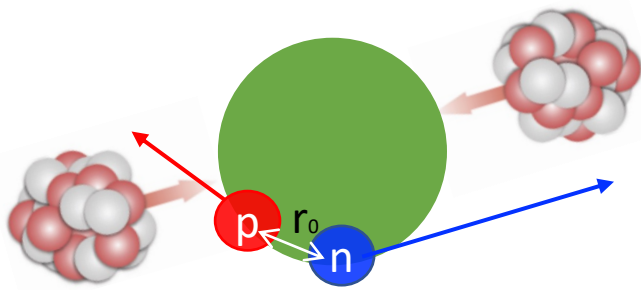
$$B_A(p_T^p) = E_A \frac{d^3 N_A}{d p_A^3} \bigg/ \left( E_p \frac{d^3 N_p}{d p_p^3} \right)^A \bigg|_{p_T^p = p_T^A / A}$$



Small distance in space  
(Only momentum correlations matter)

⇔ large  $B_A$

pp<sup>1</sup>, p—Pb<sup>2</sup>:  $r_0 = 1-1.5$  fm

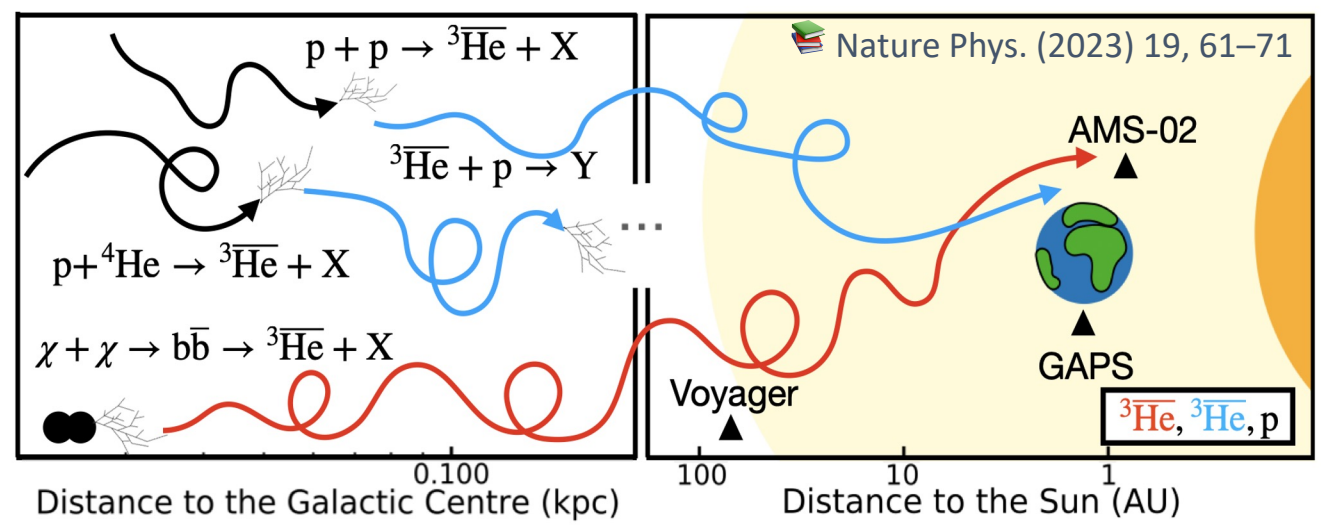


Large distance in space  
(Both momentum and space correlations matter)

⇔ small  $B_A$

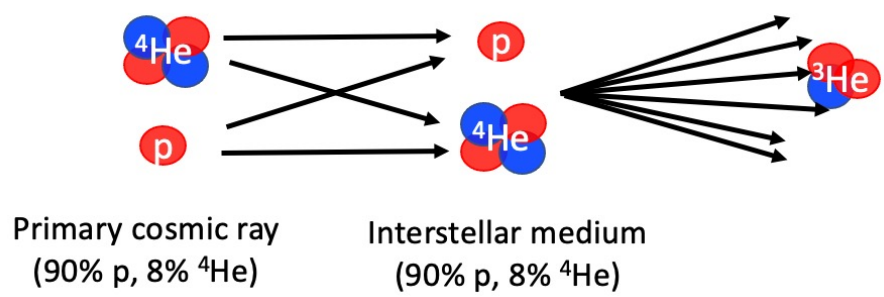
Pb—Pb<sup>3</sup>:  $r_0 = 3-6$  fm

# Astrophysics applications: Dark Matter



## Antinuclei production in our Galaxy:

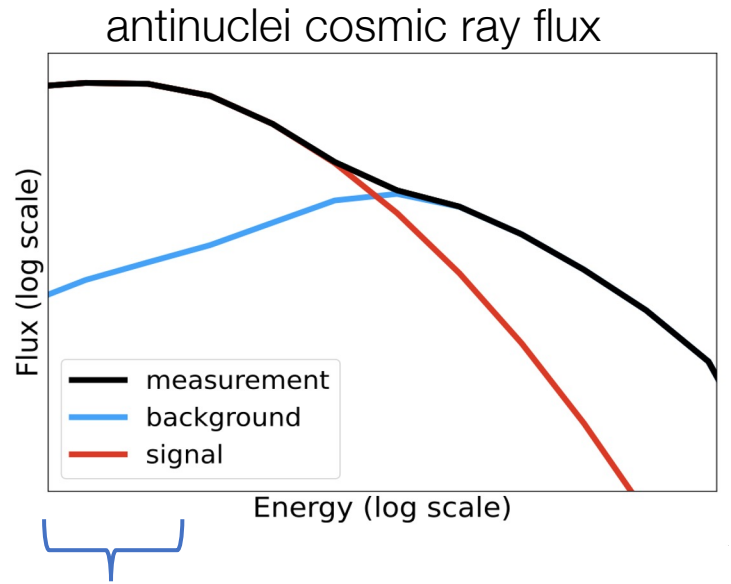
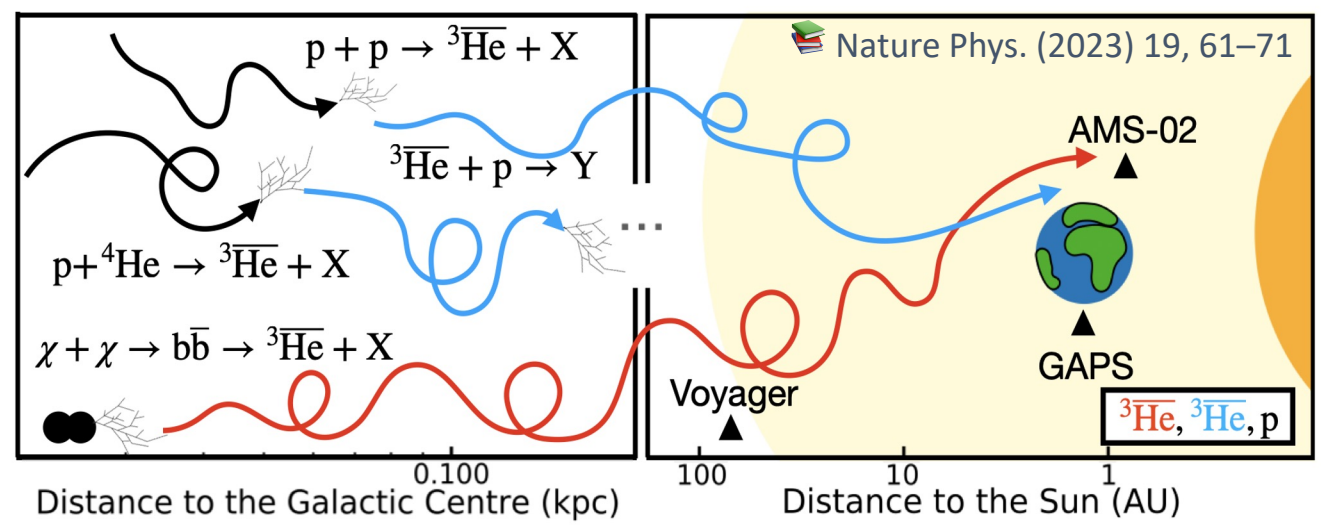
- pp, pA and (few) AA reactions between primary **cosmic rays** and the interstellar medium



- **dark-matter** annihilation processes

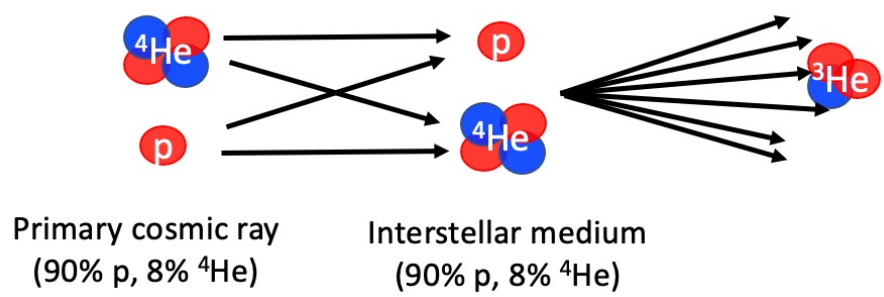


# Astrophysics applications: Dark Matter



## Antinuclei production in our Galaxy:

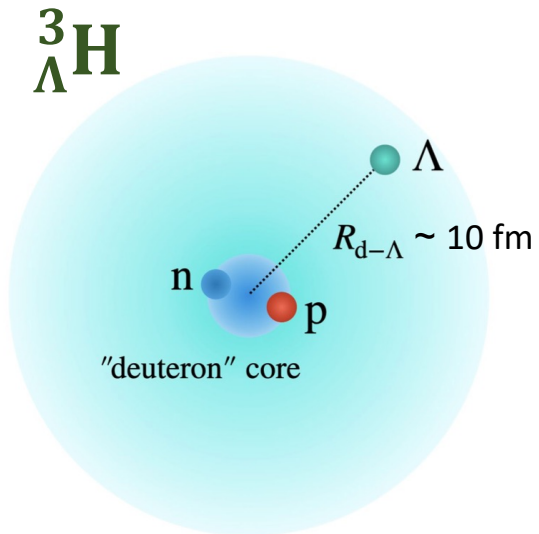
- pp, pA and (few) AA reactions between primary cosmic rays and the interstellar medium



- High Signal/Noise ratio ( $\sim 10^2 - 10^4$ ) at low  $E_{kin}$  expected by models
- To correctly interpret any future measurement, we need precise knowledge of
  1. production of antinuclei
  2. annihilation

- **dark-matter** annihilation processes

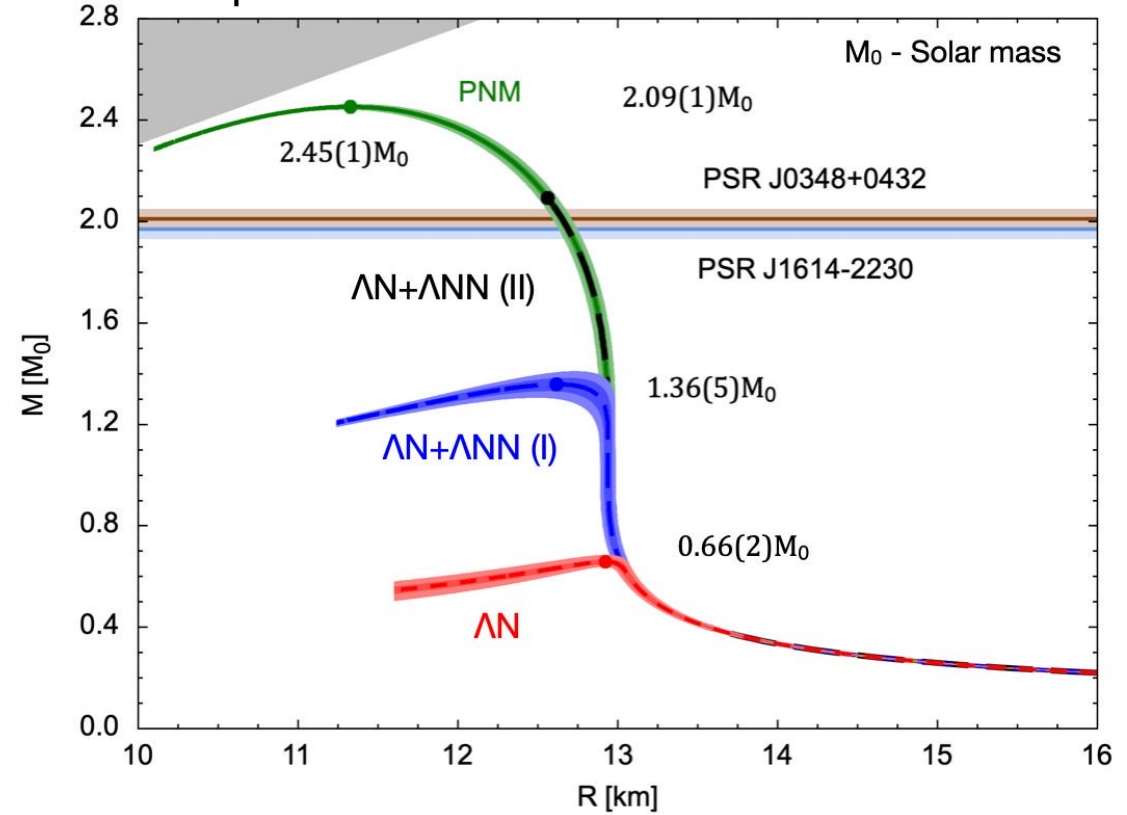
# Astrophysics applications: neutron stars



- At the LHC,  ${}^3_{\Lambda}\text{H}$  has been measured in pp, p-Pb, and Pb-Pb collisions
- ${}^3_{\Lambda}\text{H}$  powerful probe for investigating the nucleon- $\Lambda$  interaction
- Crucial for the calculation of the equation of state (EoS) and the neutron star mass-radius relation

- 3-body hyperon-nucleon interaction is key in the softening of the EoS and the consequent reduction of the predicted maximum mass
- different results on the maximum mass not necessarily incompatible with the observed neutron stars

D. Lonardonì et al., PRL 114, 092301 (2015)



# Experimental efforts at the LHC

---



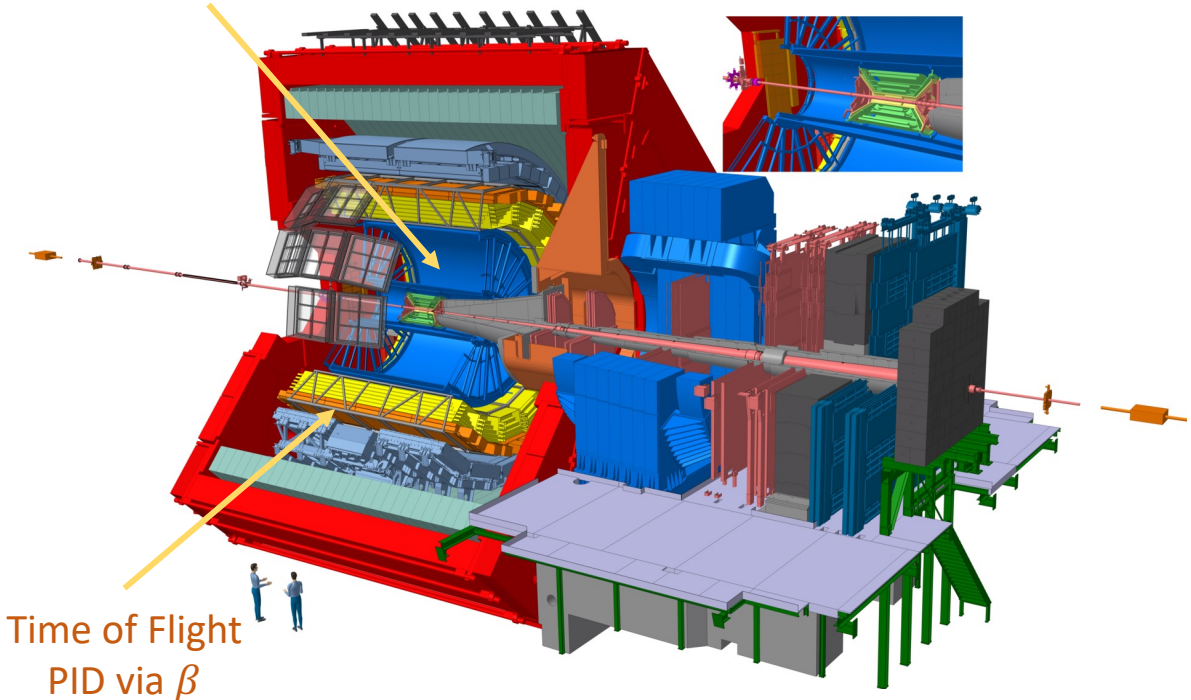


# Experimental efforts at the LHC



ALICE

Time Projection Chamber  
PID via  $dE/dx$

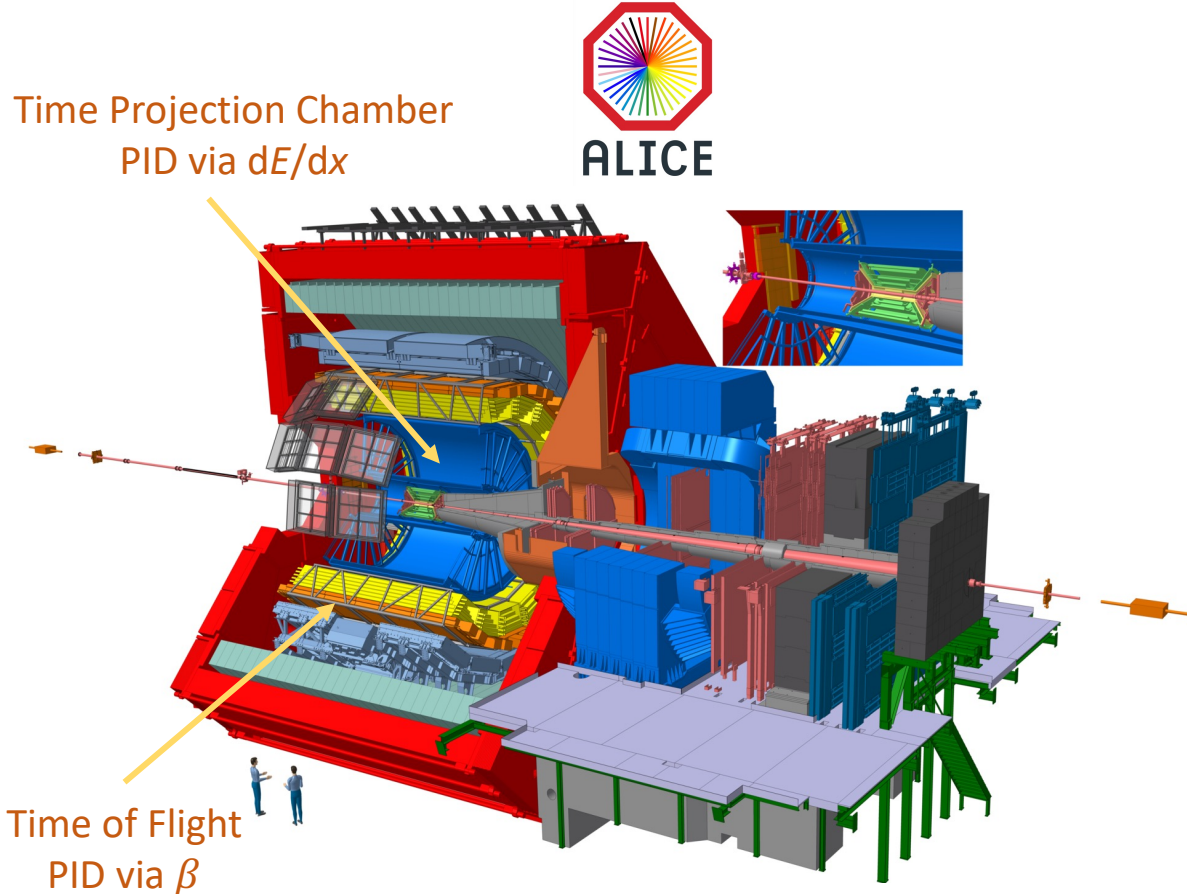


Time of Flight  
PID via  $\beta$

ALICE Collaboration, 2008 *JINST* 3 S08002

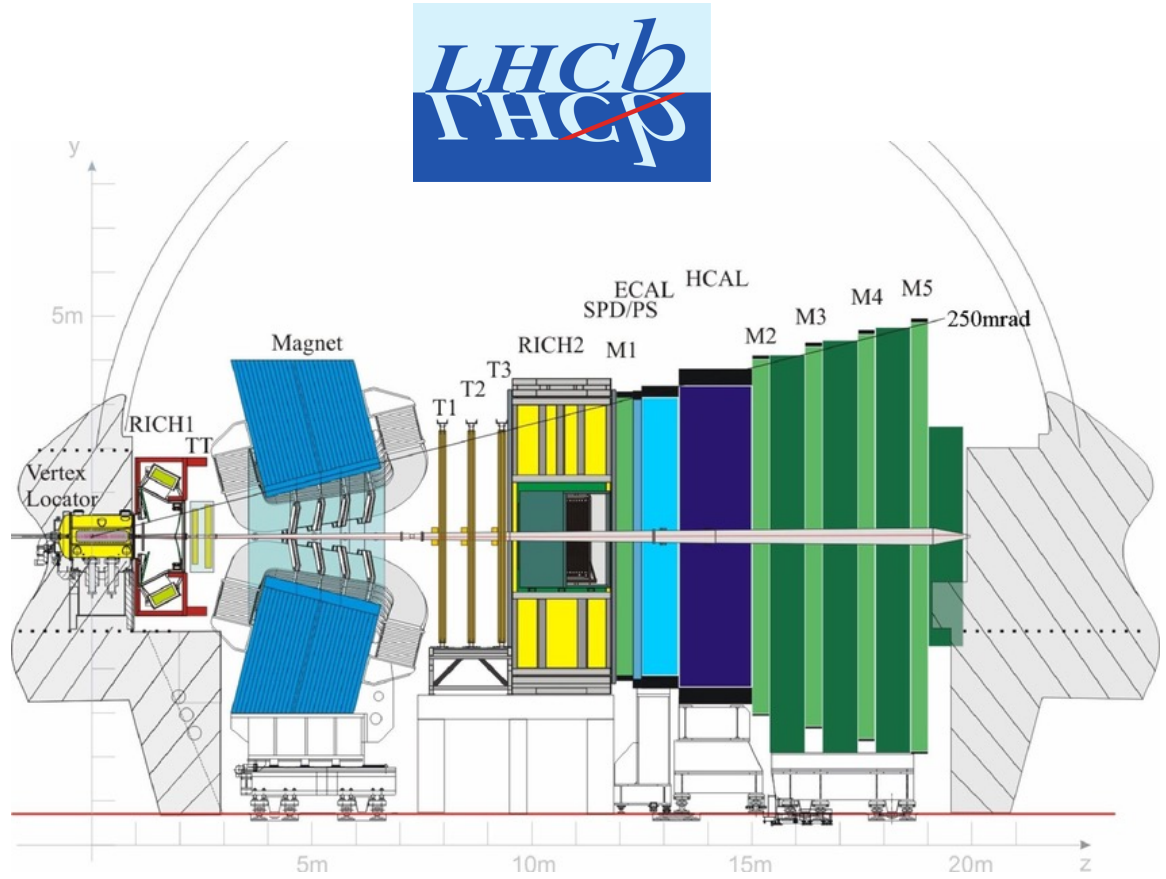
- excellent tracking & PID capabilities over broad  $p$  range
  - low material budget
- most suited detector at the LHC for the study of nuclei**

# Experimental efforts at the LHC



ALICE Collaboration, 2008 *JINST* 3 S08002

- excellent tracking & PID capabilities over broad  $p$  range
- low material budget
- **most suited detector at the LHC for the study of nuclei**



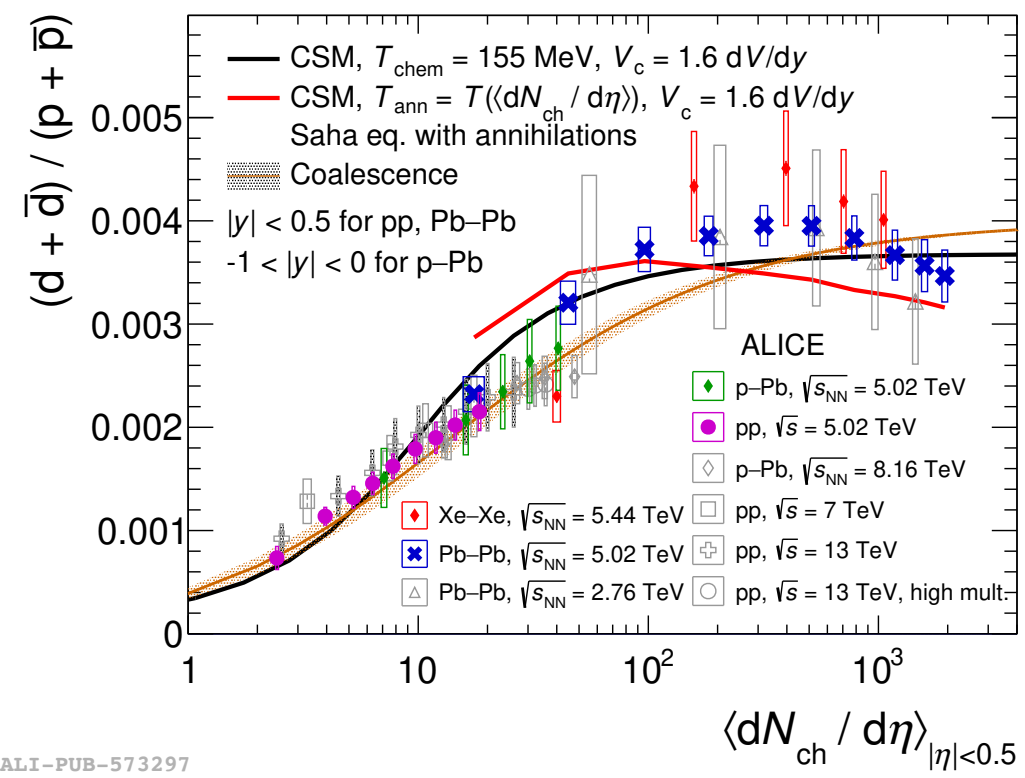
LHCb Collaboration, 2008 *JINST* 3 S08005

- excellent vertexing and PID separation for  $K$ ,  $\pi$  and  $p$  with  $O(10)$  GeV/c
- covering forward rapidity and with SMOG → several energies & systems
- **recently joined the nuclei business!**

# Testing production models with $A=2$



# Testing production models with $A=2$



ALI-PUB-573297

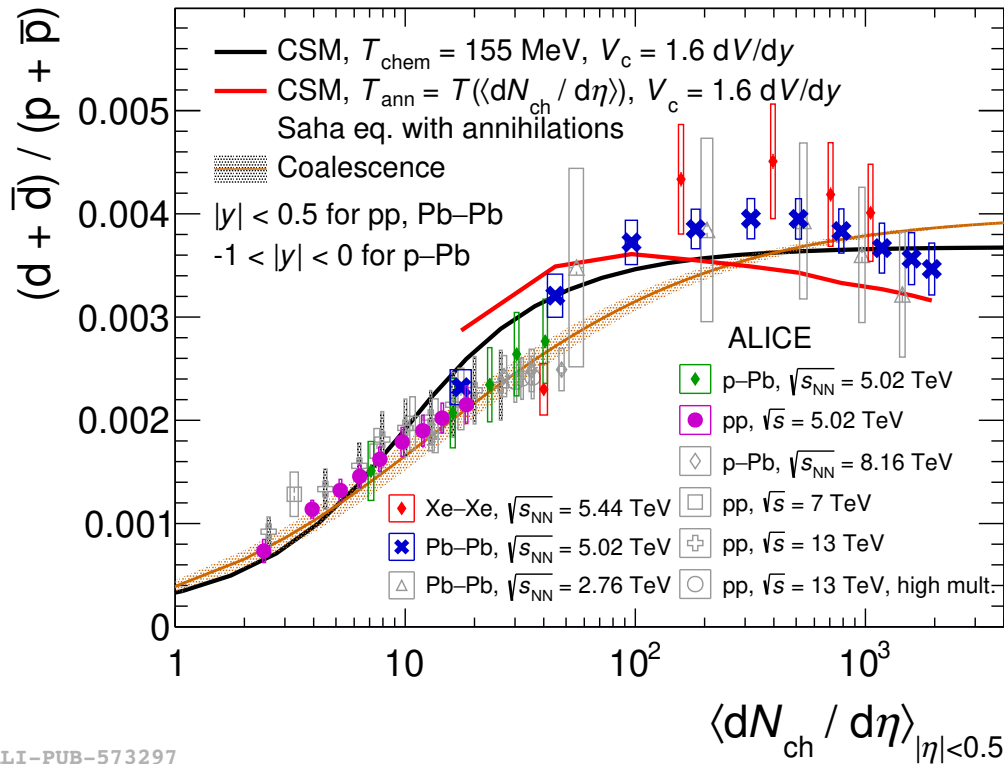
- $V_c=1.6 \text{ dV/dy}$  is the correlation volume needed to describe the net-deuteron number fluctuations in Pb–Pb collisions<sup>1</sup>
- CSM  $\rightarrow$  either with fixed chemical temperature (CSM-I) or with **annihilation** temperature depending on multiplicity<sup>2</sup> (CSM-II)
- Both CSM and **coalescence**<sup>3</sup> predictions qualitatively reproduce the trend and overall yields, but neither of the models catch all data points

<sup>1</sup> ALICE Collaboration, PRL 131 (2023) 041901

<sup>2</sup> Vovchenko, Koch, PLB 835, 137577 (2022)

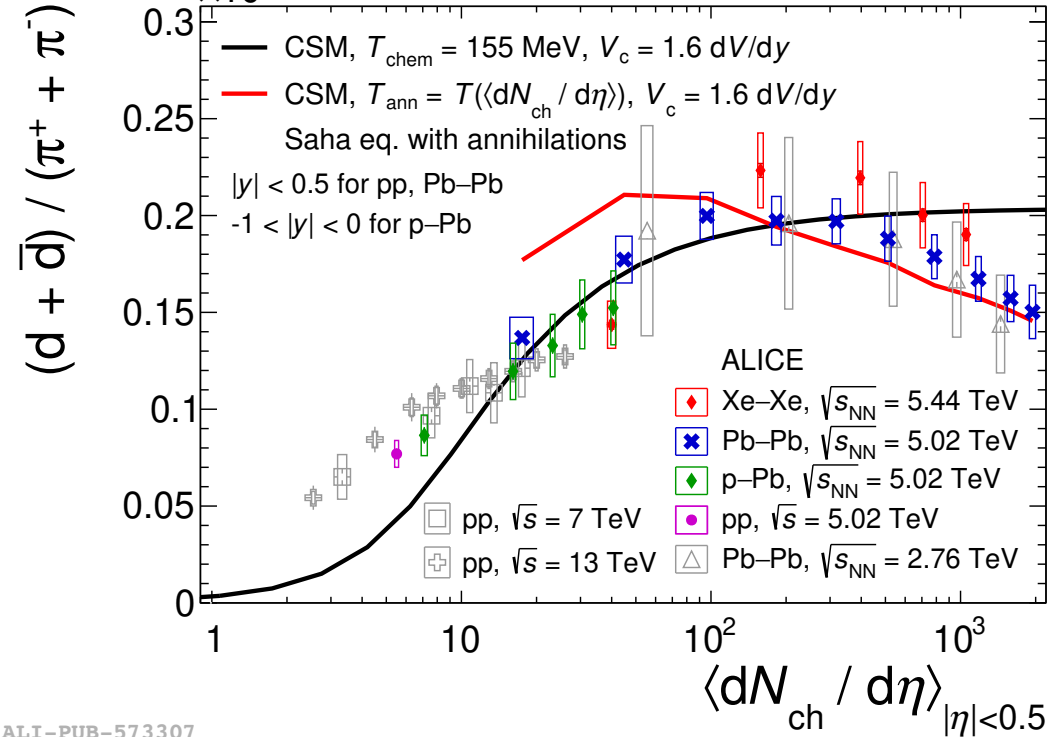
<sup>3</sup> Sun, Ko, Doenigus, PLB 792 (2019) 132-137

# Testing production models with $A=2$



ALI-PUB-573297

ALI-PUB-573307



ALICE Collaboration, [arXiv:2405.19826](https://arxiv.org/abs/2405.19826)

- $V_c=1.6 \text{ dV/dy}$  is the correlation volume needed to describe the net-deuteron number fluctuations in Pb–Pb collisions<sup>1</sup>
- CSM  $\rightarrow$  either with fixed chemical temperature (CSM-I) or with **annihilation** temperature depending on multiplicity<sup>2</sup> (CSM-II)
- Both CSM and **coalescence**<sup>3</sup> predictions qualitatively reproduce the trend and overall yields, but neither of the models catch all data points
- CSM-I at low multiplicity does not reproduce  $d/\pi$  ratio, but CSM-II at high multiplicity catches the decreasing trend

<sup>1</sup> ALICE Collaboration, PRL 131 (2023) 041901

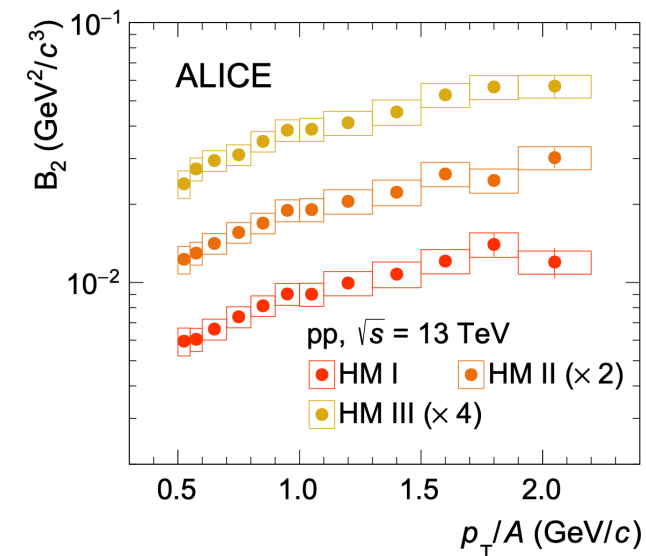
<sup>2</sup> Vovchenko, Koch, PLB 835, 137577 (2022)

<sup>3</sup> Sun, Ko, Doenigus, PLB 792 (2019) 132-137

# Testing coalescence model using $B_2$

- Important observable in accelerator measurements: coalescence parameter  $B_A$

$$B_A(p_T^p) = \frac{1}{2\pi p_T^A} \frac{d^2 N_A}{dy dp_T^A} \bigg/ \left( \frac{1}{2\pi p_T^p} \frac{d^2 N_p}{dy dp_T^p} \right)^A$$

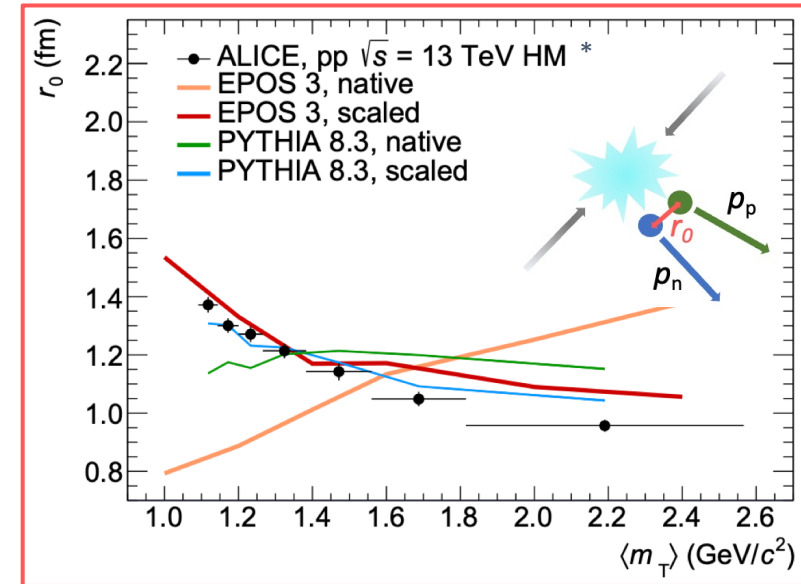


# Testing coalescence model using $B_2$

- Important observable in accelerator measurements: coalescence parameter  $B_A$

$$B_A(p_T^p) = \frac{1}{2\pi p_T^A} \frac{d^2 N_A}{dy dp_T^A} \bigg/ \left( \frac{1}{2\pi p_T^p} \frac{d^2 N_p}{dy dp_T^p} \right)^A$$

- Comparison to state-of-the-art coalescence models based on Wigner formalism showed that there are 2 key ingredients:
  - *emission source size*



\* ALICE Collaboration, PLB 811 (2020) 135849  
 ALICE Collaboration, JHEP 01 (2022) 106

Kachelrieß et al., EPJA 56 1 (2020) 4  
 Kachelrieß et al., EPJA 57 5 (2021) 167

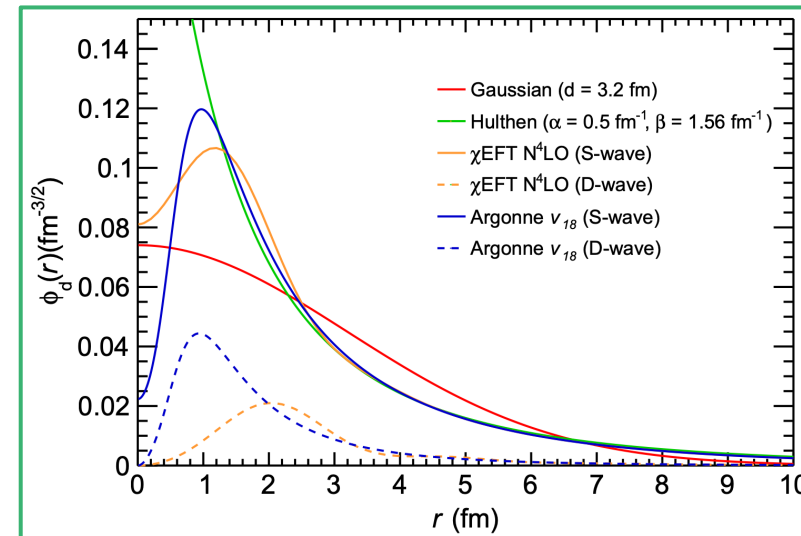
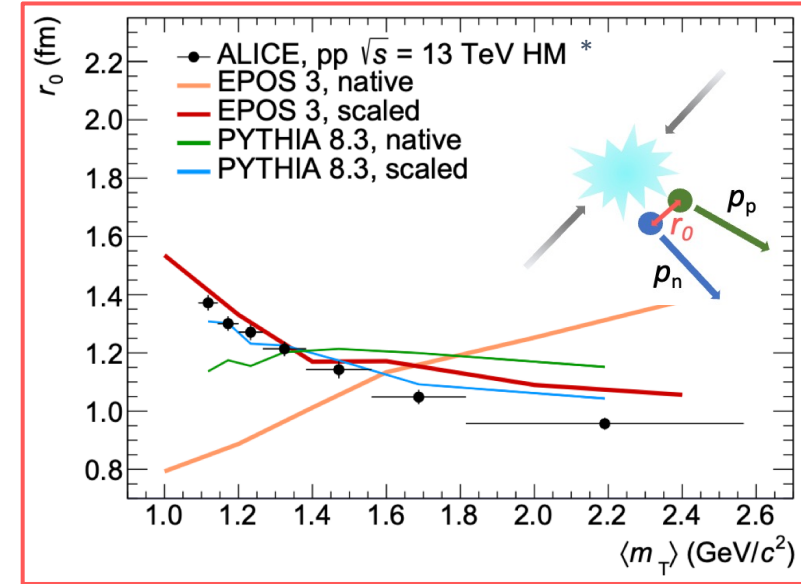
Mahlein et al., EPJC 83 (2023) 9, 804

# Testing coalescence model using $B_2$

- Important observable in accelerator measurements: coalescence parameter  $B_A$

$$B_A(p_T^p) = \frac{1}{2\pi p_T^A} \frac{d^2 N_A}{dy dp_T^A} \bigg/ \left( \frac{1}{2\pi p_T^p} \frac{d^2 N_p}{dy dp_T^p} \right)^A$$

- Comparison to state-of-the-art coalescence models based on Wigner formalism showed that there are 2 key ingredients:
  - *emission source size*
  - *deuteron wave function*



\* ALICE Collaboration, PLB 811 (2020) 135849  
 ALICE Collaboration, JHEP 01 (2022) 106

Kachelrieß et al., EPJA 56 1 (2020) 4  
 Kachelrieß et al., EPJA 57 5 (2021) 167

Mahlein et al., EPJC 83 (2023) 9, 804



# Testing coalescence model using $B_2$

- Important observable in accelerator measurements: coalescence parameter  $B_A$

$$B_A(p_T^p) = \frac{1}{2\pi p_T^A} \frac{d^2 N_A}{dy dp_T^A} \bigg/ \left( \frac{1}{2\pi p_T^p} \frac{d^2 N_p}{dy dp_T^p} \right)^A$$

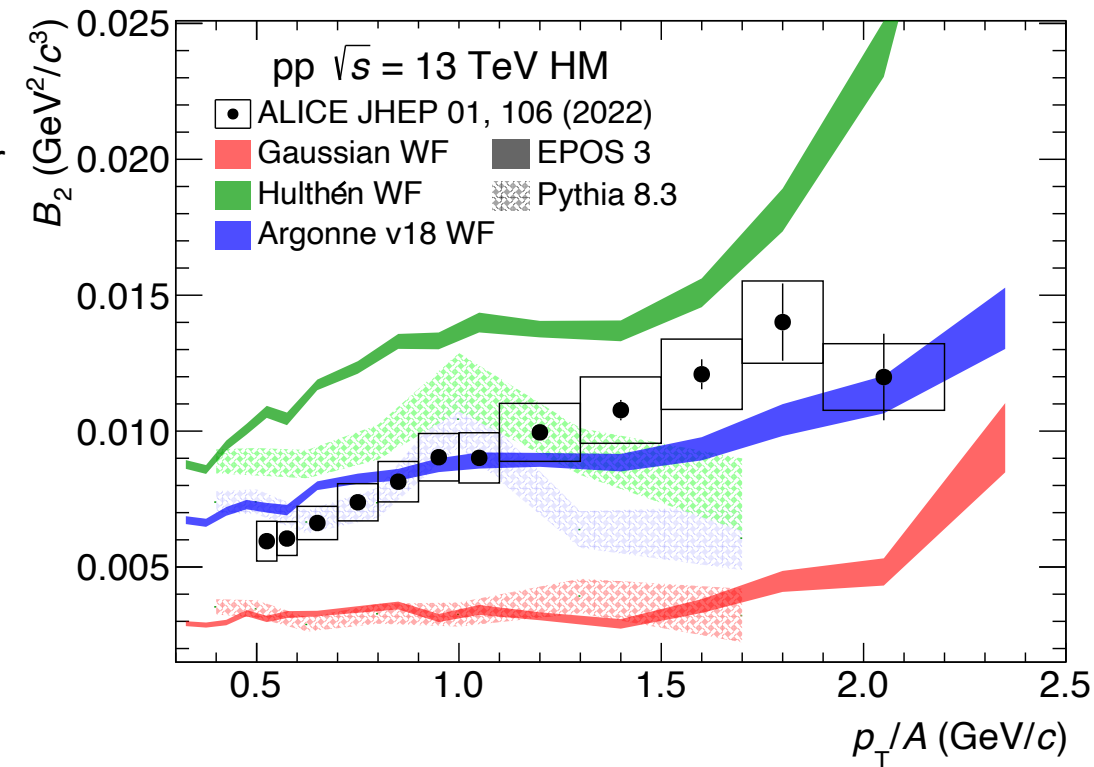
- Comparison to state-of-the-art coalescence models based on Wigner showed that there are 2 key ingredients:

- *emission source size*
- *deuteron wave function*

State-of-the-art coalescence model describes deuteron momentum distributions and coalescence parameter, using realistic WF and measured  $r_0$ !



Production measurements can be used to constrain the nuclear wavefunction!



\* ALICE Collaboration, PLB 811 (2020) 135849

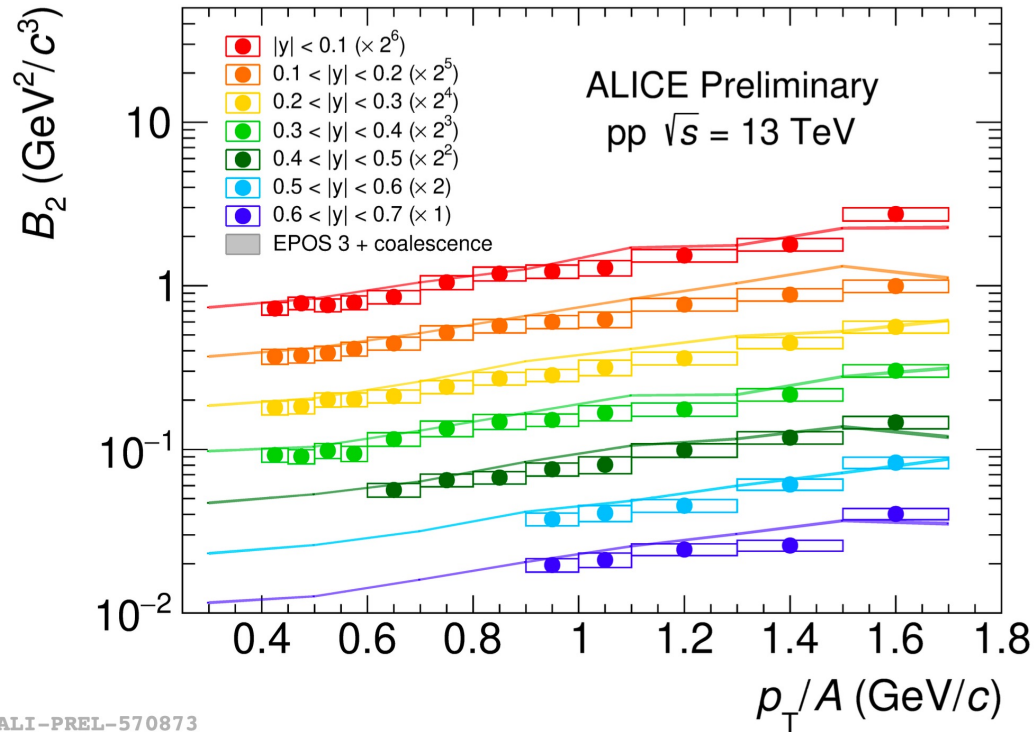
ALICE Collaboration, JHEP 01 (2022) 106

Kachelrieß et al., EPJA 56 1 (2020) 4

Kachelrieß et al., EPJA 57 5 (2021) 167

Mahlein et al., EPJC 83 (2023) 9, 804

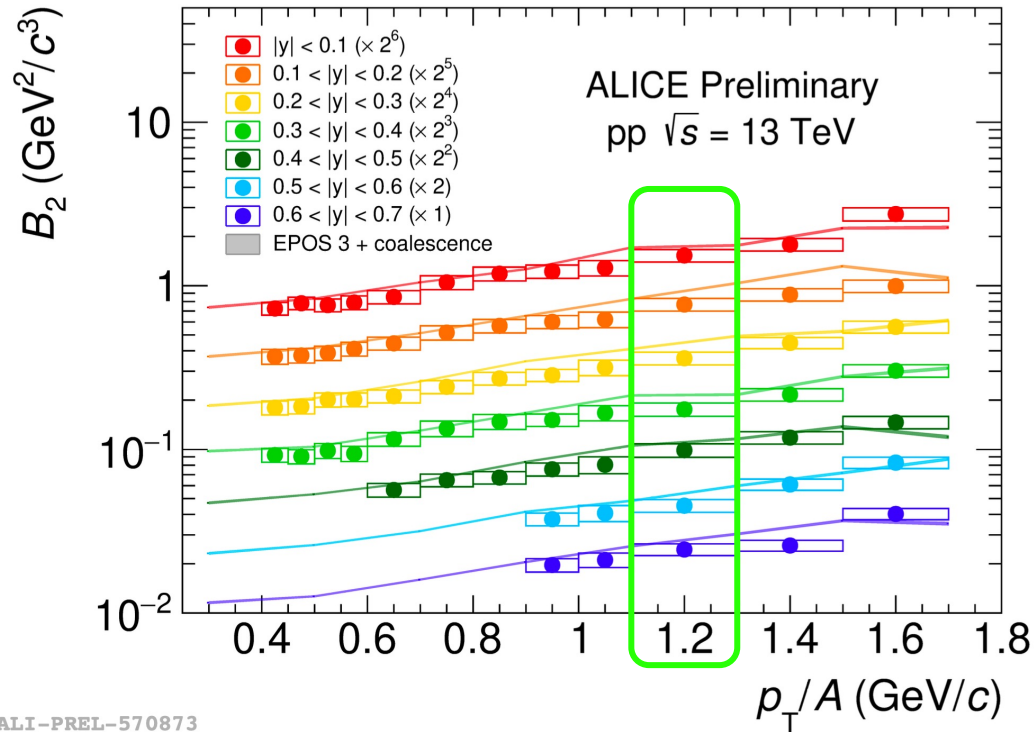
# $B_2$ vs rapidity with ALICE



- ALICE measurements cover the midrapidity region ( $|y| < 0.5$ ), while astrophysical models extrapolate to forward region
- Current acceptance of ALICE detector allows one to extend the measurement of antinuclei up to  $|y| = 0.7$

ALI-PREL-570873

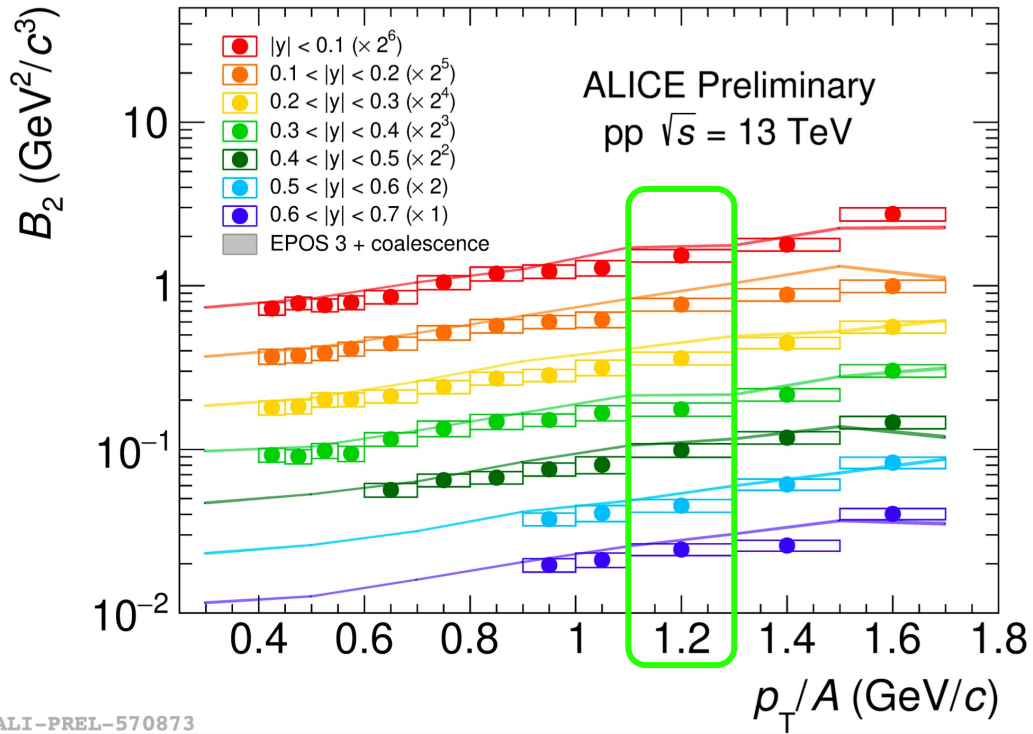
# $B_2$ vs rapidity with ALICE



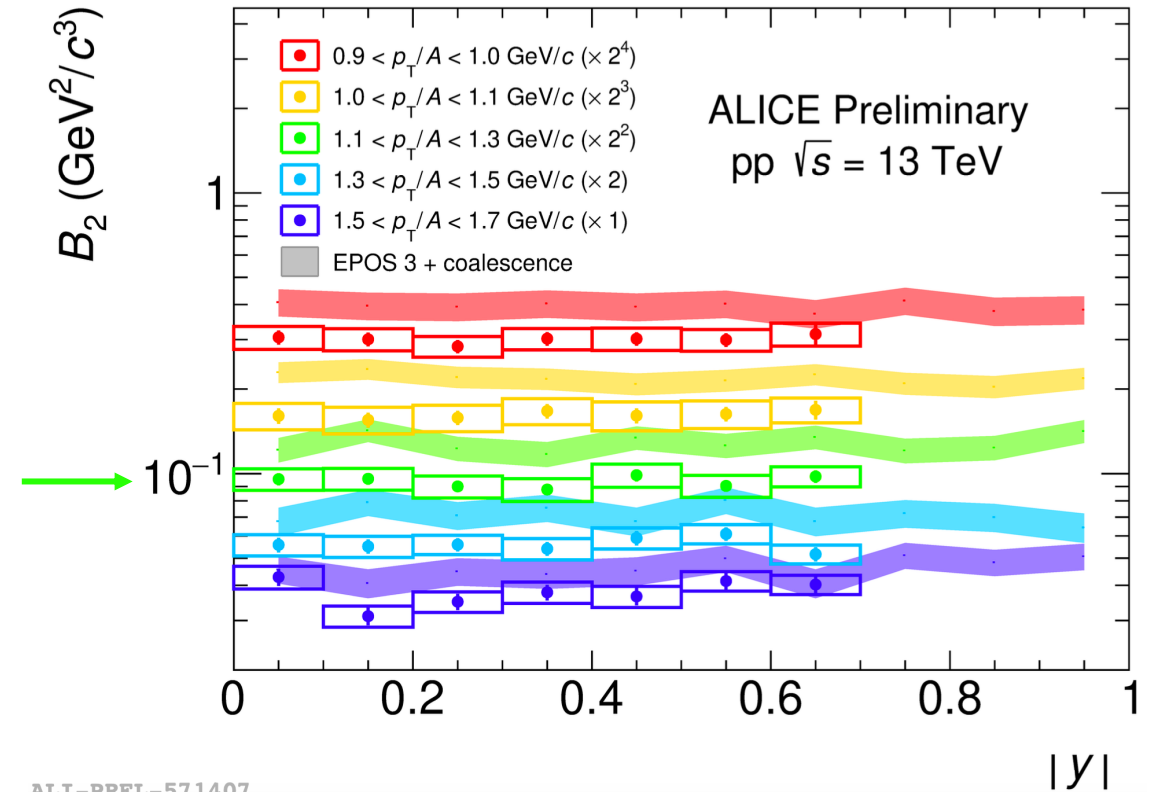
- ALICE measurements cover the midrapidity region ( $|y| < 0.5$ ), while astrophysical models extrapolate to forward region
- Current acceptance of ALICE detector allows one to extend the measurement of antinuclei up to  $|y| = 0.7$

ALI-PREL-570873

# $B_2$ vs rapidity with ALICE



- ALICE measurements cover the midrapidity region ( $|y| < 0.5$ ), while astrophysical models extrapolate to forward region
- Current acceptance of ALICE detector allows one to extend the measurement of antinuclei up to  $|y| = 0.7$

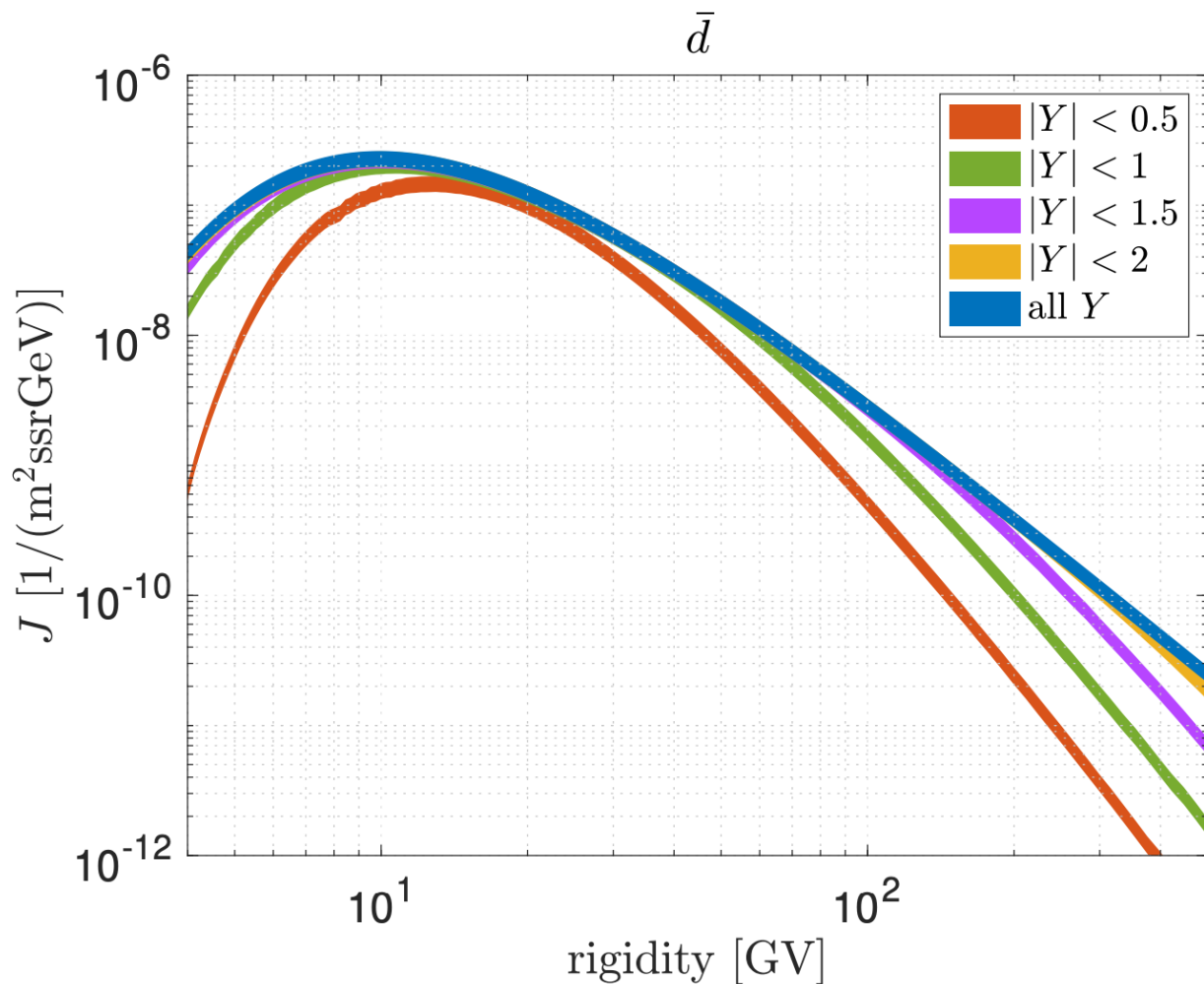


- Rapidity and  $p_T$  dependence of  $B_2$  is extrapolated to forward rapidity using coalescence model + Pythia 8.3 and EPOS as event generators

ALI-PREL-570873

ALI-PREL-571407

# Flux of antinuclei in CRs



- Model predictions based on ALICE measurements are used as input to calculate antideuteron flux from cosmic rays\* → dominant background in dark matter searches
- **Most of the antideuteron yield from  $|y| < 1.5$ , in reach with:**
  - future ALICE3<sup>(1)</sup> detector acceptance ( $|y| \lesssim 4$ )
  - LHCb experiment with fixed target
  - CMS in Run4
- Extrapolation to **lower energies** ( $\sim \text{GeV}$ ) is needed for astrophysical models

\* K. Blum, [Phys. Rev. D 96, 103021 \(2017\)](https://arxiv.org/abs/1703.07501)

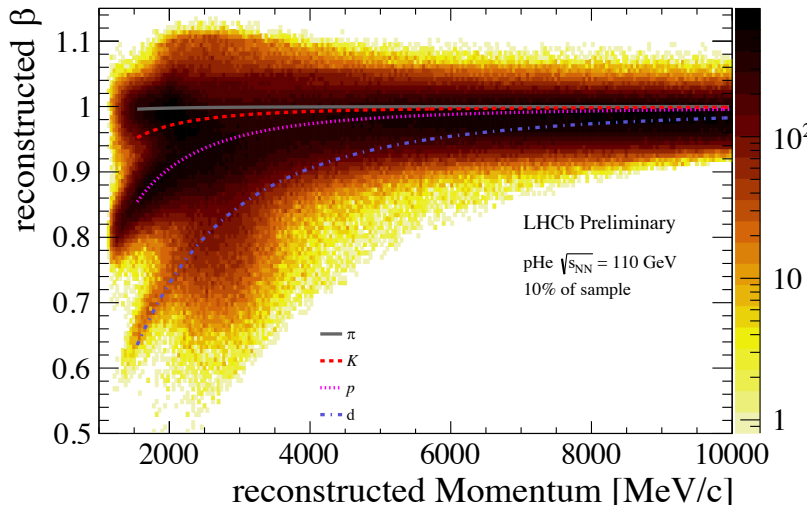
<sup>1</sup> ALICE Collaboration, [arXiv:2211.02491](https://arxiv.org/abs/2211.02491)

K. Blum, [arXiv:2306.13165](https://arxiv.org/abs/2306.13165)

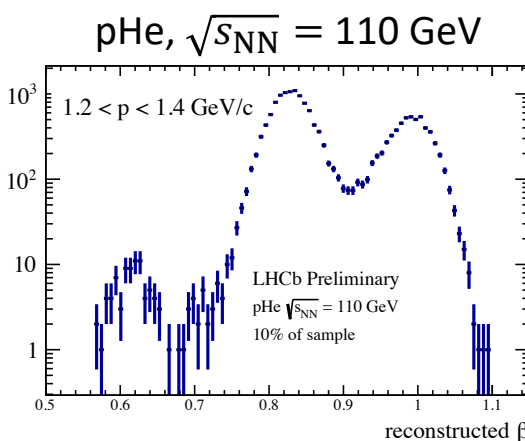


# (anti)deuterons at forward rapidity

- LHCb can be used as a fixed-target experiment (**SMOG**)
- Collect physics samples with different **targets** and different **centre of mass energies** ( $\sqrt{s_{NN}} \in [30, 115]$  GeV)



**Time-of-Flight**  
→ identification of **d**,  
separation of  ${}^3\text{He}$ ,  ${}^4\text{He}$



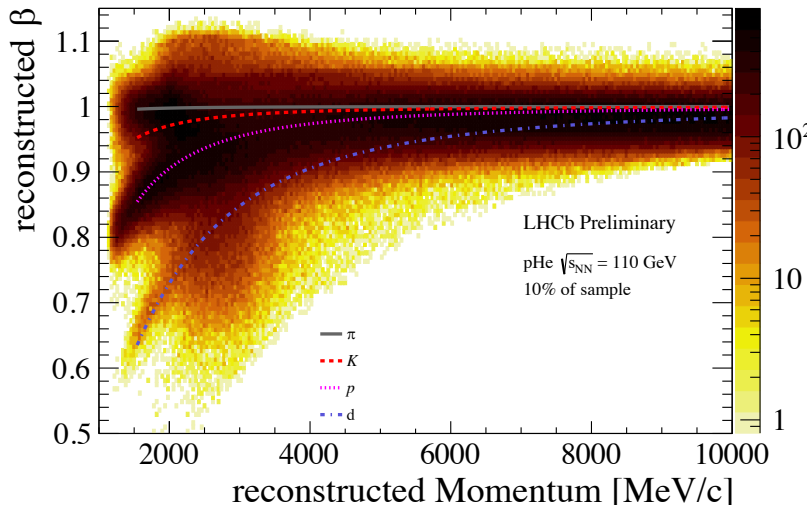
$$2 \lesssim |\eta| \lesssim 5$$

# (anti)deuterons at forward rapidity

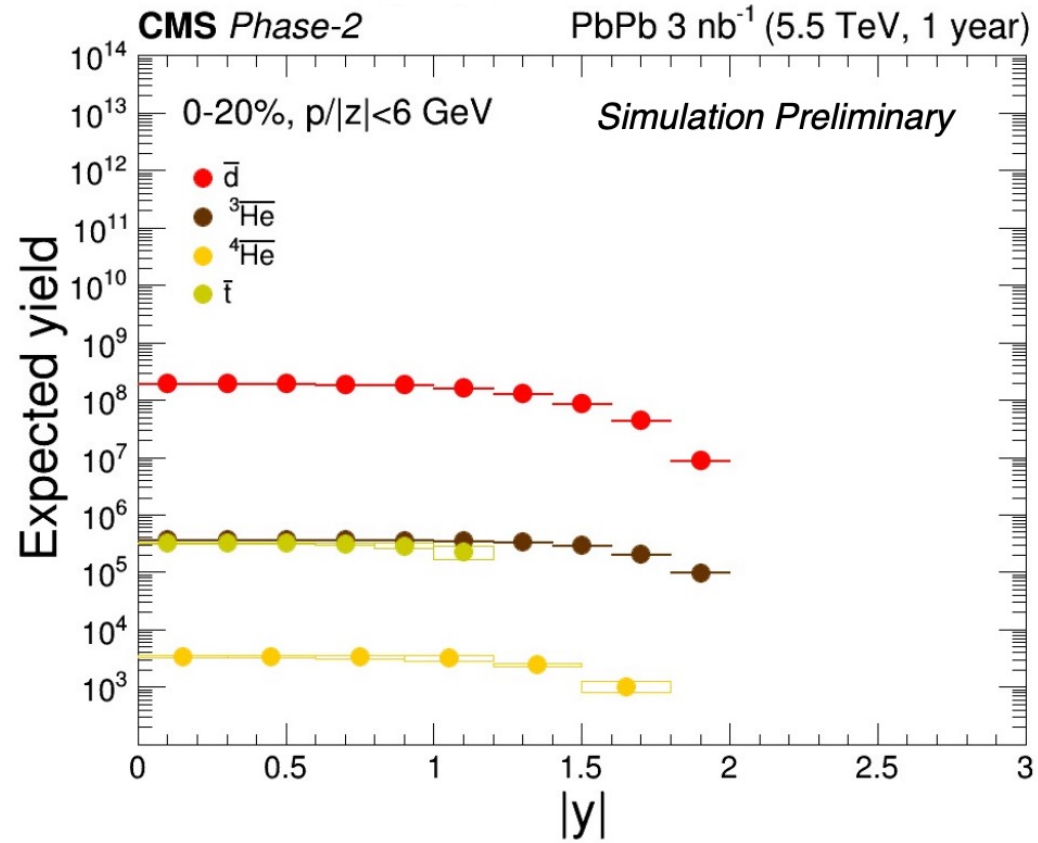
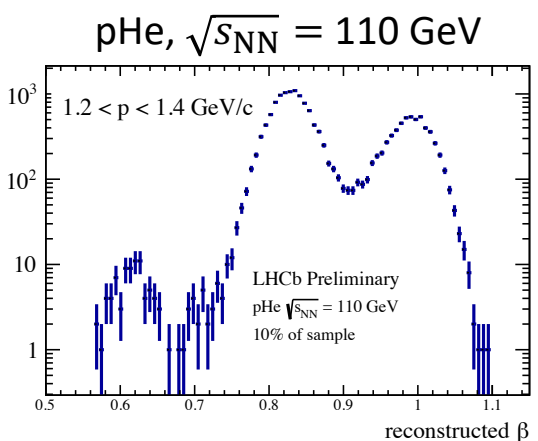
- LHCb can be used as a fixed-target experiment (**SMOG**)
- Collect physics samples with different **targets** and different **centre of mass energies** ( $\sqrt{s_{NN}} \in [30, 115]$  GeV)



CMS program in LHC Run4  
( $|\eta| \lesssim 2$ )

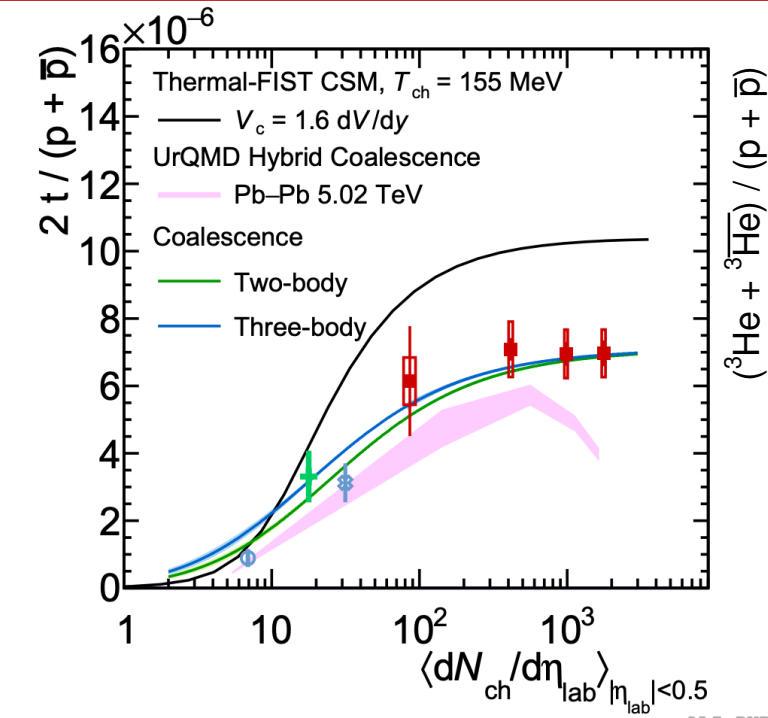


**Time-of-Flight**  
→ identification of **d**,  
separation of  ${}^3\text{He}$ ,  ${}^4\text{He}$

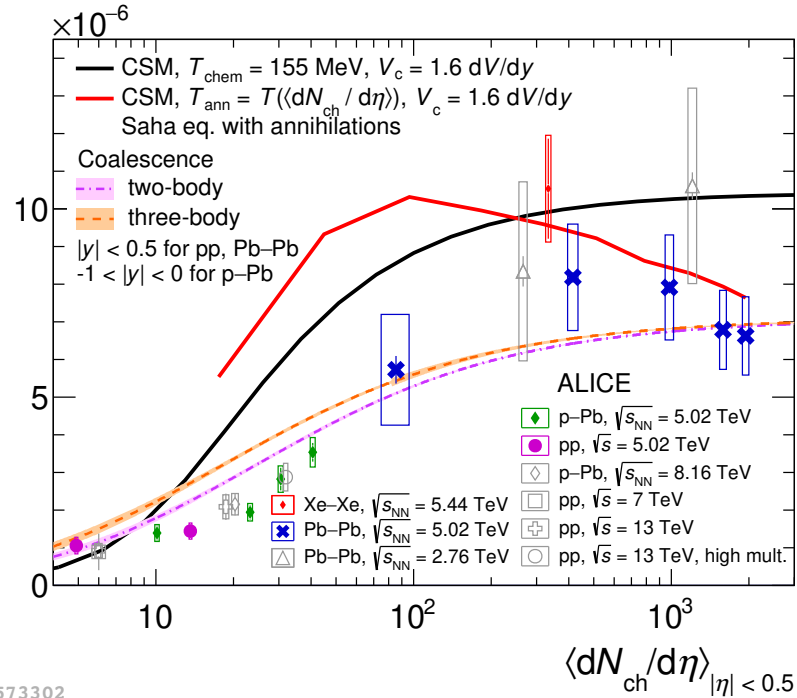


$2 \lesssim |\eta| \lesssim 5$

# Testing production models with A=3

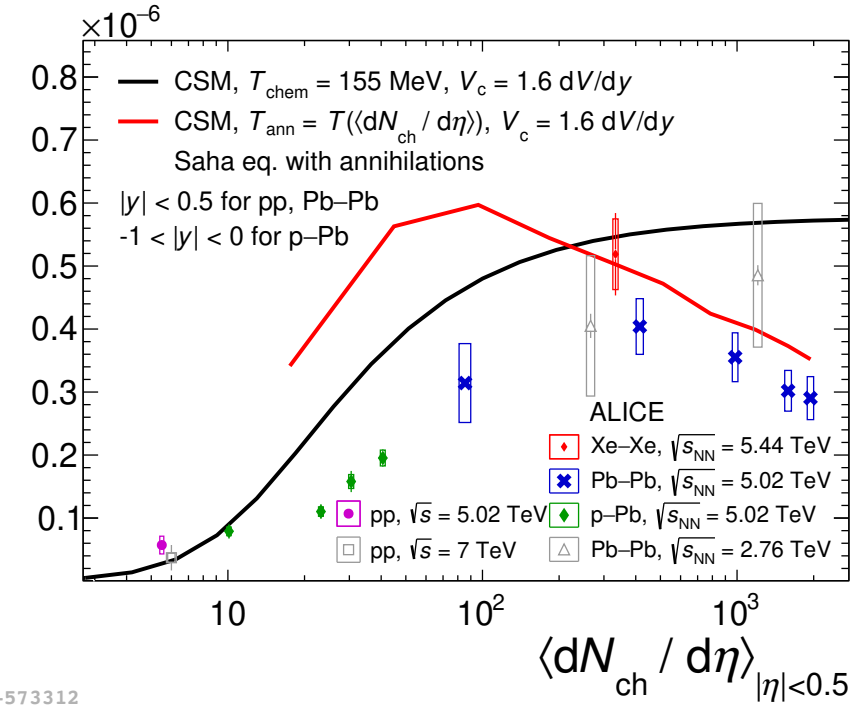
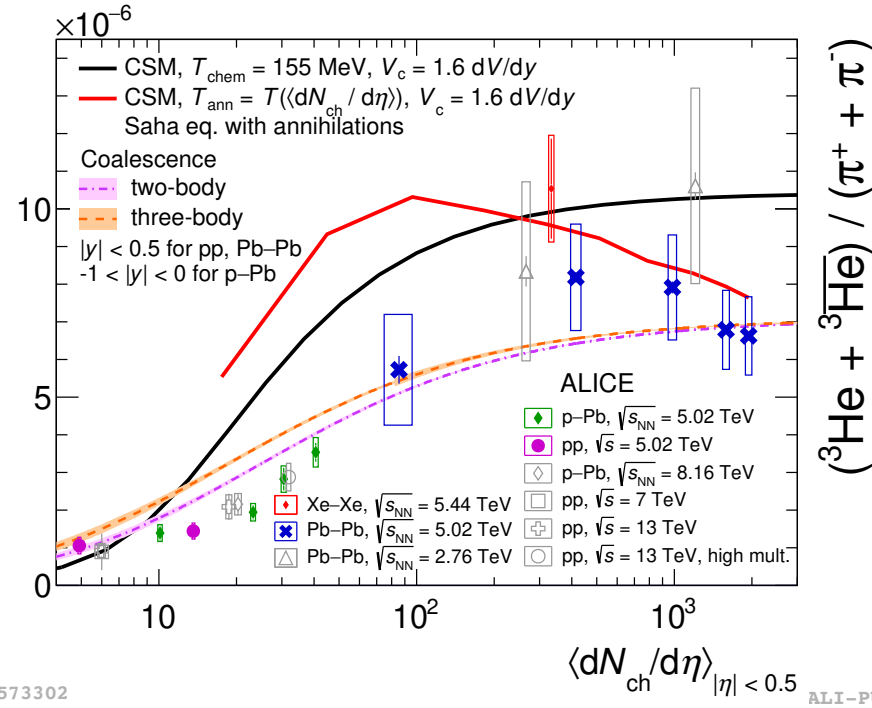
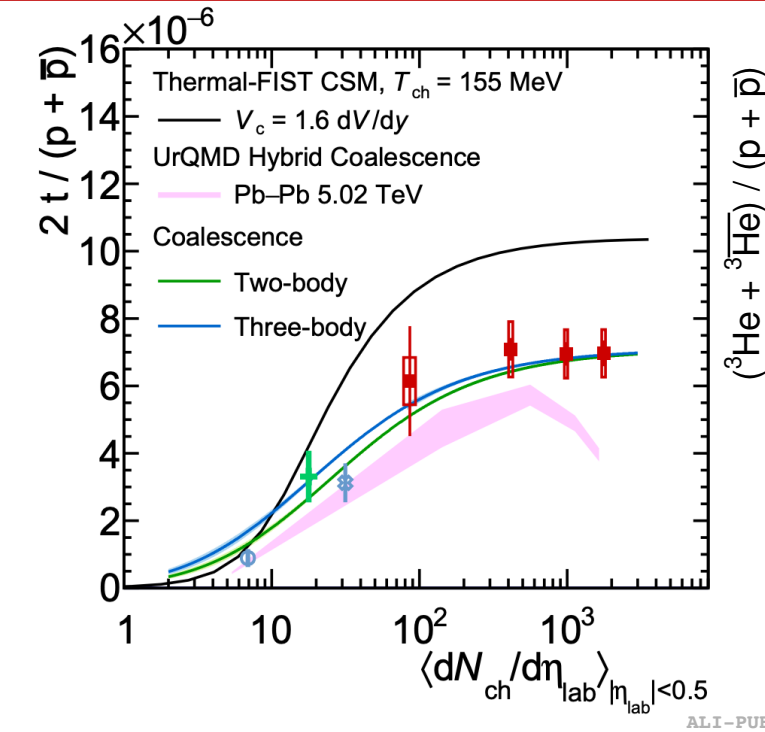


ALI-PUB-573302



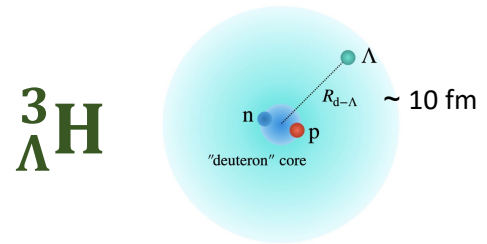
- Measurements of yields of nuclei with A=3 challenge the models
- Neither of the CSM models or **coalescence** predictions reproduce the trend of the ratios, but qualitatively reproduce the overall yields

# Testing production models with A=3



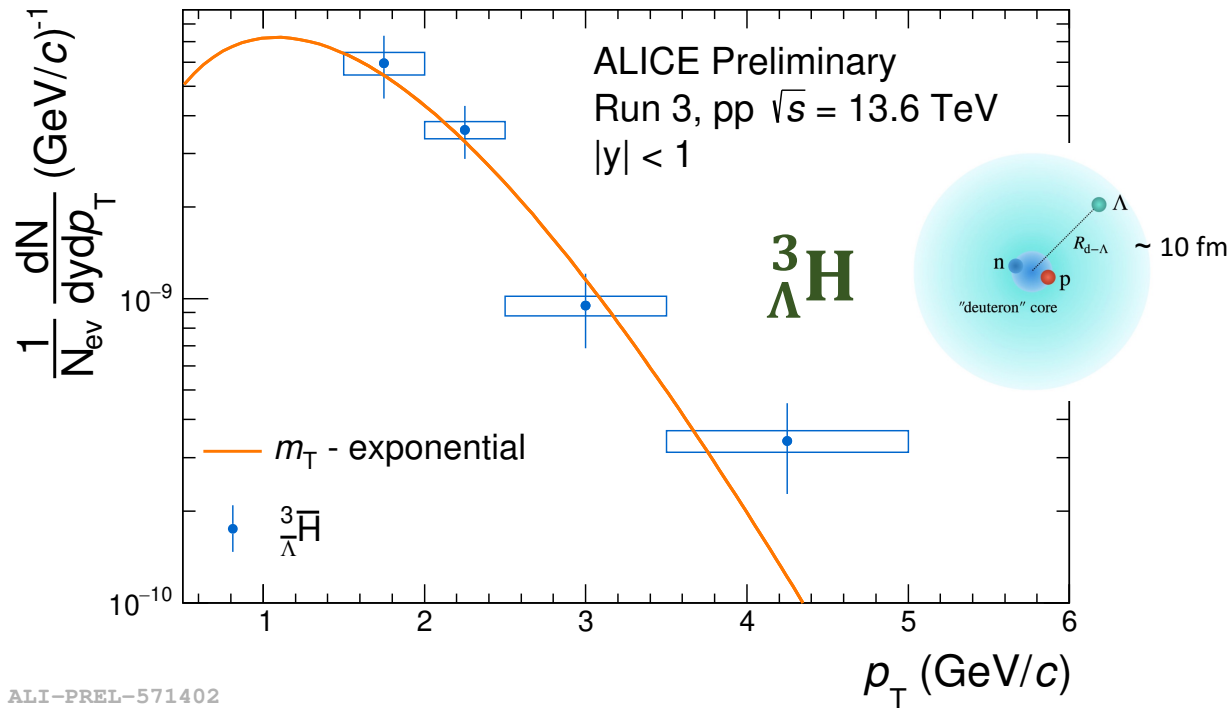
- Measurements of yields of nuclei with A=3 challenge the models
- Neither of the CSM models or **coalescence** predictions reproduce the trend of the ratios, but qualitatively reproduce the overall yields
- As for  $d/\pi$  and  $d/p$  ratios, **CSM-II** at high multiplicity catches the decreasing trend

# Testing production models with hypertriton



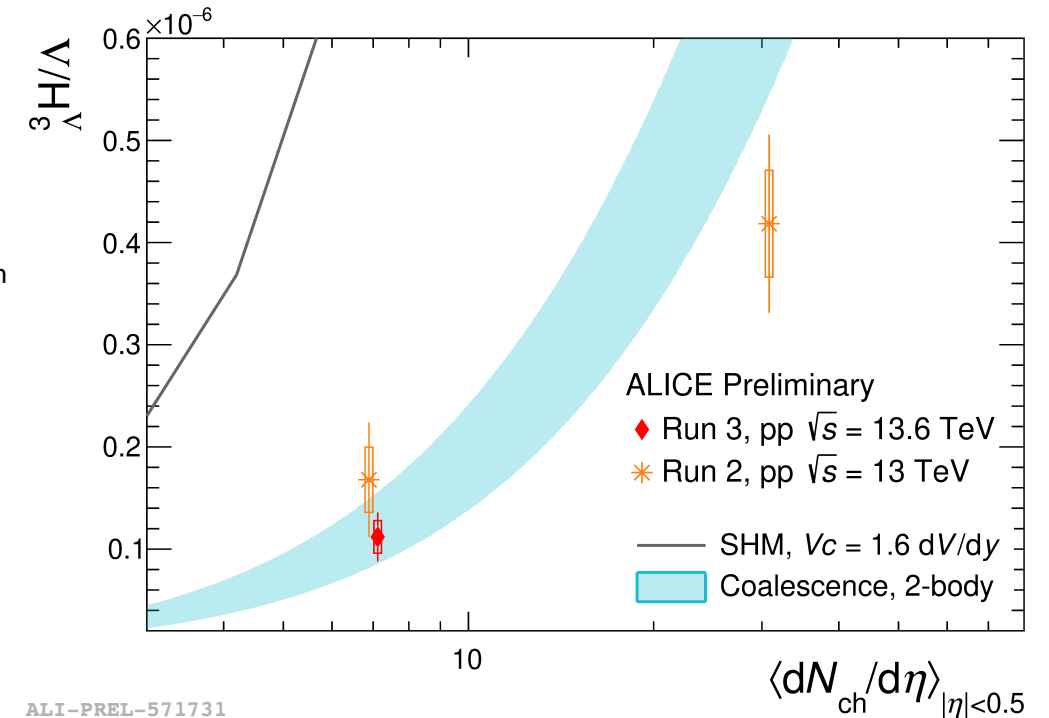
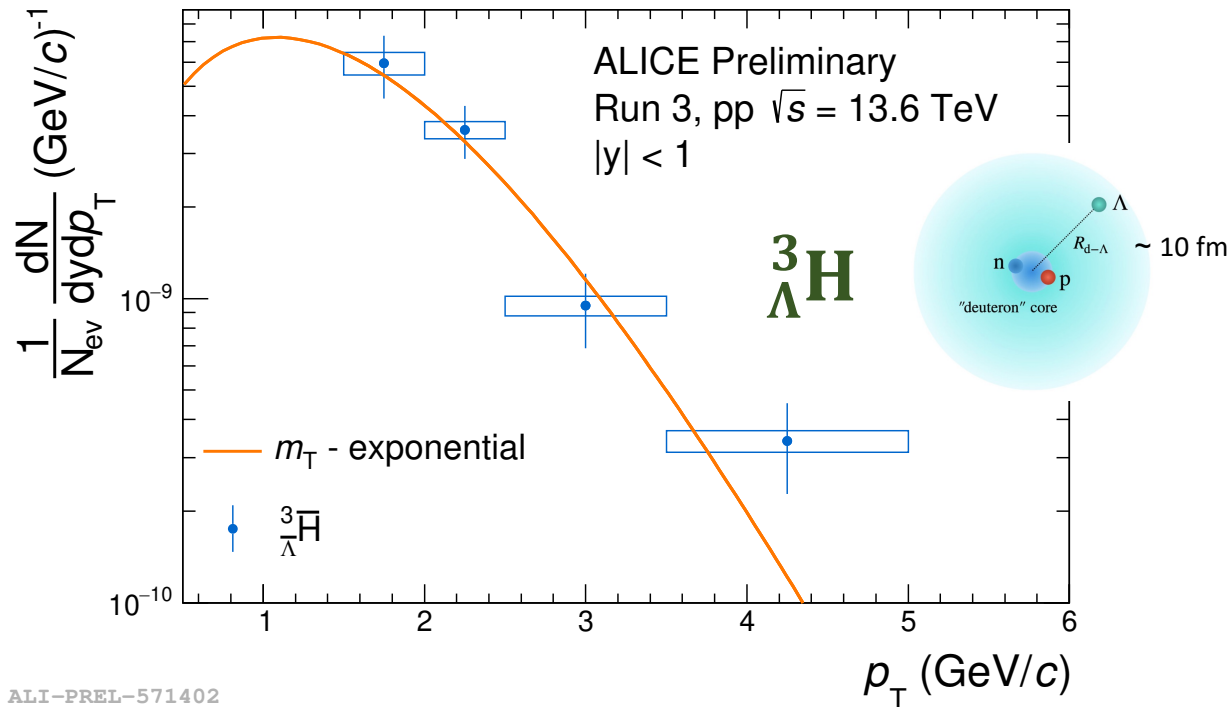


# Testing production models with hypertriton



- In small collision systems (as pp) size of system created in the collision is smaller or equal to that of the nucleus under study
- Coalescence is sensitive to the **interplay** between the **size of the collision system** and the spatial extension of the **nucleus wave function**

# Testing production models with hypertriton



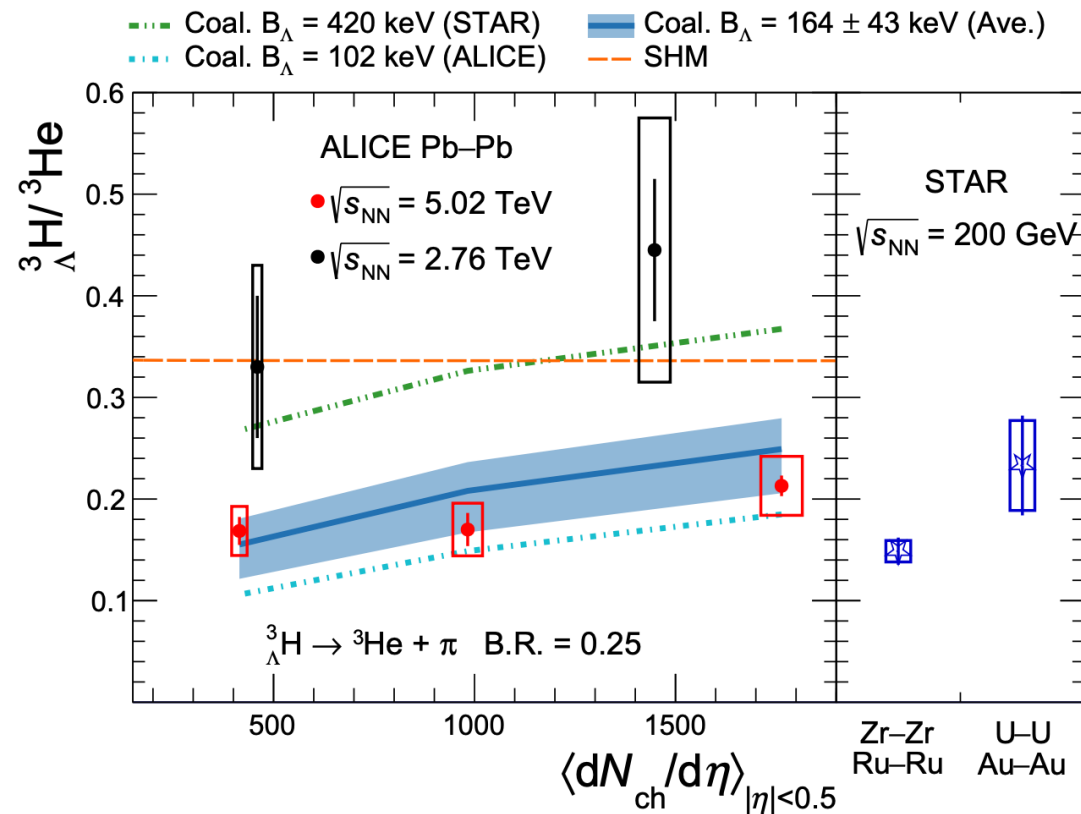
- In small collision systems (as pp) size of system created in the collision is smaller or equal to that of the nucleus under study
- Coalescence is sensitive to the **interplay** between the **size of the collision system** and the spatial extension of the **nucleus wave function**
- $\frac{^3\text{H}}{\Lambda}$  ratio provides a powerful tool to investigate nuclear production mechanism → For small systems model **predictions are quite different**

# Hypertriton in Pb—Pb: test of production models

- ${}^3_{\Lambda}\text{H}/{}^3\text{He}$  ratio allows for testing the production models

vs.  $\langle dN_{\text{ch}}/d\eta \rangle_{|\eta|<0.5}$

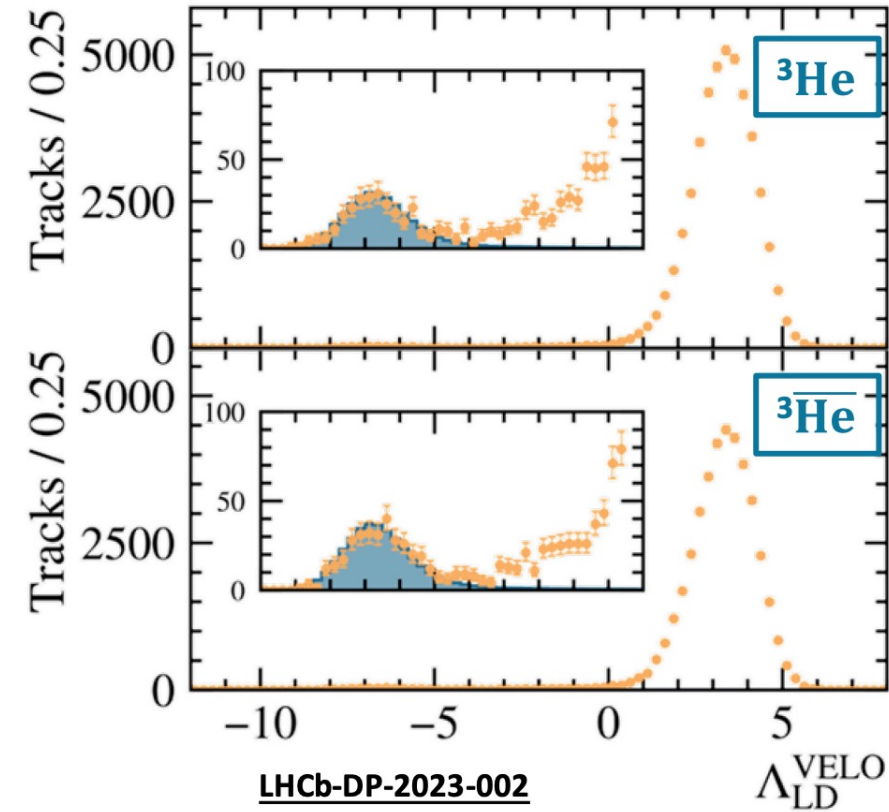
- **SHM** predicts a flat ratio: sensitive to their similar masses ( $m_{{}^3_{\Lambda}\text{H}}=2.991$  and  $m_{{}^3\text{He}}=2.809$  GeV/ $c^2$ ), but insensitive to their size [ $r_{{}^3\text{He}}$ : 1.76 fm,  $r_{{}^3_{\Lambda}\text{H}}(\text{np}\Lambda)$ : 4.9 fm ( $B_{\Lambda}=2.35$  MeV),  $r_{{}^3_{\Lambda}\text{H}}(\text{d}\Lambda)$ : 10 fm ( $B_{\Lambda}\sim 0.13$  MeV)]
- **coalescence**  $\rightarrow$  interplay between the spatial extension of the nucleus wavefunction and the system size
- better agreement with coalescence



# Identification of ${}^3\text{He}$ and ${}^3_{\Lambda}\text{H}$ at LHCb

- Bethe-Bloch:  $Z=2$  particles deposits  $\sim 4$  times the energy of  $Z=1$  particles  
→ **He**: higher ADC counts and wider cluster size

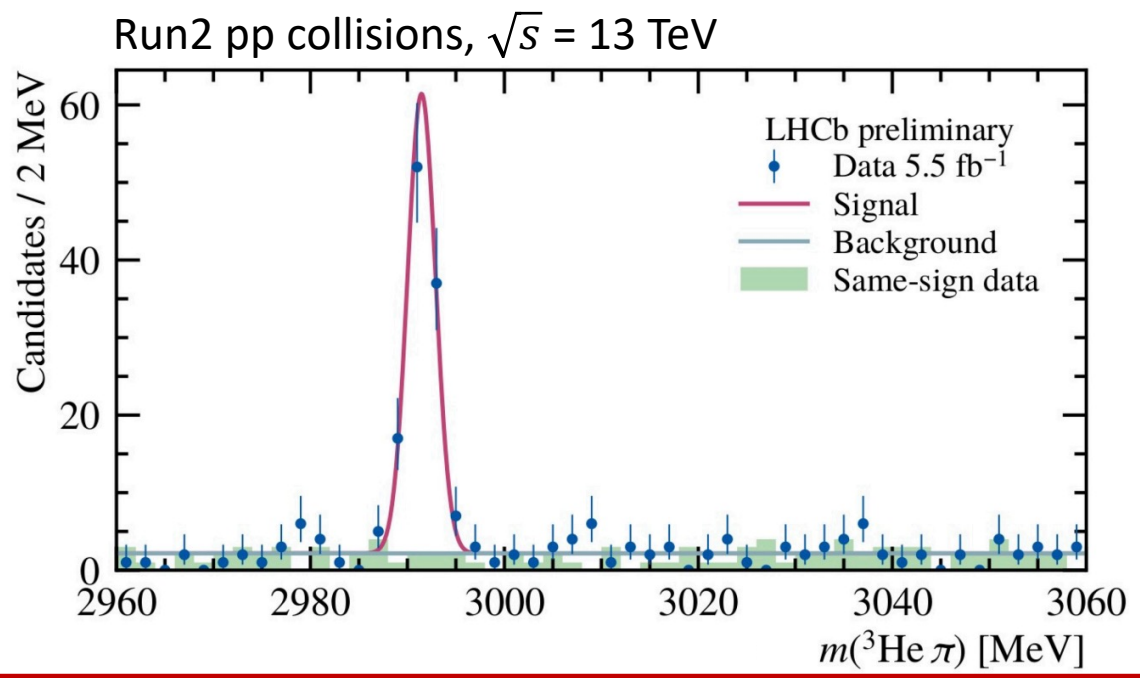
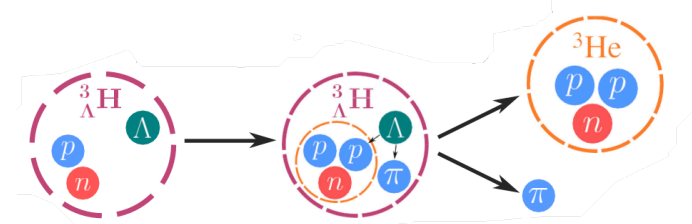
**First (anti-)Helium candidates  
observed in  $pp$  in LHCb data!**



# Identification of ${}^3\text{He}$ and ${}^3_\Lambda\text{H}$ at LHCb

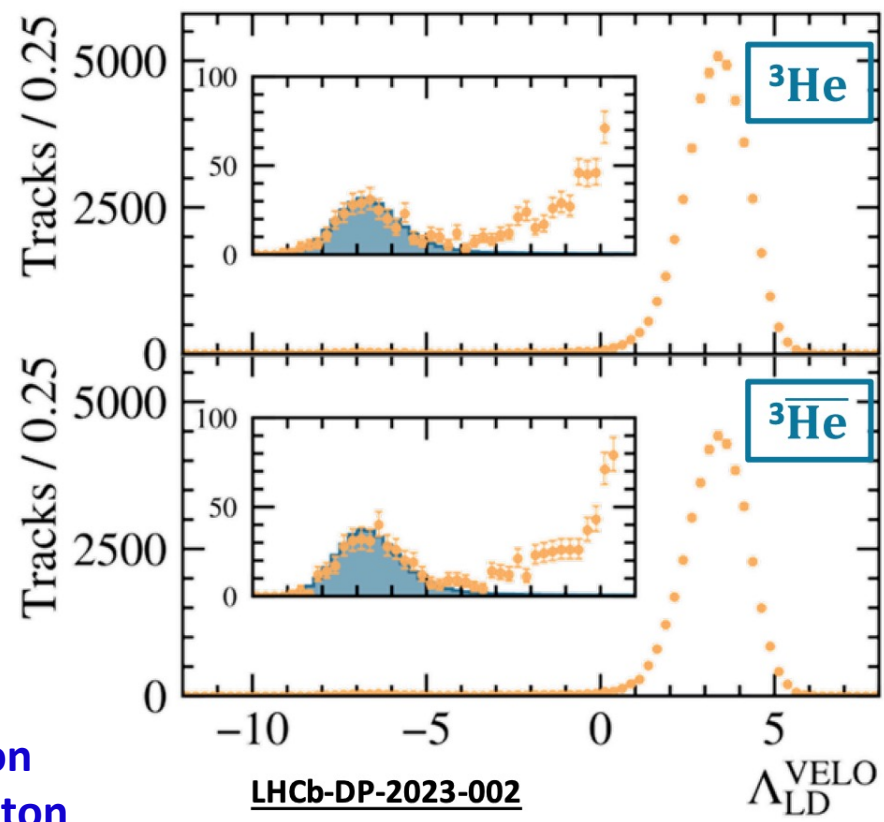
- Bethe-Bloch:  $Z=2$  particles deposits  $\sim 4$  times the energy of  $Z=1$  particles  
 $\rightarrow$  **He**: higher ADC counts and wider cluster size
- Application of  ${}^3\text{He}$  identification:
- Reconstruction of hypertriton** through the 2-body mesonic decay

$${}^3_\Lambda\text{H} \rightarrow {}^3\text{He} + \pi^- \text{ and c.c.}$$



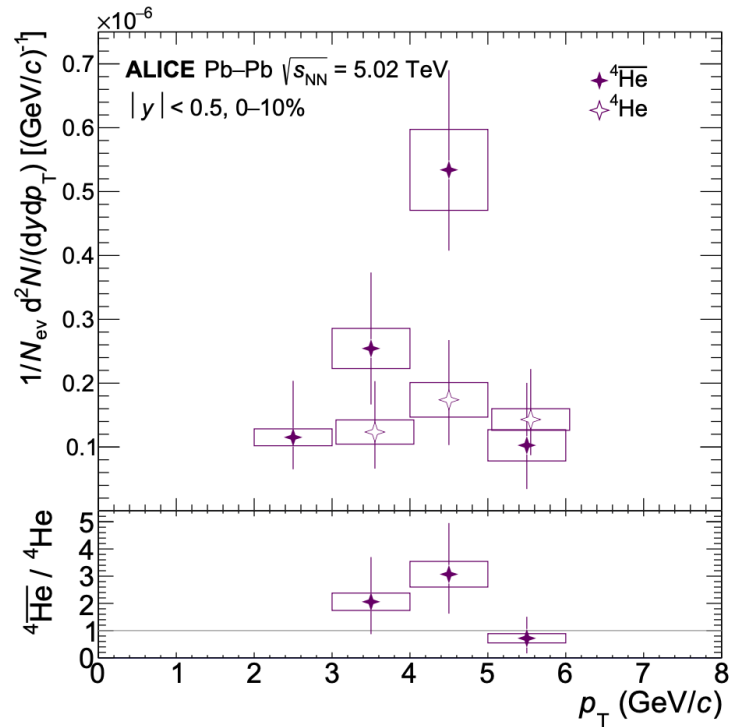
Yields:  
 **$61 \pm 8$  Hypertriton**  
 **$46 \pm 7$  antihypertriton**  
 Statistical mass precision  
**0.16 MeV**

**First (anti-)Helium candidates observed in  $pp$  in LHCb data!**



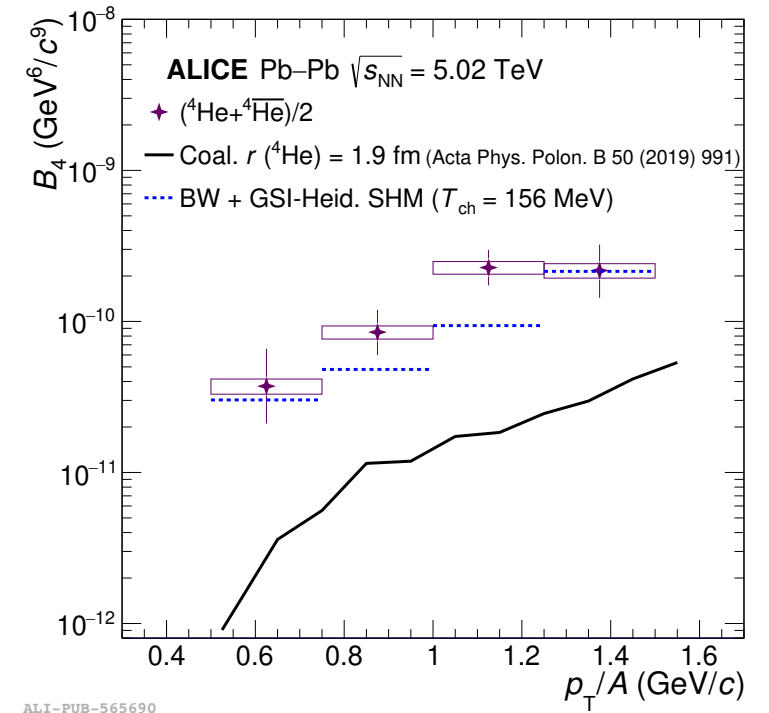
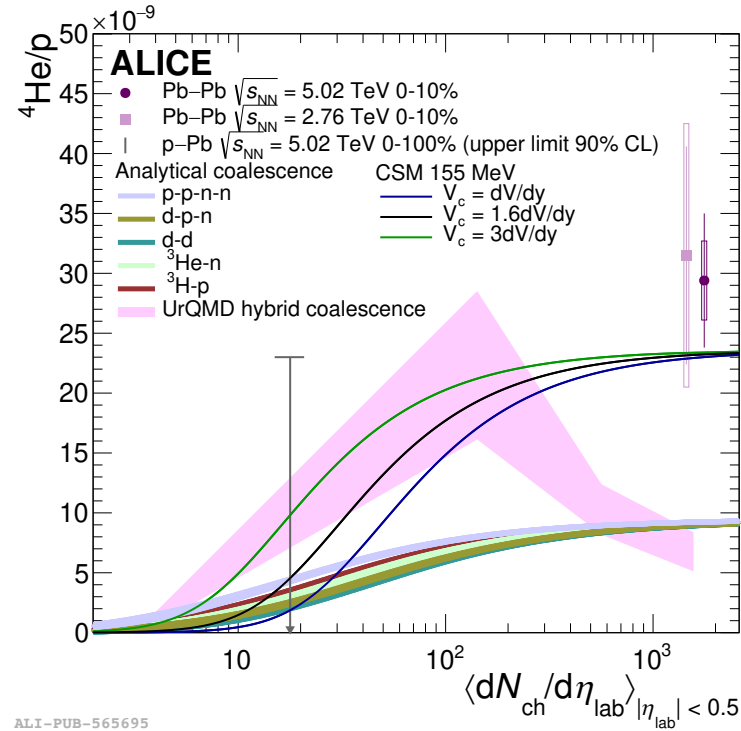
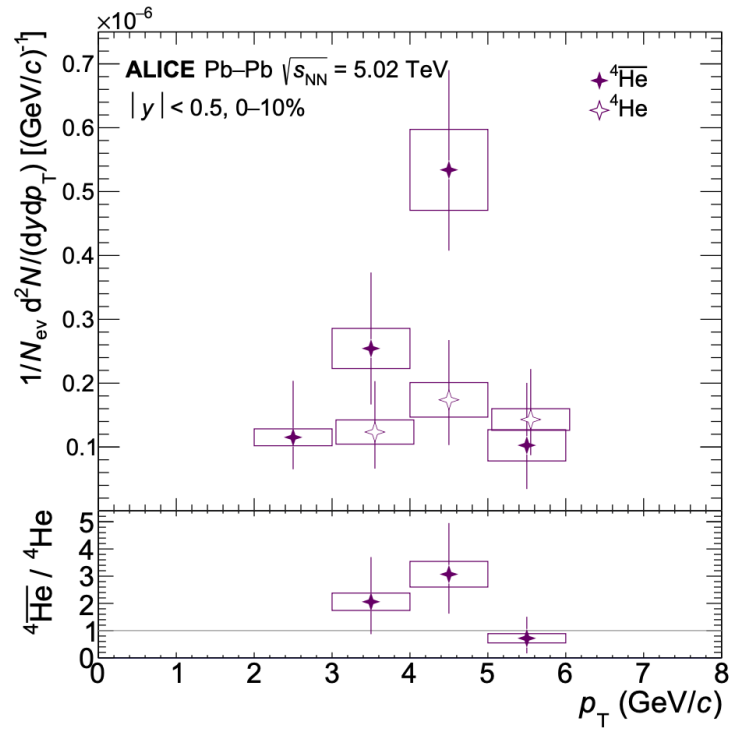


# Measurement of A=4 nuclei in Pb—Pb



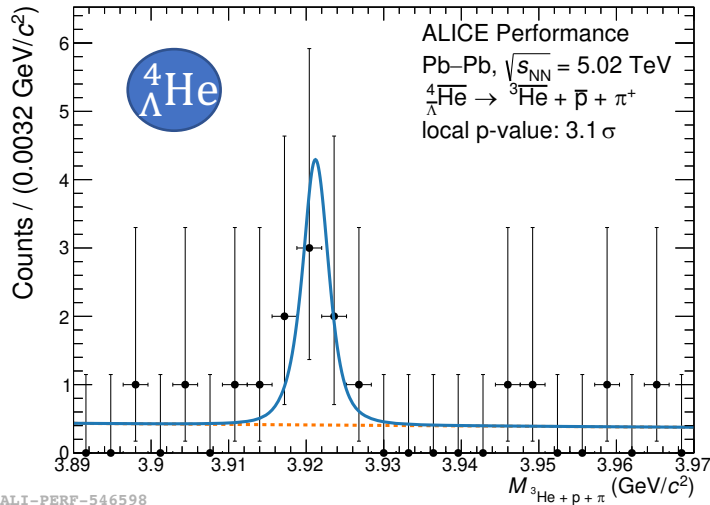
- $^4He$  is very compact and more bound than lighter nuclei:  $E_B \sim 28$  MeV,  $r \sim 1.7$  fm

# Measurement of A=4 nuclei in Pb—Pb

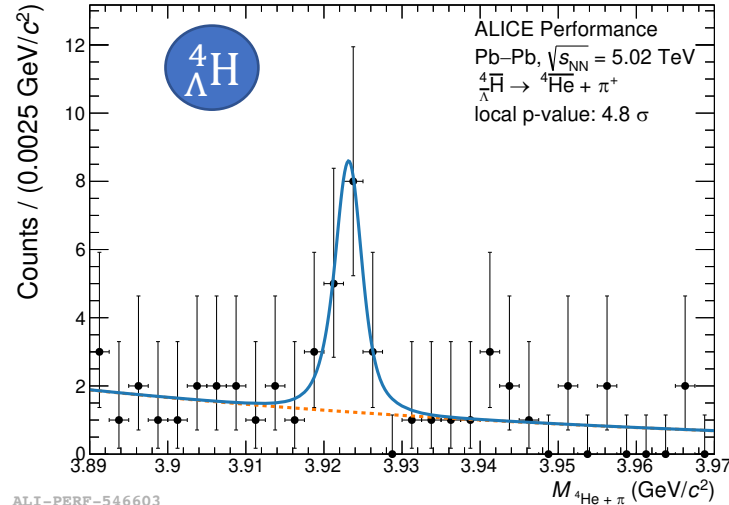


- $^4\text{He}$  is very compact and more bound than lighter nuclei:  $E_B \sim 28$  MeV,  $r \sim 1.7$  fm
- $^4\text{He}/p$  ratio &  $B_4$  in agreement with SHM, but the only available measurements are from Pb—Pb collisions  $\rightarrow$  data needed at intermediate multiplicity where models differ
- Blast Wave using common parameters with the other nuclei describes  $B_4$

# Hypernuclei in the A=4 sector

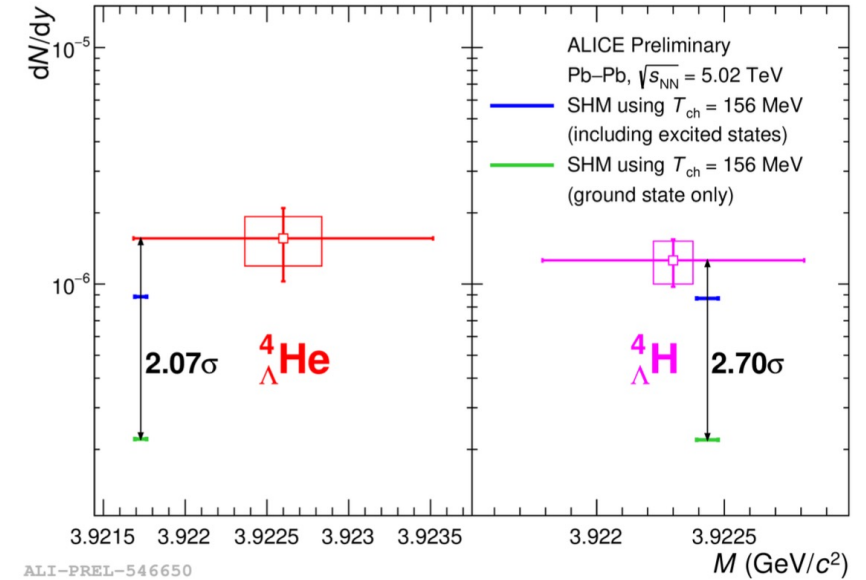


ALI-PERF-546598



ALI-PERF-546603

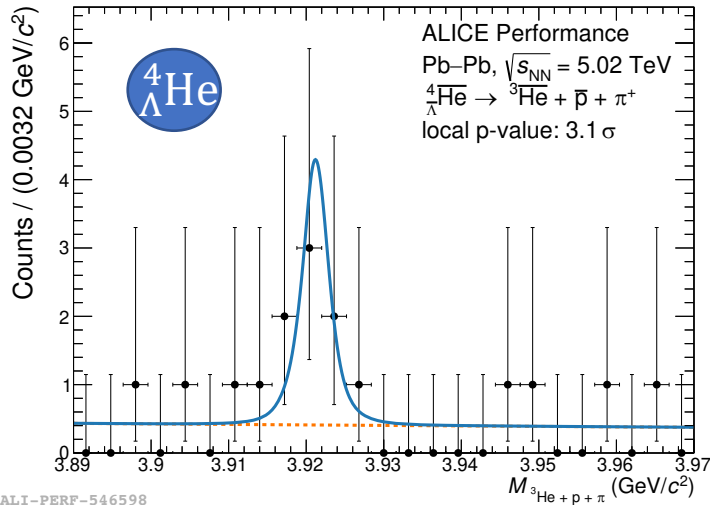
**Pb—Pb**



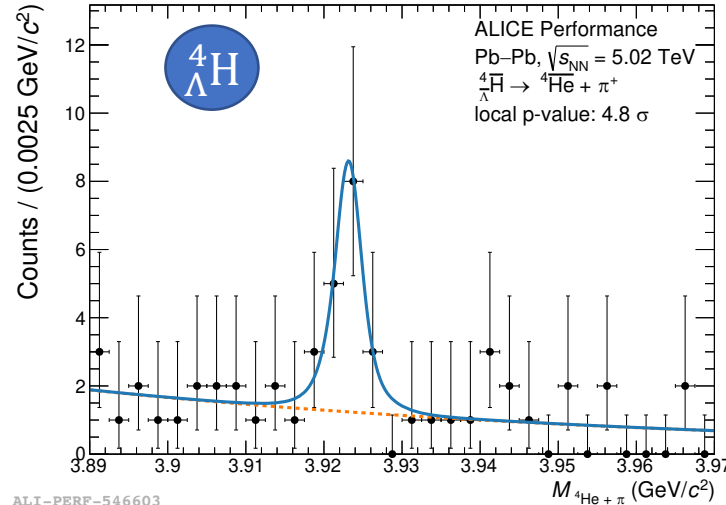
ALI-PREL-546650

- First ever observation of anti- ${}^4_{\Lambda}\text{He}$ !
  - **Hypernuclei with A=4** in Pb-Pb collisions are compared to predictions of SHM
    - penalty factor  $\sim 300$  from  ${}^4_{\Lambda}\text{He}$  to  ${}^4_{\Lambda}\text{H}$  due to strangeness content
  - But their yield may be enhanced due to larger binding energy wrt A=3 & existence of excited states (spin degeneracy)
- Measured yields in **agreement** with the presence of **excited states**

# Hypernuclei in the A=4 sector

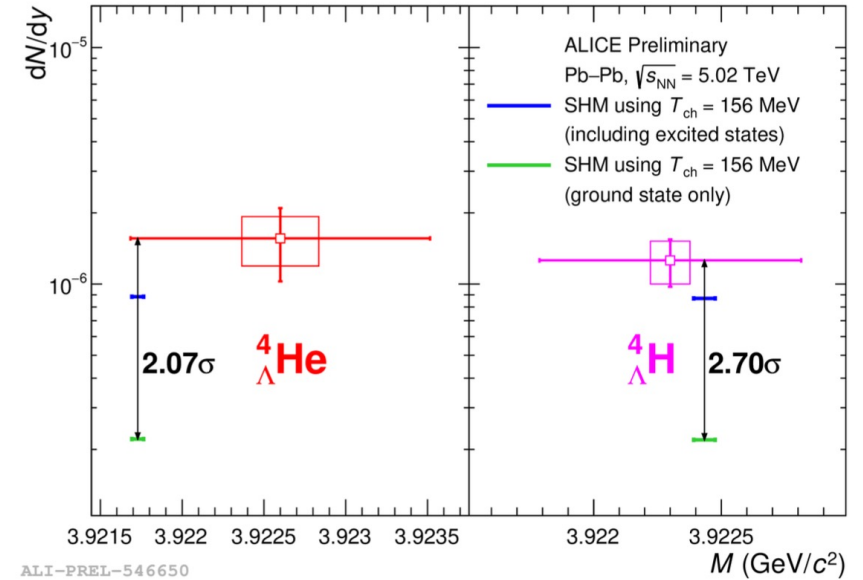


ALI-PERF-546598



ALI-PERF-546603

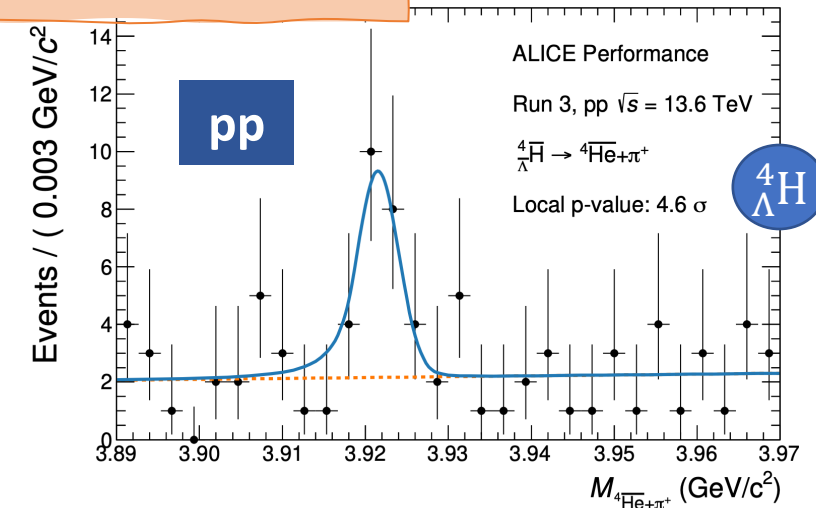
**Pb—Pb**



ALI-PREL-546650

*More to come with LHC Run3 data!*

- First ever observation of anti- ${}^4_{\Lambda}\text{He}$ !
  - **Hypernuclei with A=4** in Pb-Pb collisions are compared to predictions of SHM
    - penalty factor  $\sim 300$  from  ${}^4_{\Lambda}\text{He}$  to  ${}^4_{\Lambda}\text{H}$  due to strangeness content
  - But their yield may be enhanced due to larger binding energy wrt A=3 & existence of excited states (spin degeneracy)
- Measured yields in **agreement** with the presence of **excited states**



ALI-PERF-546499

**pp**

**${}^4_{\Lambda}\text{H}$**

- Measurements of the production of (anti)(hyper)nuclei is fundamental to investigate the **hadronization mechanism**
- The models on the market describe **different aspects** of the production but none of them can describe all observations, at all multiplicities and at all collision energies
- We have **many observables** that have significantly **different model predictions** → powerful probes to distinguish among the models
- Now the **experimental challenge** is to get **precision measurements** to finally close the debate

- Measurements of the production of (anti)(hyper)nuclei is fundamental to investigate the **hadronization mechanism**
- The models on the market describe **different aspects** of the production but none of them can describe all observations, at all multiplicities and at all collision energies
- We have **many observables** that have significantly **different model predictions** → powerful probes to distinguish among the models
- Now the **experimental challenge** is to get **precision measurements** to finally close the debate
- Other powerful tools to distinguish among the models, not covered in this talk, are the  ${}^3\text{He}/{}^3\text{H}$  ratio vs  $p_T$ ,  ${}^3\text{H}/{}^3\text{He}$  ratio vs  $p_T$ , elliptic flow  $v_2$  of nuclei and hypernuclei, nuclei in and out of jets,  ${}^3\text{H}\cdot p/d^2$  ratio vs  $dN_{ch}/d\eta$  etc...

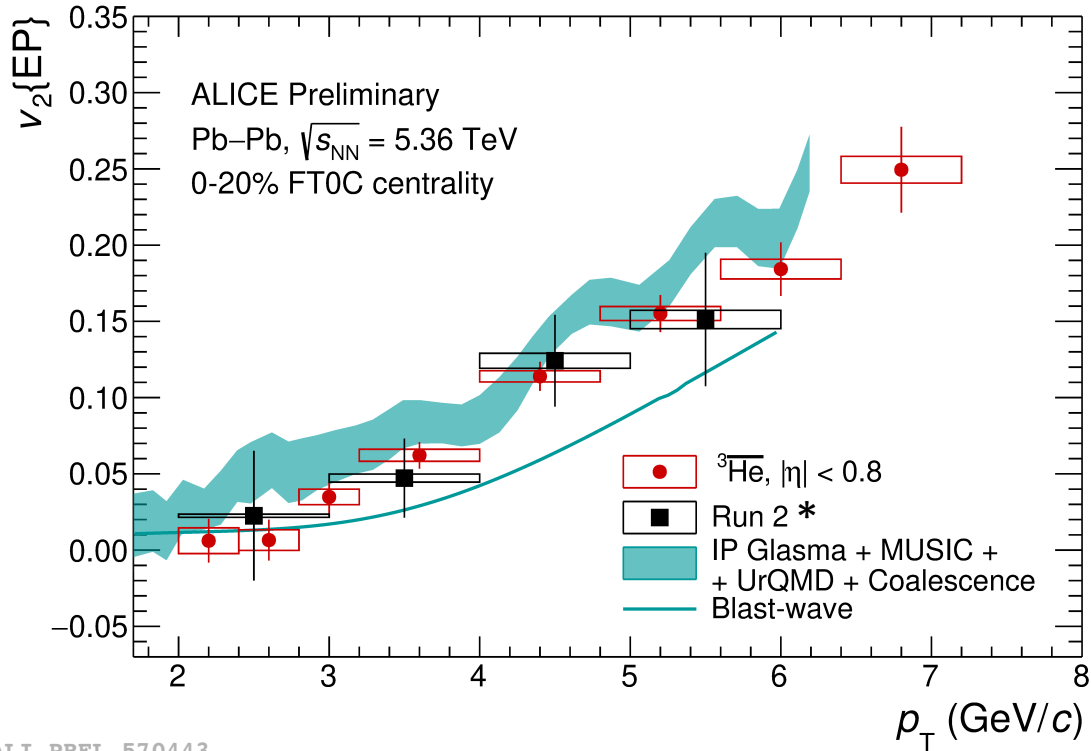


- Measurements of the production of (anti)(hyper)nuclei is fundamental to investigate the **hadronization mechanism**
- The models on the market describe **different aspects** of the production but none of them can describe all observations, at all multiplicities and at all collision energies
- We have **many observables** that have significantly **different model predictions** → powerful probes to distinguish among the models
- Now the **experimental challenge** is to get **precision measurements** to finally close the debate
- Other powerful tools to distinguish among the models, not covered in this talk, are the  ${}^3\text{He}/{}^3\text{H}$  ratio vs  $p_T$ ,  ${}^3\text{H}/{}^3\text{He}$  ratio vs  $p_T$ , elliptic flow  $v_2$  of nuclei and hypernuclei, nuclei in and out of jets,  ${}^3\text{H}\cdot p/d^2$  ratio vs  $dN_{\text{ch}}/d\eta$  etc...

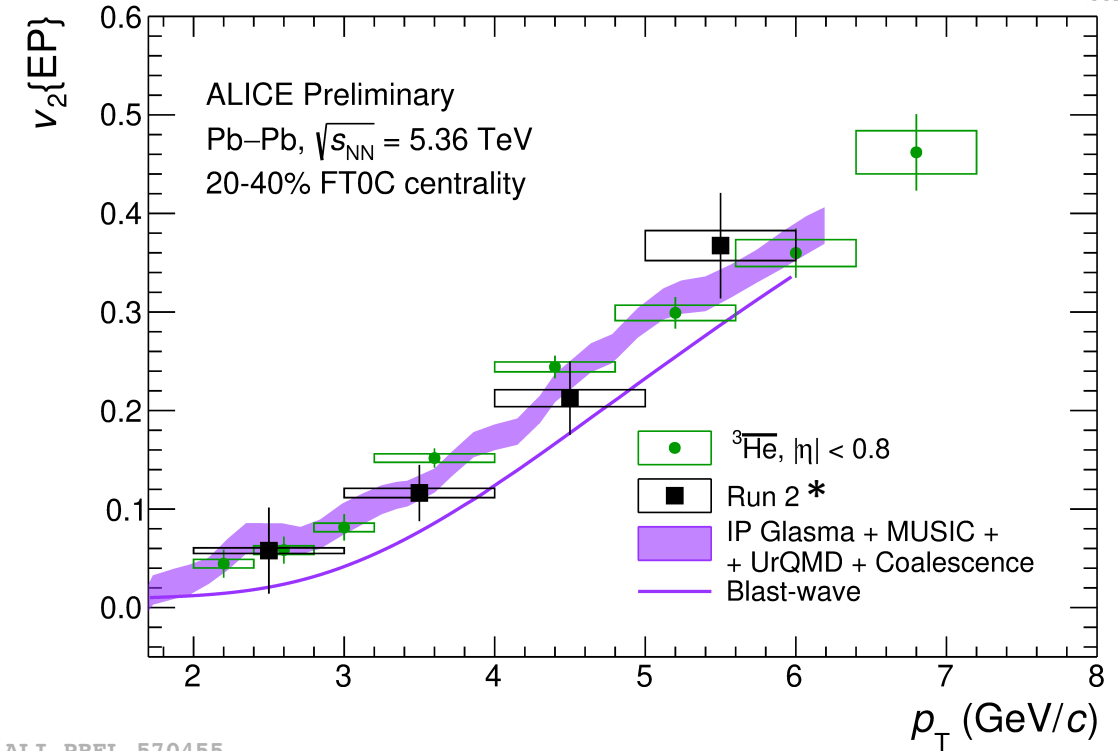
*Thank You...*



# $v_2$ of $^3\text{He}$ : another test of production models



ALI-PREL-570443

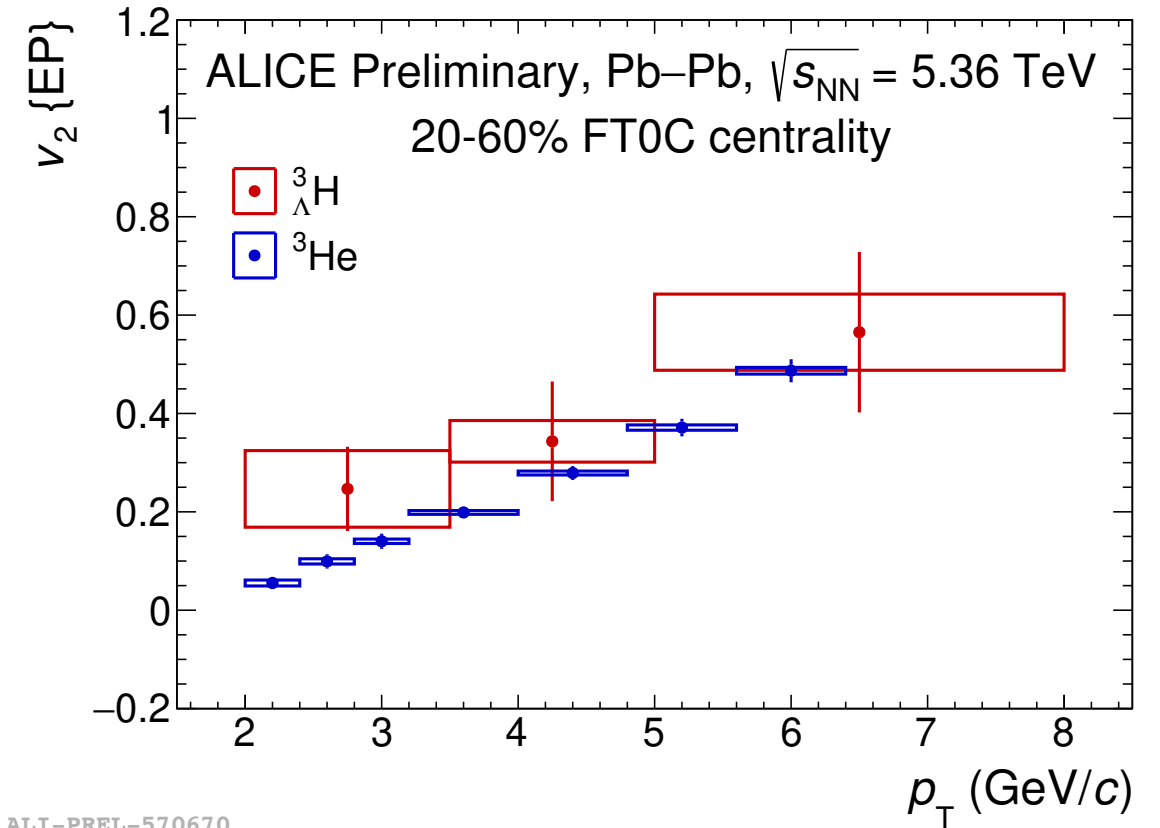
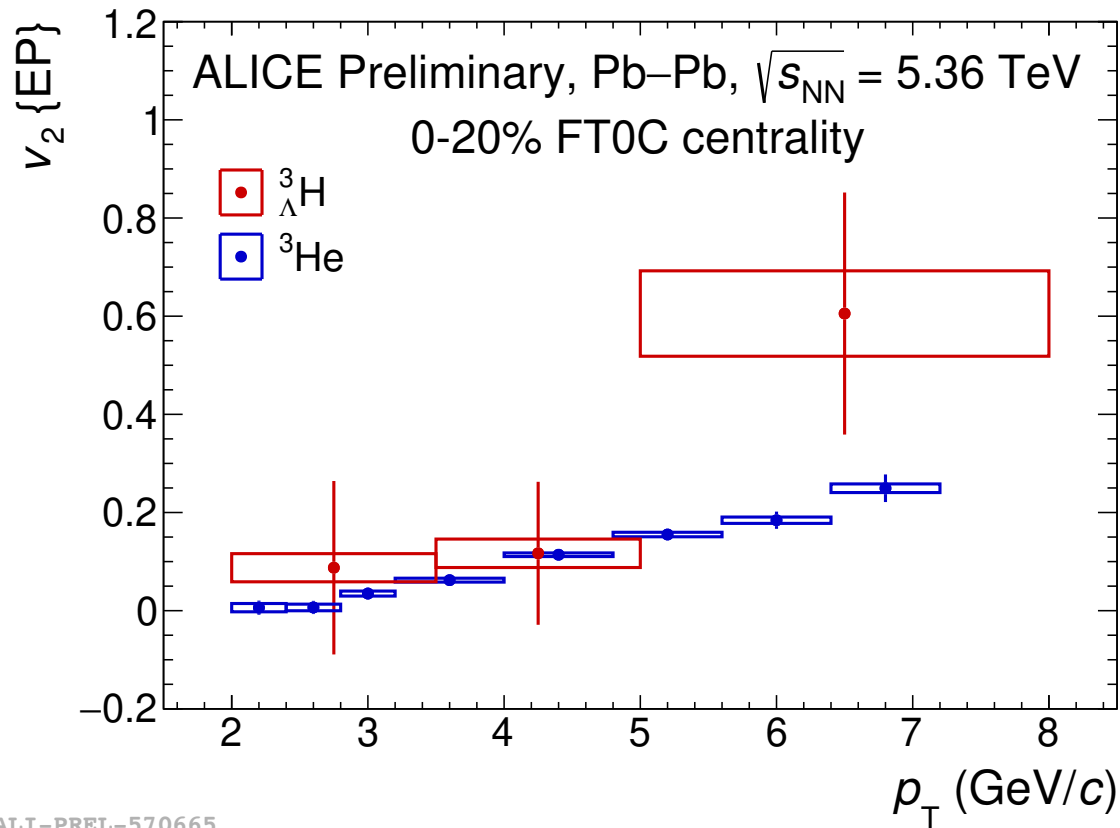


ALI-PREL-570455

- ALICE Run3 statistics seems sensitive to the different production models using the elliptic flow  $v_2$
- **Coalescence** is sensitive to a different production in-plane and out-of-plane
- Data are compared with the predictions of
  - Blast Wave model that uses the fit parameters of pi, K, p
  - coalescence model + hydrodynamics

# Elliptic flow of hypertriton measured by ALICE

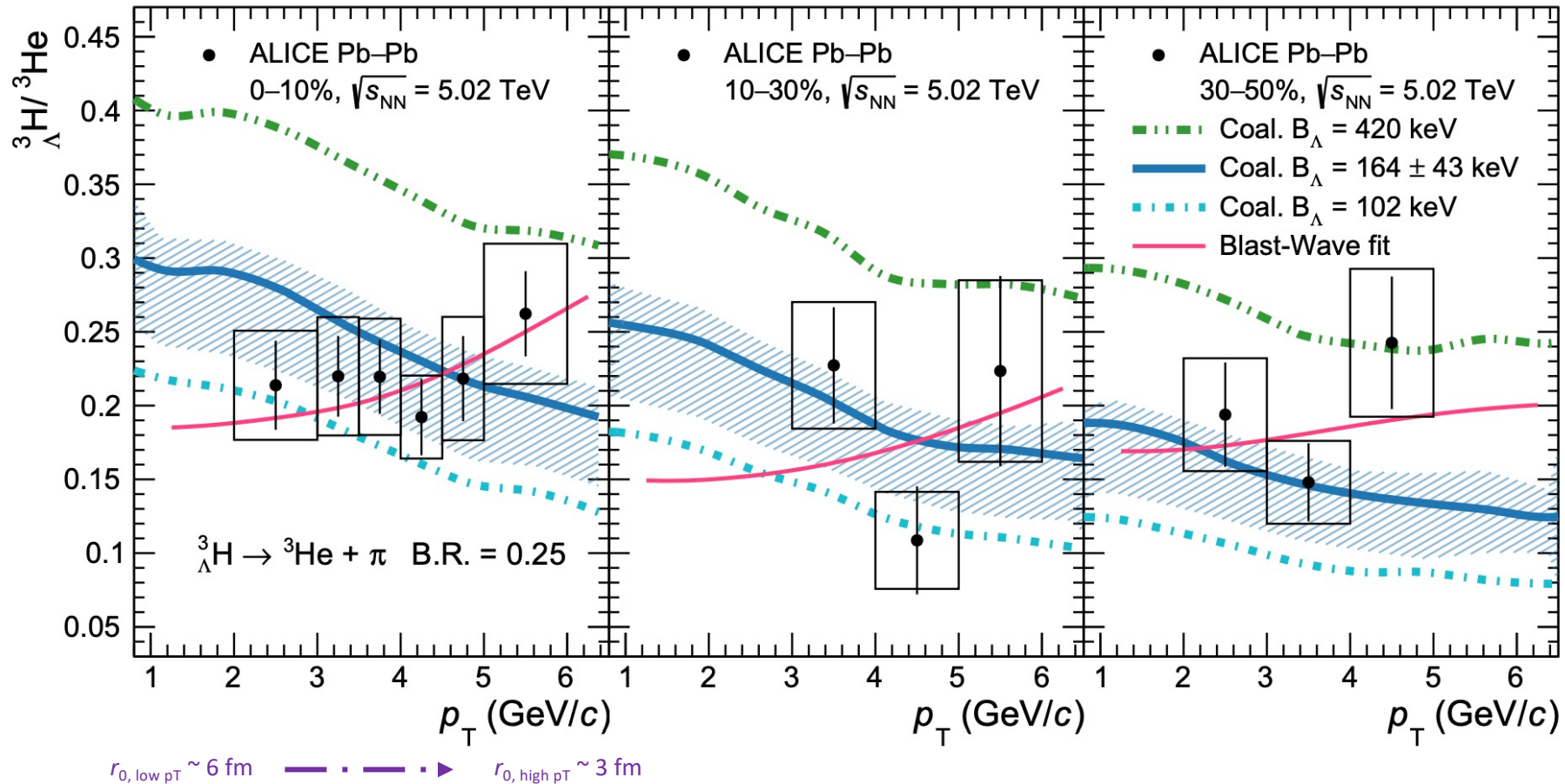
- ALICE delivered the first experimental measurement of hypertriton elliptic flow!
- Compatible with  ${}^3\text{He}$   $v_2$ , due to their similar masses
- Large uncertainties



# Hypertriton in Pb—Pb: test of production models

- ${}^3\text{H}/{}^3\text{He}$  ratio allows for testing the production models

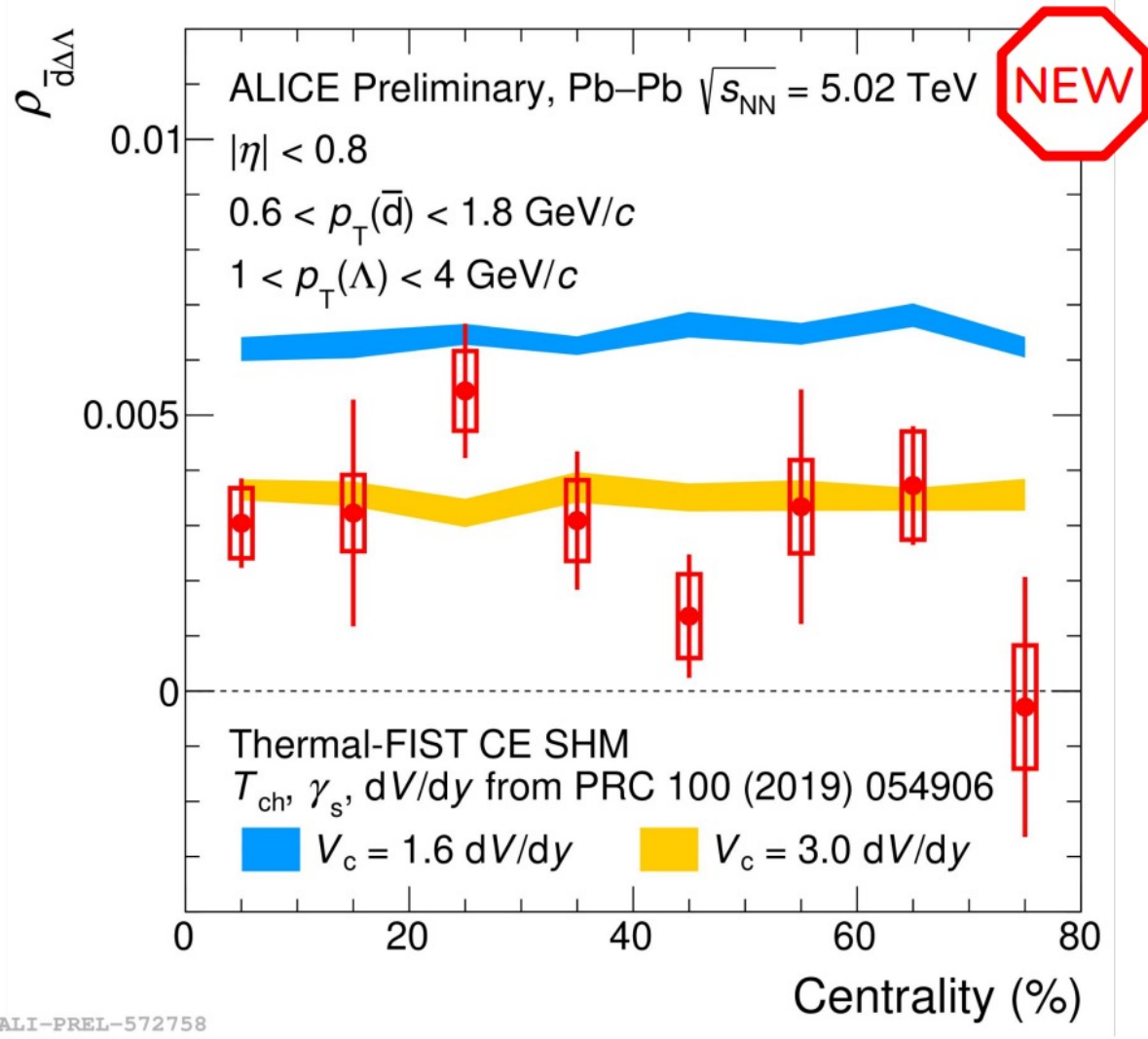
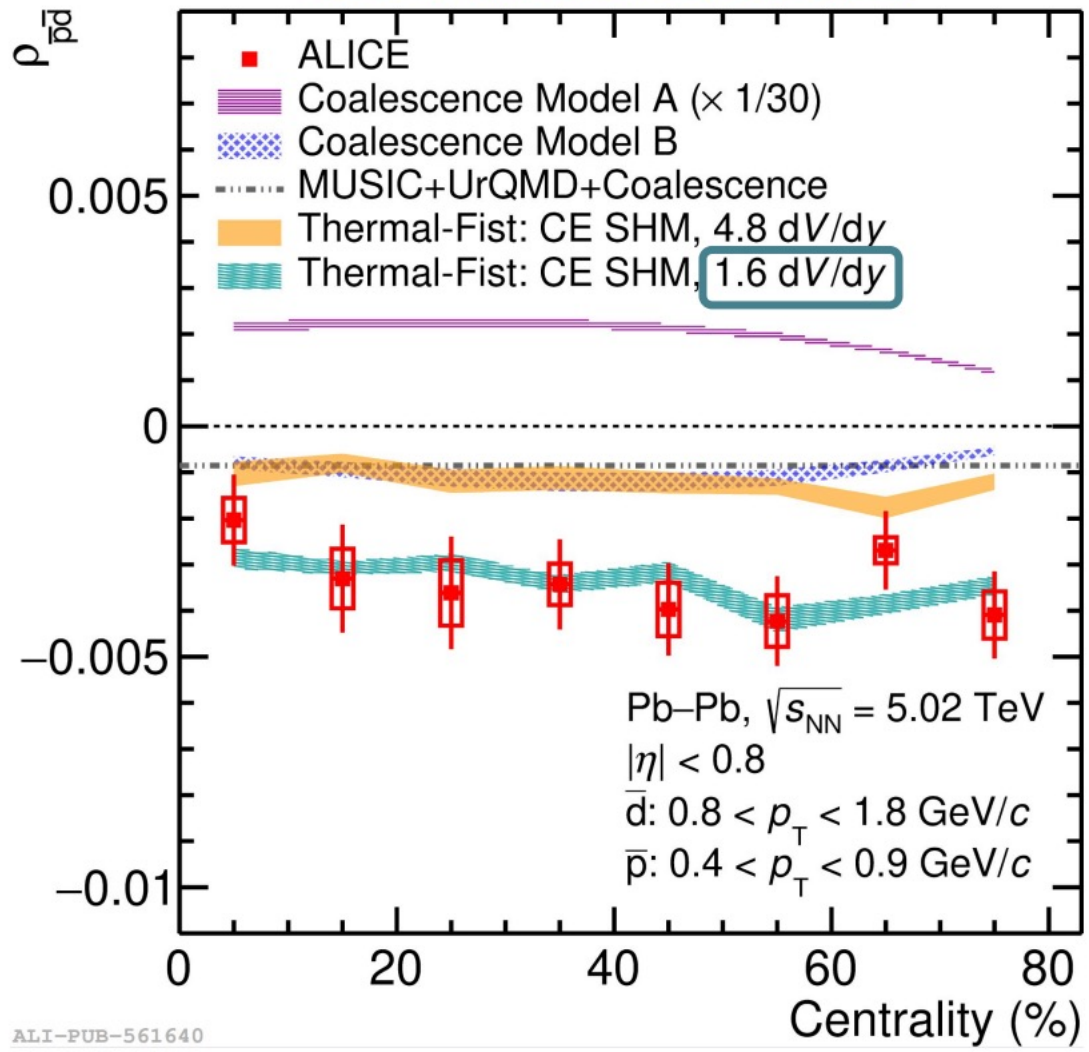
- vs.  $p_T$
- Radial flow picture (Blast-Wave): higher mass states have a harder momentum spectrum
  - Coalescence: at large momentum smaller source radius, hence the state with the larger wave-function will get suppressed



# Event-by-event fluctuations at the LHC



ALICE Coll., Phys. Rev. Lett. 131, 041901 (2023)

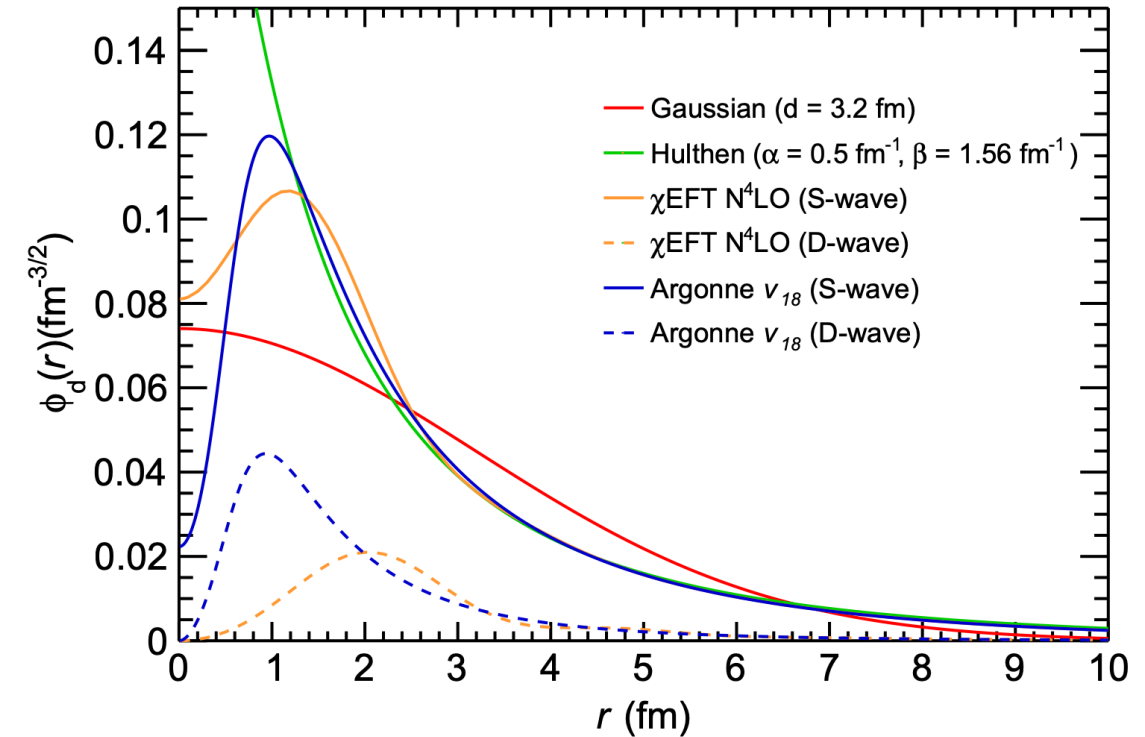
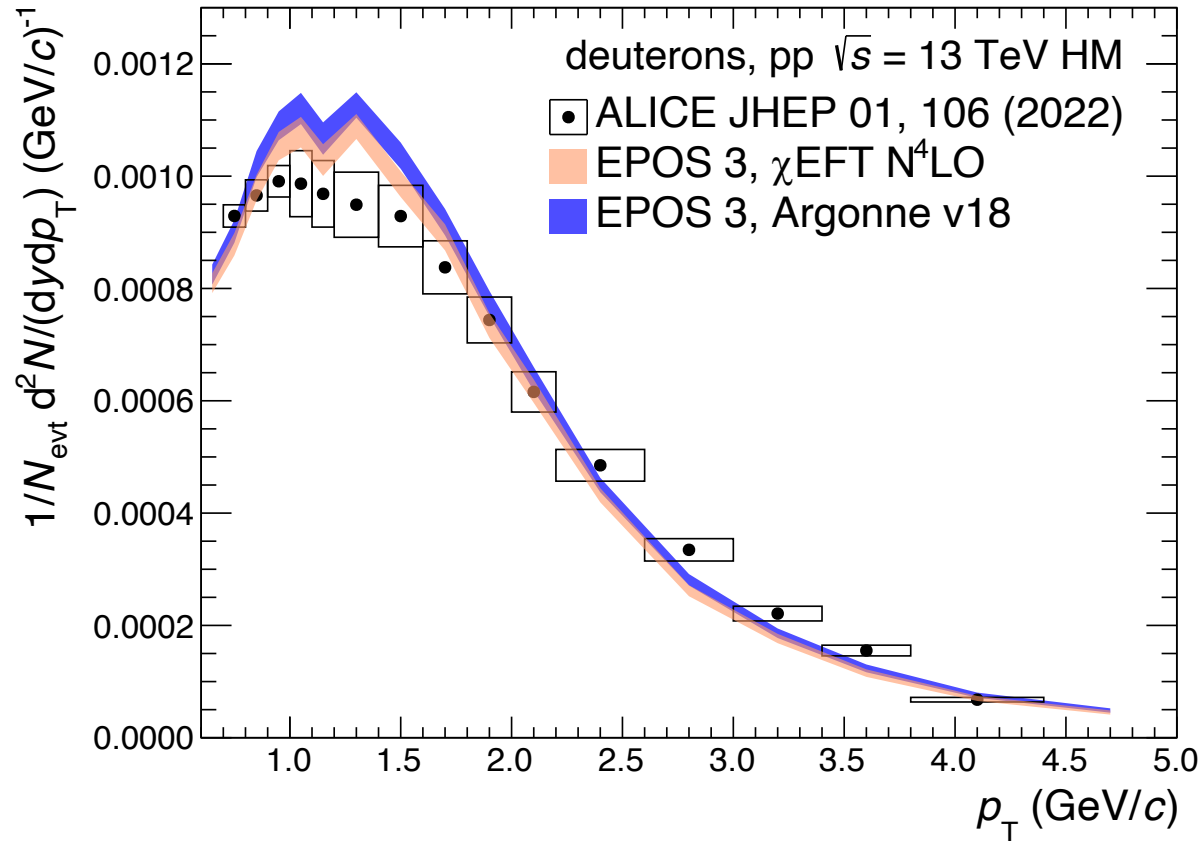




# Testing coalescence model using $B_2$

Difference between the 2 WFs is  $\sim 4\%$

→ Production of deuterons is not affected by the short-range interactions ( $< 2$  fm)



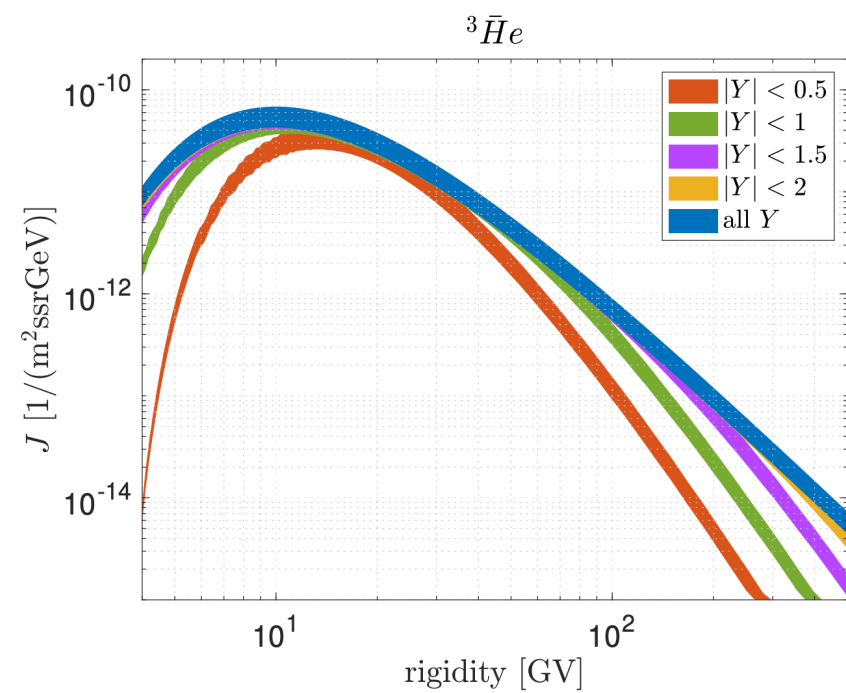
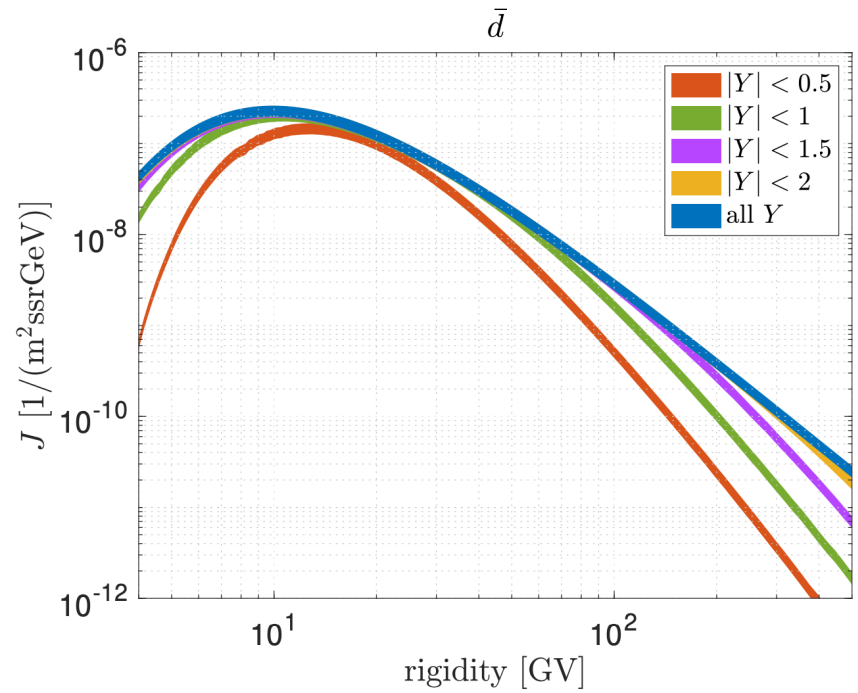
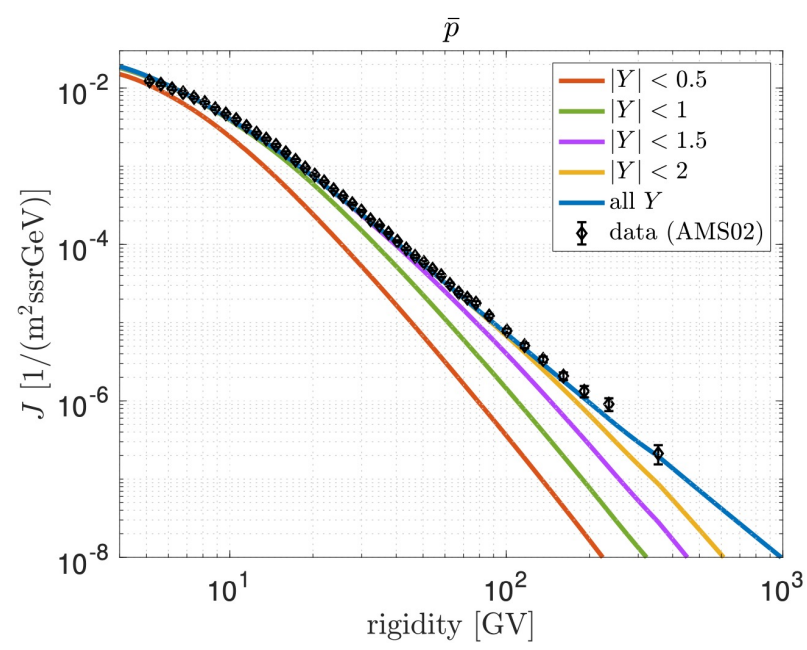
- **Hulthén\***: Favoured by low energy scattering experiments
- **Argonne  $v_{18}$ \*\***: phenomenological potential constrained to p-n scattering
- **$\chi$ EFT**: Favoured by modern nuclear interaction experiments (e.g. Femtoscopy)

\* Scheibl et al., PRC 59 (1999) 1585-1602

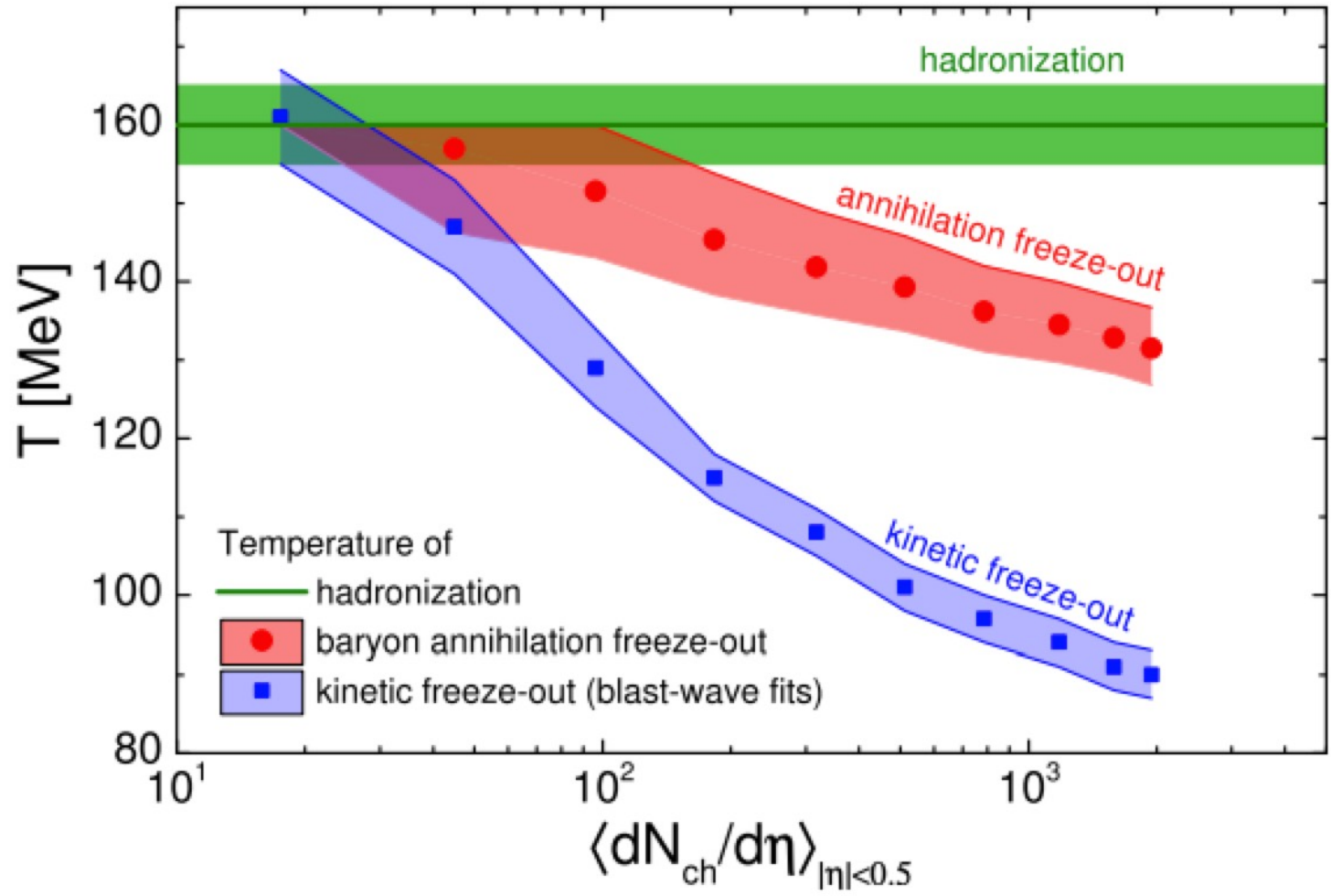
\*\* Wiringa et al., PRC 51 (1995) 38-51

\*\*\* D. R. Entem et al., PRC 96 2 (2017) 024004

# Flux of antinuclei in CRs



K. Blum, [Phys. Rev. D 96, 103021 \(2017\)](https://arxiv.org/abs/1703.02521)  
 K. Blum, [arXiv:2306.13165](https://arxiv.org/abs/2306.13165)  
 M. Aguilar et al. (AMS02 Coll.), [PRL 117, 091103 \(2016\)](https://arxiv.org/abs/1603.04467)



- Correlation volume fixed to 1.6 dV/dy
- Needed to describe the net-deuteron number fluctuations in PbPb collisions.
- Smaller than that of net-proton number fluctuations (3-5)dV/dy
- Temperature of annihilation depends on multiplicity

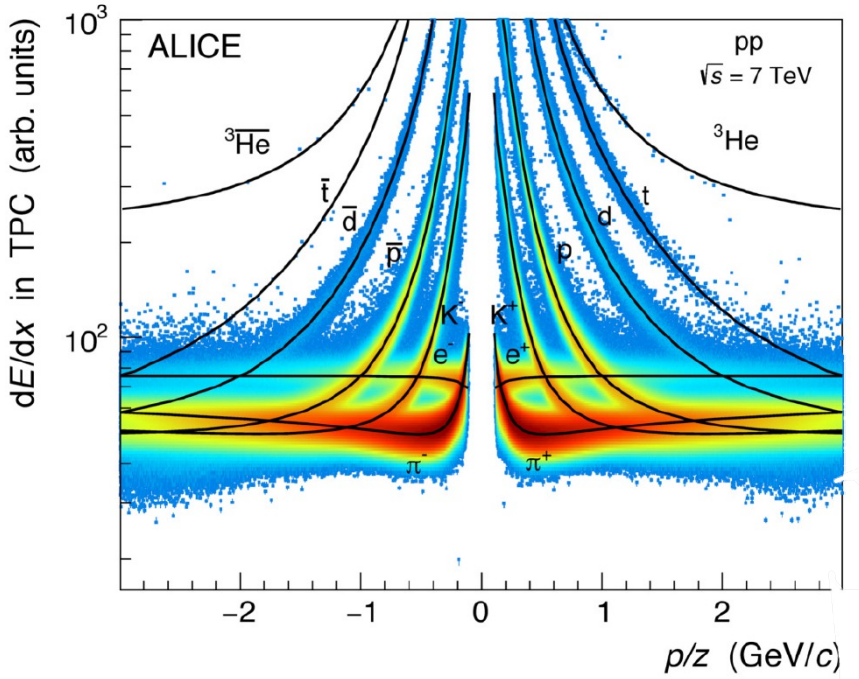
PLB 835, 137577 (2022)

For each multiplicity, the hadronic phase starts with hadronization at 160 MeV and expands in the state of partial chemical equilibrium which includes baryon annihilation reactions to reach chemical equilibrium at annihilation temperature

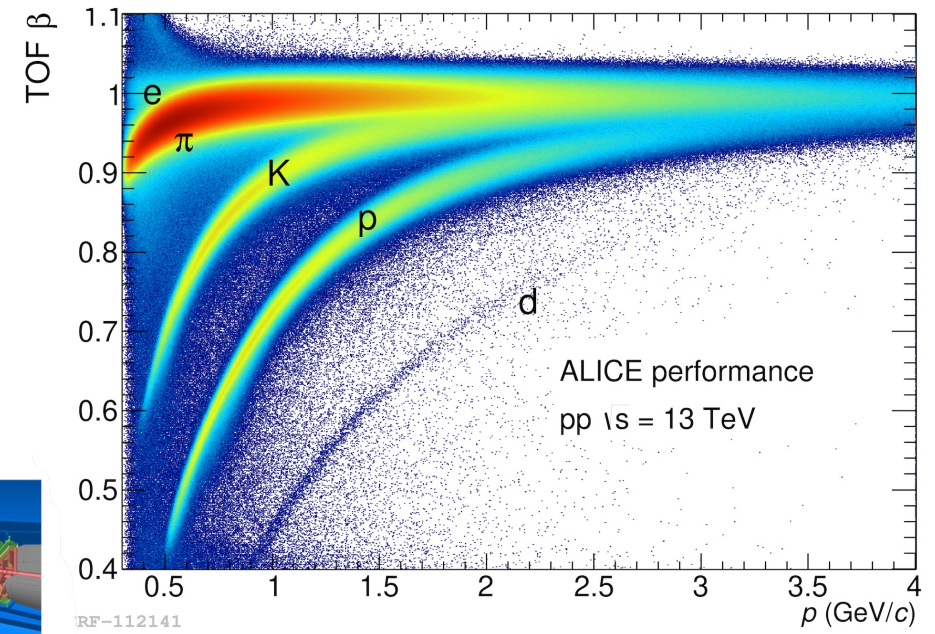


# Identification of nuclei with ALICE

Low  $p$  region (below 1 GeV/c) → PID via  $dE/dx$  measurements in TPC

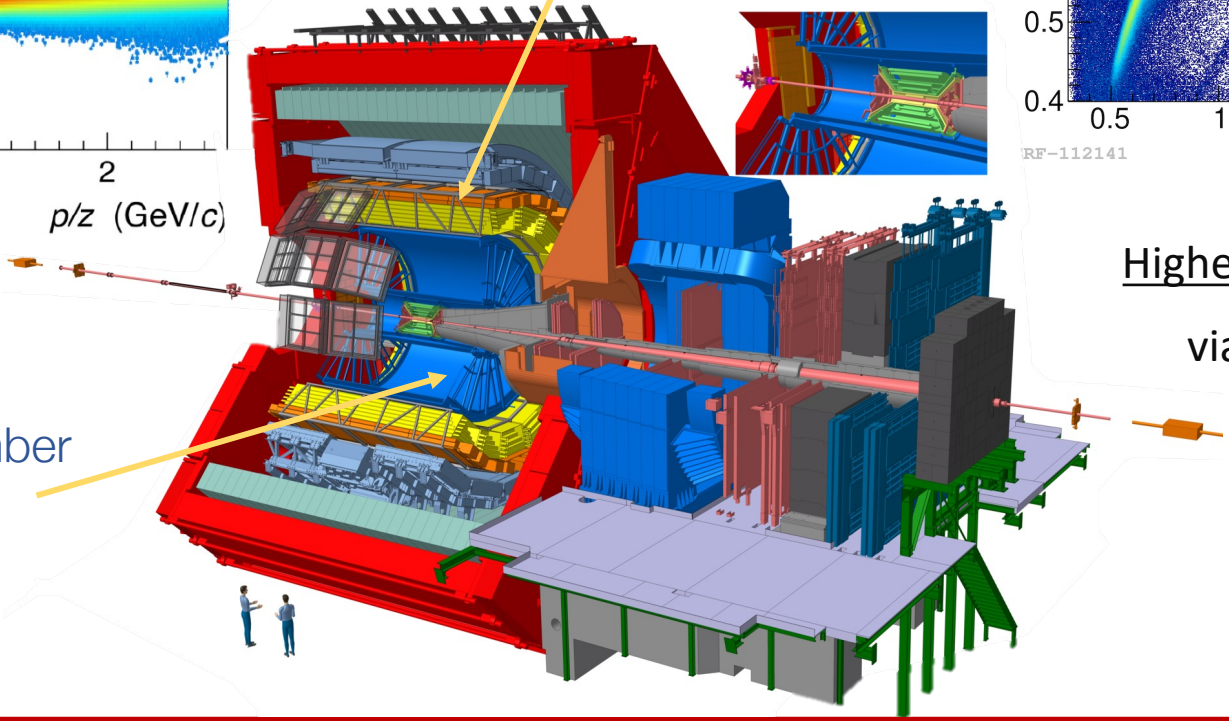


Time Of Flight  
PID via  $\beta$   
 $\sigma_{PID} \sim 70$  ps



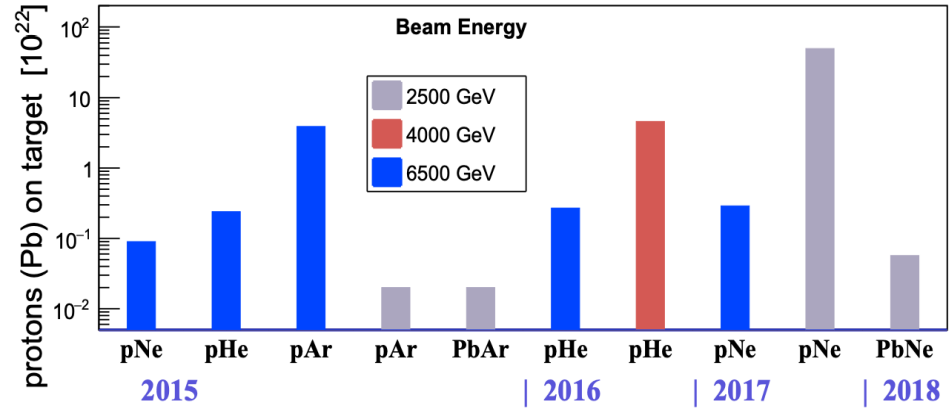
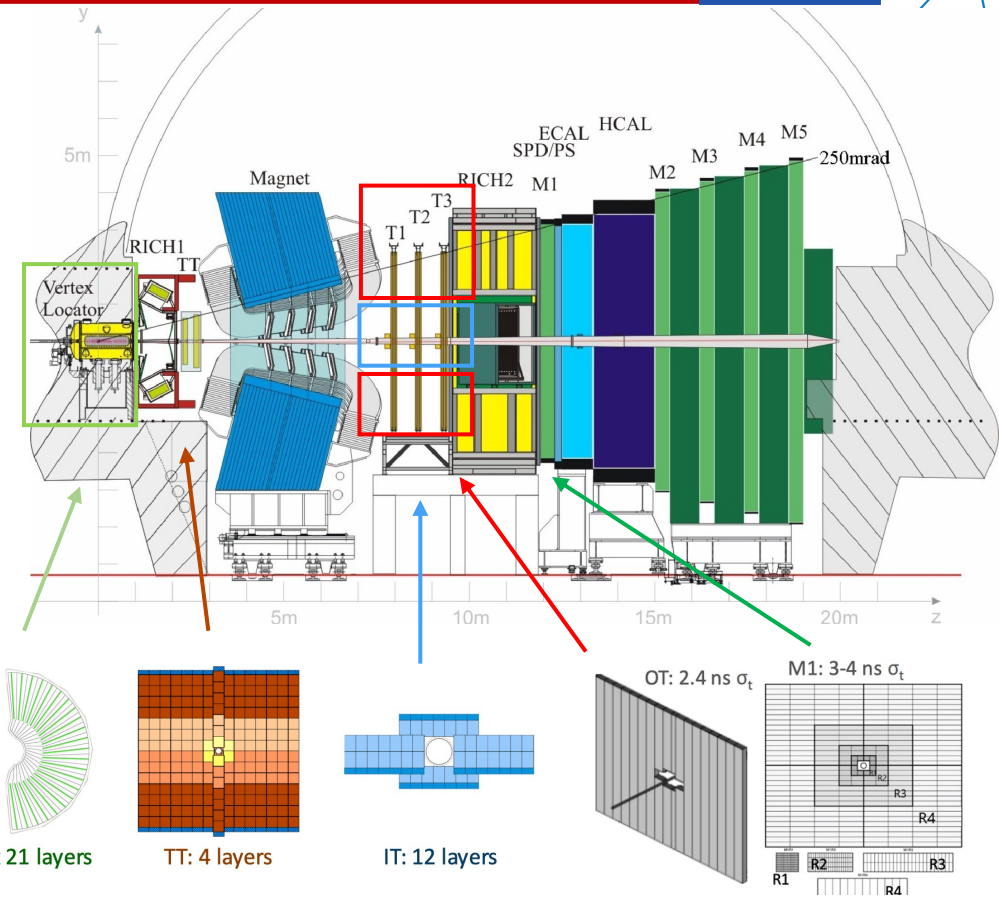
Higher  $p$  region (above 1 GeV/c) → PID via velocity  $\beta$  measurements in TOF

Time Projection Chamber  
tracking, PID via  $dE/dx$   
 $\sigma_{dE/dx} \sim 6\%$



# Identification of nuclei with LHCb

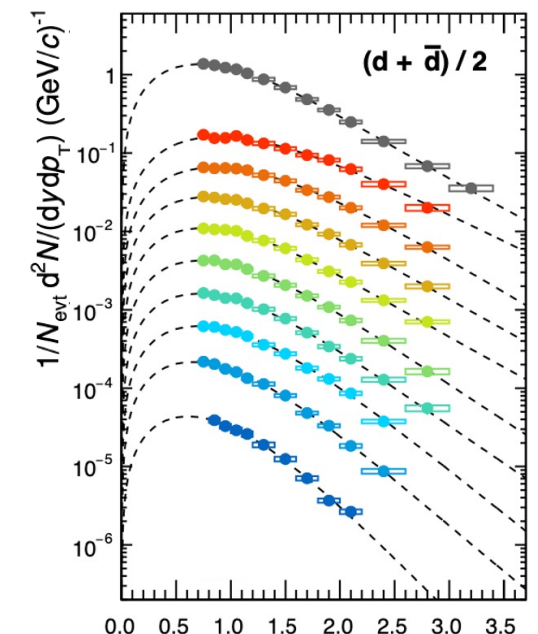
- LHCb detector not initially designed to identify light (anti)nuclei
- Use  $dE/dx \propto Z^2$  from the silicon detectors (VELO, TT, IT)
  - identification of **Helium**, good separation for  $Z \geq 2$
- Time-of-Flight** (OT, M1)  $\rightarrow \beta = \Delta t / L$ 
  - identification of **d**, separation of  $^3\text{He}$ ,  $^4\text{He}$
- With **SMOG** can be used as a fixed-target experiment
- Collect physics samples with different **targets** and different **centre of mass energies**



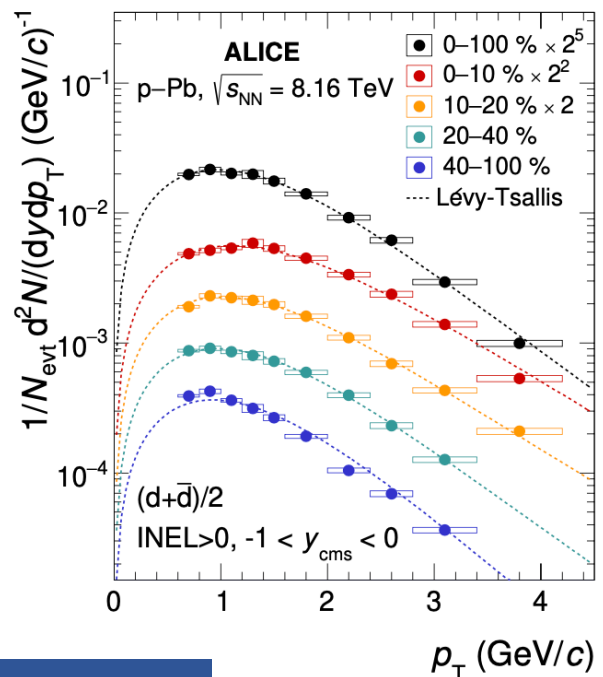
LHCb Collaboration, [JINST 3 S08005 \(2008\)](#)

- Energy range  $\sqrt{s_{NN}} \in [30, 115]$  GeV for beam energy in  $[0.45, 7]$  TeV  $\rightarrow$  Unexplored gap between SPS and LHC/RHIC

# Measurement of (anti)nuclei with A=2

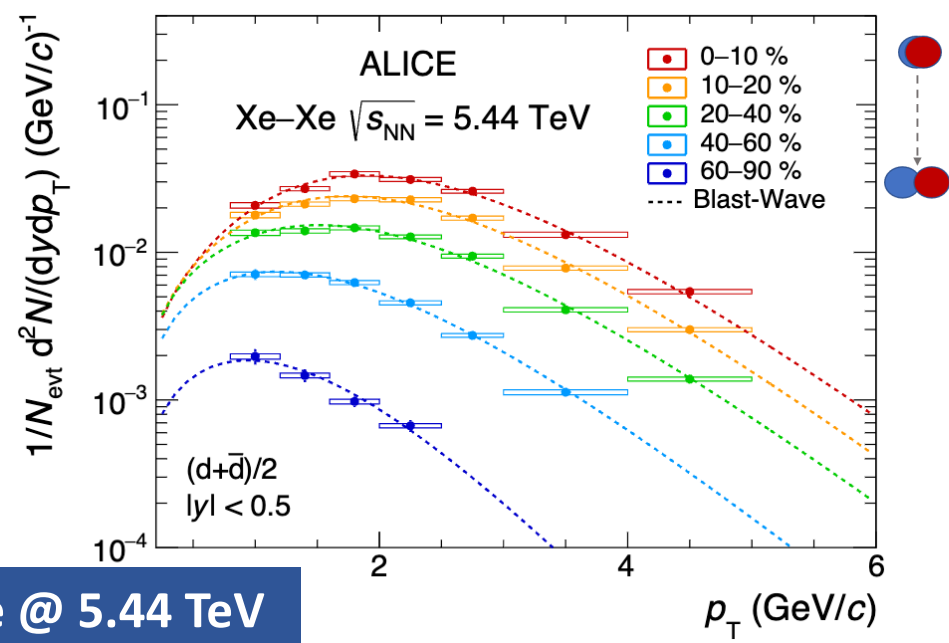


pp @ 5.02 TeV



p-Pb @ 8.16 TeV

- Deuterons have been measured in narrow multiplicity classes in all systems, from pp to heavy-ions
- Momentum distributions fitted to extrapolate the yield in the unmeasured regions

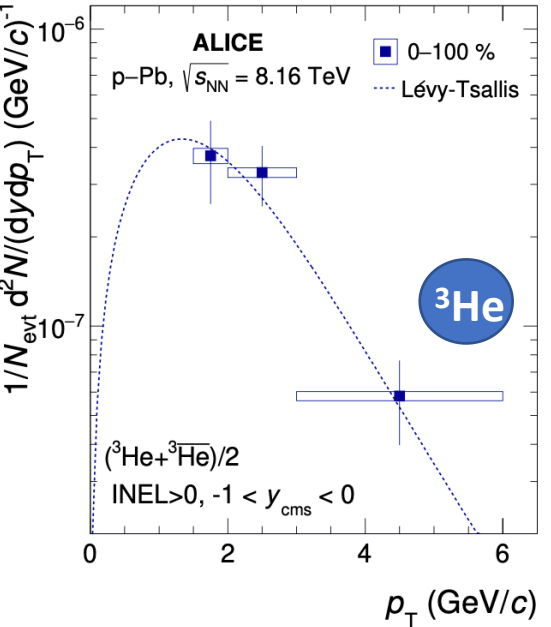


Xe-Xe @ 5.44 TeV

pp: ALICE Collaboration, EPJC (2022) 82:289  
 p-Pb: ALICE Collaboration, PLB 846 (2023) 137795  
 Xe-Xe: ALICE Collaboration, [arXiv:2405.19826](https://arxiv.org/abs/2405.19826)  
 Pb-Pb: ALICE Collaboration, [arXiv:2311.11758](https://arxiv.org/abs/2311.11758)

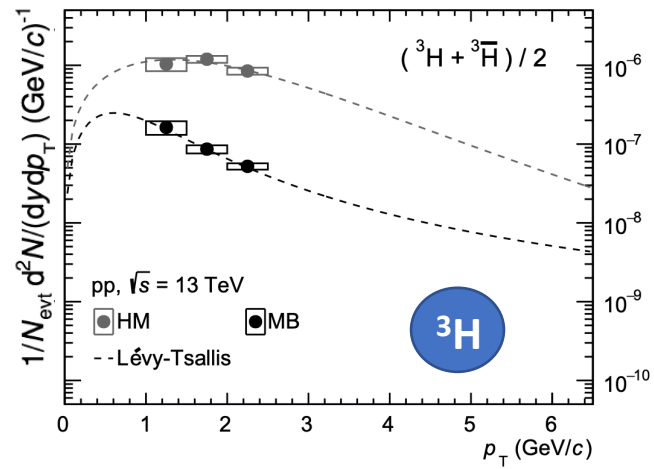


# Measurement of (anti)nuclei with A=3



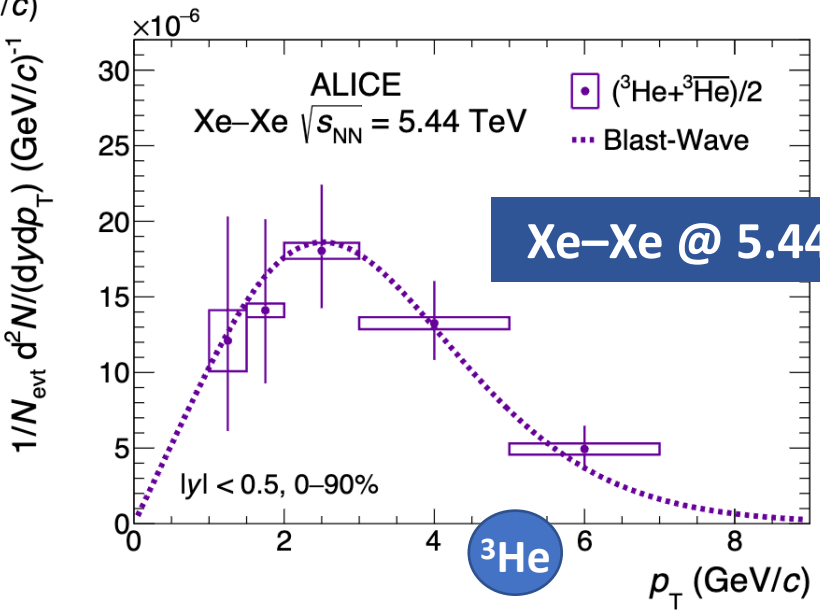
**p-Pb @ 8.16 TeV**

pp: ALICE Collaboration, JHEP 01 (2022) 106  
 p-Pb: ALICE Collaboration, PLB 846 (2023) 137795  
 Xe-Xe: ALICE Collaboration, arXiv:2405.19826  
 Pb-Pb: ALICE Collaboration, arXiv:2405.19839

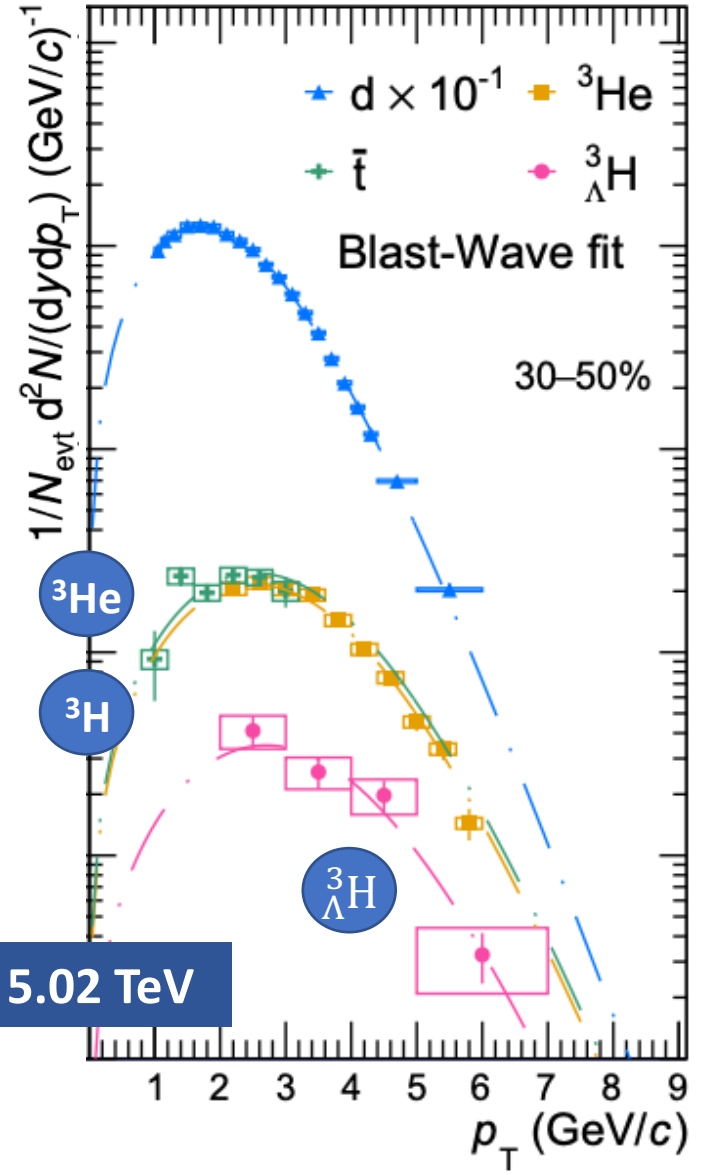


**pp @ 13 TeV**

(anti) ${}^3\text{He}$ , (anti) ${}^3\text{H}$  and (anti) ${}^3_{\Lambda}\text{H}$  have been measured in all collision systems by ALICE



**Xe-Xe @ 5.44 TeV**



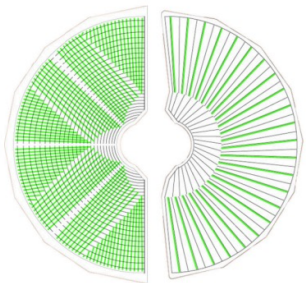
**Pb-Pb @ 5.02 TeV**

# Identification of nuclei with A=3 with LHCb

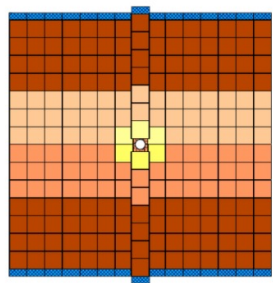
LHCb detector not designed to identify light (anti)nuclei

Use information from the tracking system

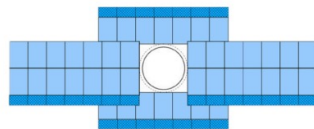
**1** Ionisation losses in silicon sensors:  $Z^2$  dependence in Bethe-Bloch  
 → dE/dx in VELO, TT, IT to identify He



VELO: 2 x 21 layers

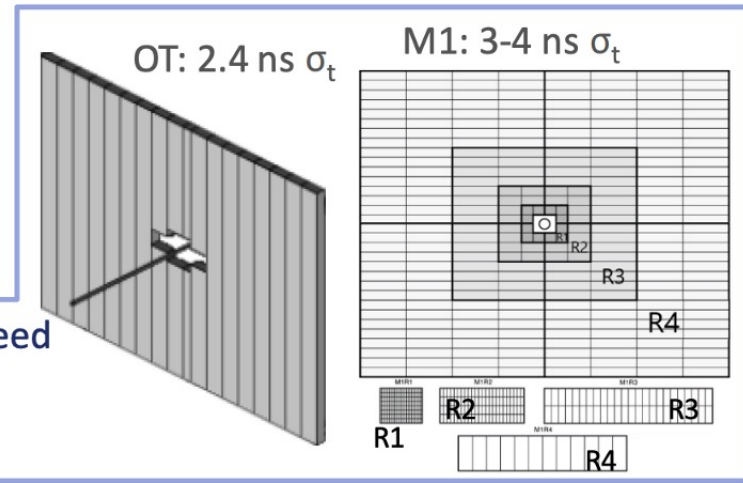
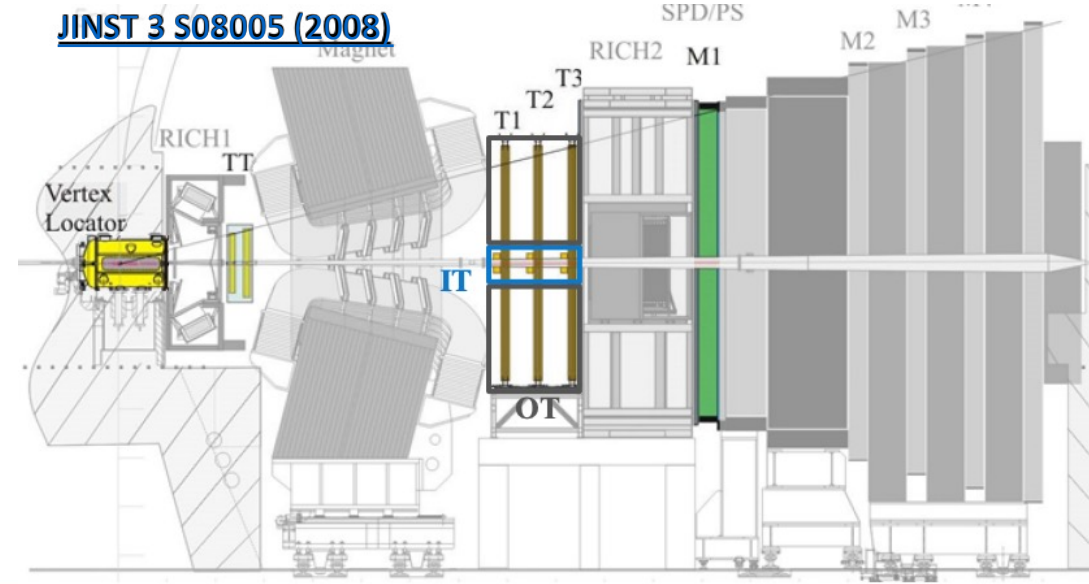


TT: 4 layers



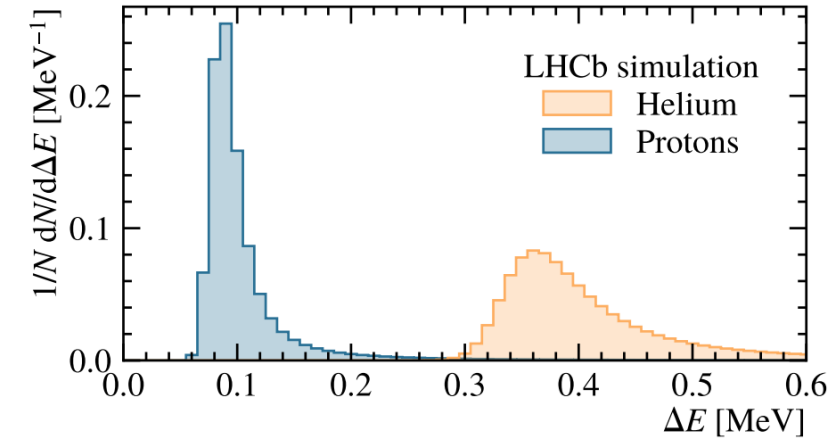
IT: 12 layers

**2** Light nuclei slower than c:  $M$  dependence of particle speed  
 → Time-of-flight in OT and M1 to identify d,  
 distinguish  $^3\text{He}$  and  $^4\text{He}$



- excellent vertexing ( $\sigma_{IP} = 15+29/p_T$  [GeV]  $\mu\text{m}$ ,  $\sigma_p = 0.5\% - 1.0\%$ )
  - excellent PID separation for K,  $\pi$  and p with O(10) GeV/c

# Identification of $^3\text{He}$ with LHCb



Bethe-Bloch:  $Z=2$  particles deposits  $\sim 4$  times the energy of  $Z=1$  particles  
 $\rightarrow$  He: higher ADC counts and wider cluster size

**First (anti-)Helium candidates observed in  $pp$  in LHCb data!**

Define Likelihood discriminators based on cluster size and ADC counts:

$$\mathcal{L}^X = \left( \prod_{i=1}^n \text{PDD}_i^X \right)^{1/n}, \quad X = \{\text{He, Bkg}\}$$

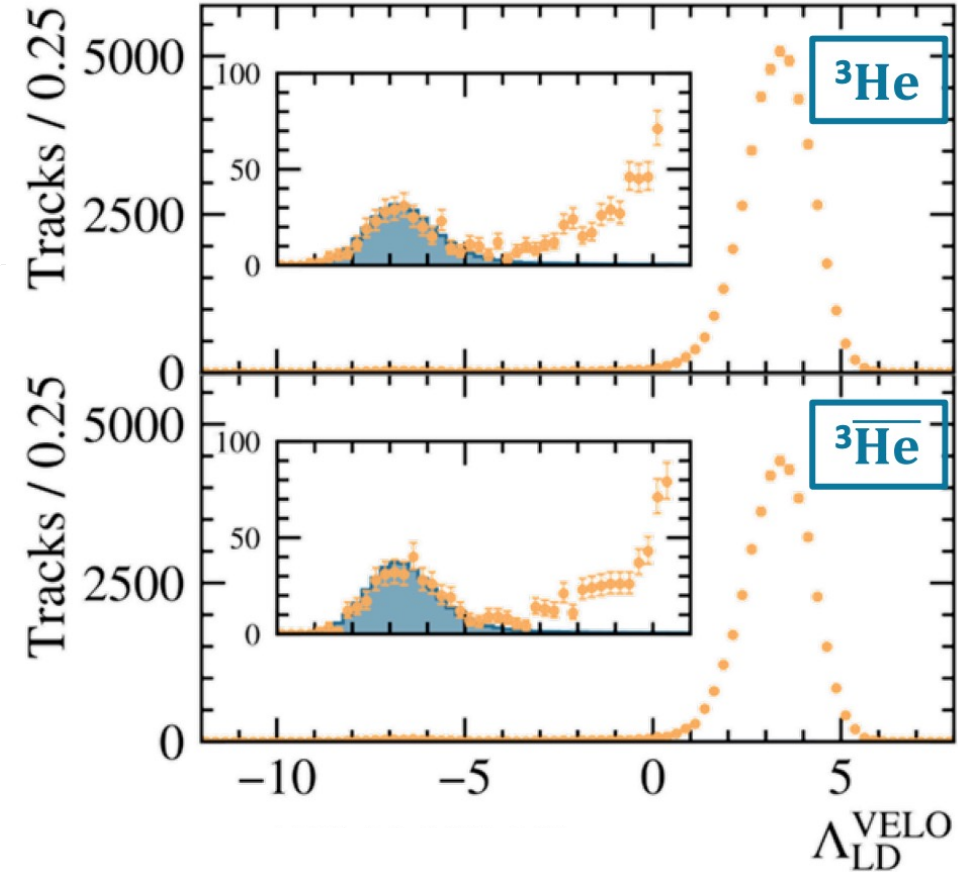
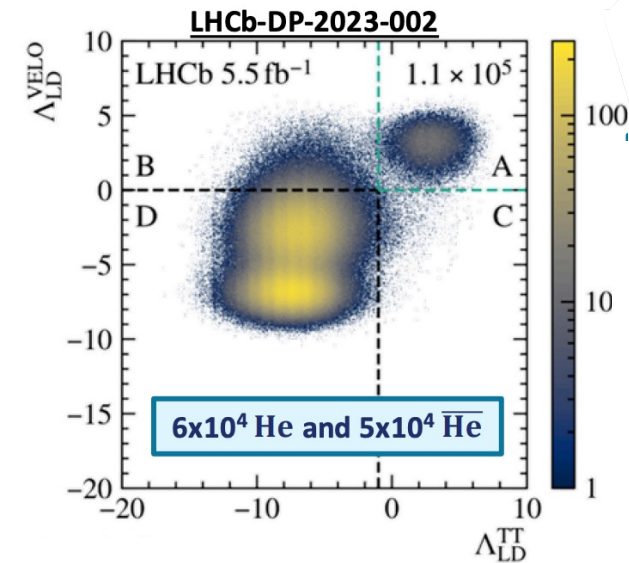
$$\Lambda_{\text{LD}} = \log \mathcal{L}^{\text{He}} - \log \mathcal{L}^{\text{Bkg}}$$

One discriminator for each subdetector:

- $\Lambda_{\text{LD}}^{\text{VELO}}$
- $\Lambda_{\text{LD}}^{\text{TT}}$
- $\Lambda_{\text{LD}}^{\text{IT}}$

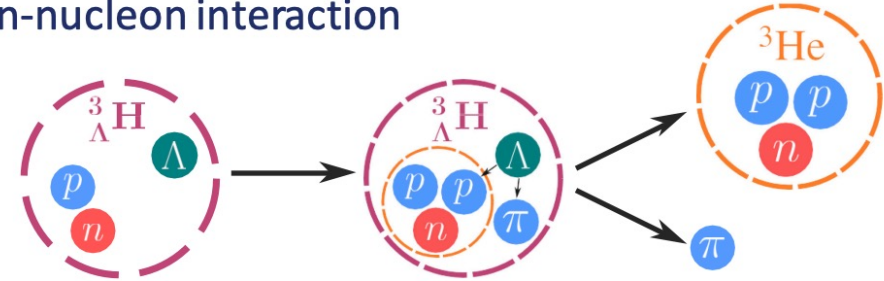
**Performance:**

- MisID probability:  $\mathcal{O}(10^{-12})$
- Signal efficiency:  $\sim 50\%$



- Hypertriton life-time and binding energy gives access to hyperon-nucleon interaction  
→ Constrains on maximum mass of neutron stars

**Search for 2-body decay into He:**



## Results:

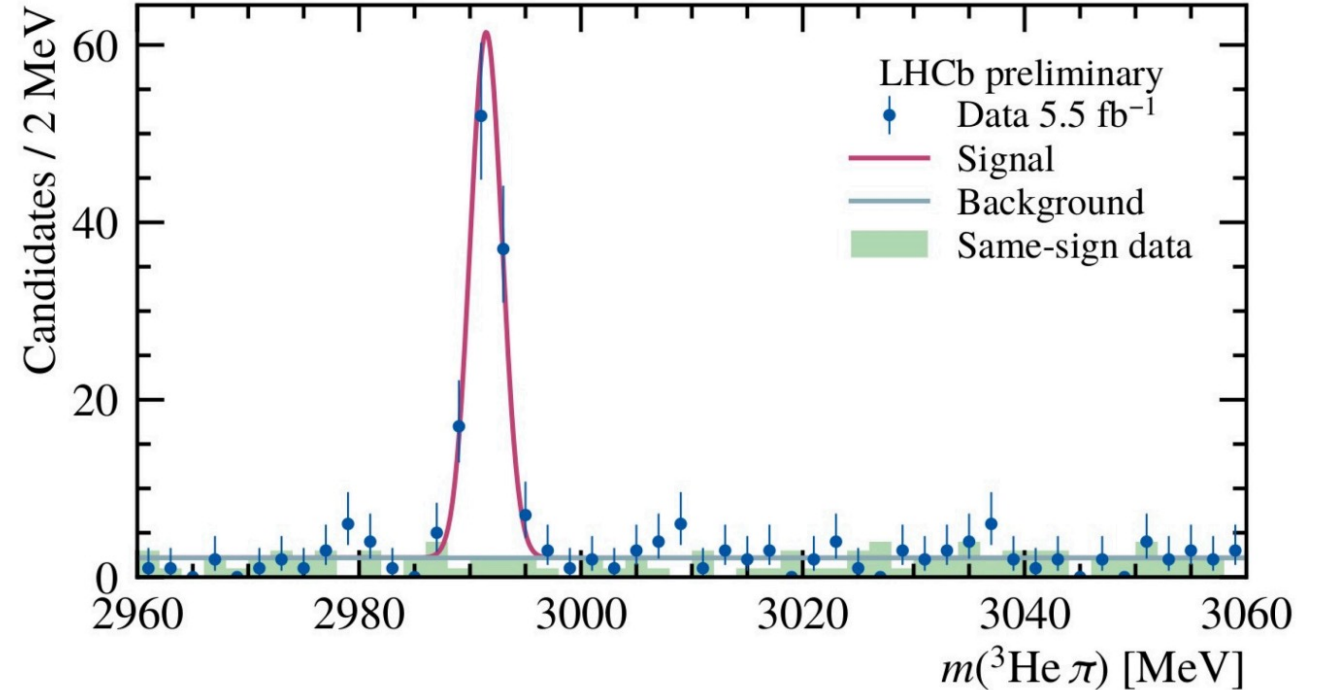
(Run2  $pp$  collisions at  $\sqrt{s} = 13$  TeV)

### • Yields:

- $61 \pm 8$  Hypertriton
- $46 \pm 7$  anti-Hypertriton

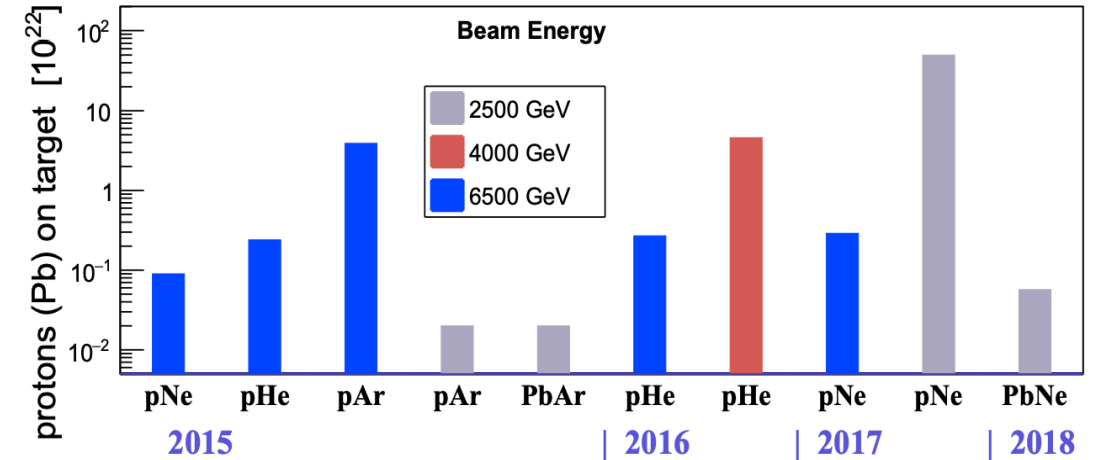
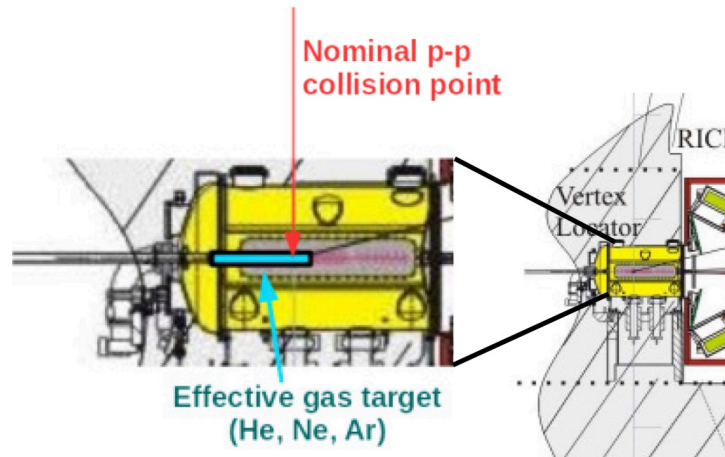
- Statistical mass precision: 0.16 MeV

This measurement shows the applicability of  ${}^3\text{He}$  reconstruction and paves the way for future measurements of astrophysical interest





- The *System for Measuring Overlap with Gas (SMOG)* can inject gas in LHC beam pipe around  $\pm 20$  m from the LHCb IP
- SMOG exploited for LHCb **fixed-target physics programme**  
 → Collected physics samples with different **targets** and different **centre of mass energies**



Unique opportunities at the LHC:

- Collisions with targets of mass number  $A$  intermediate between  $p$  and  $Pb$  → **Reproduce CR interactions (pp, pHe)**
- Energy range  $\sqrt{s_{NN}} \in [30, 115]$  GeV for beam energy in  $[0.45, 7]$  TeV → Unexplored gap between SPS and LHC/RHIC

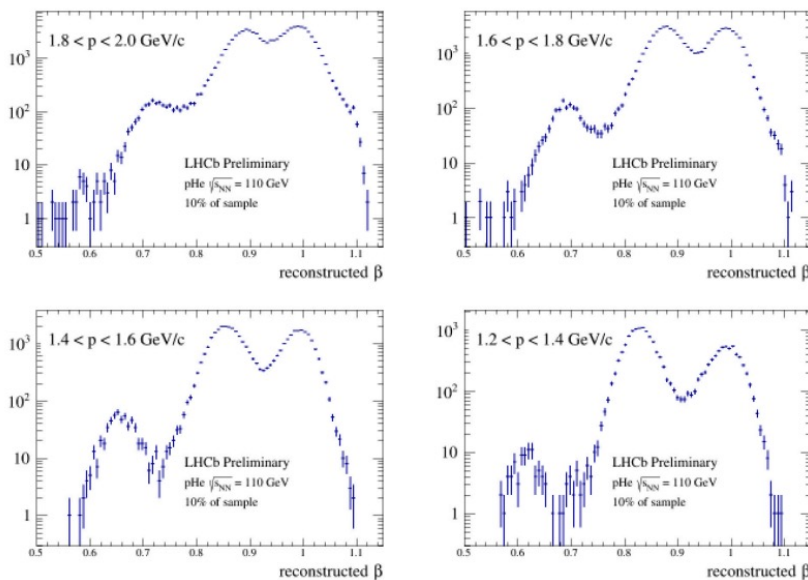
**LHCb contribution is relevant for astrophysics applications!**

LHCb is now also capable of measuring (anti)deuterons

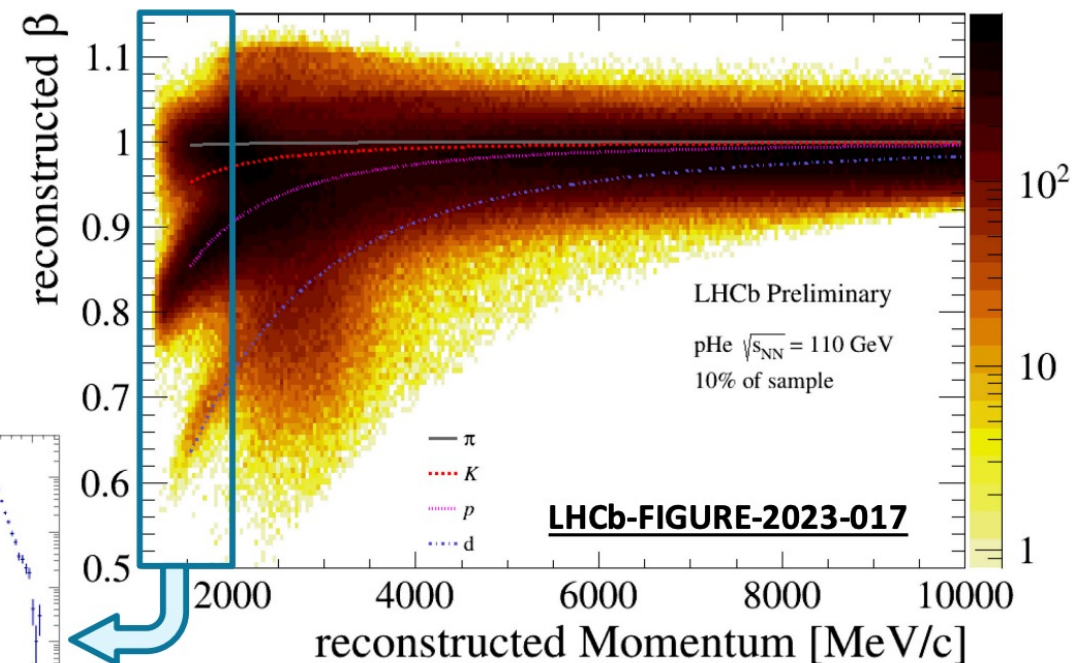
- *Time-of-flight based technique*
- Reconstructed tracks refitted to determine  $\beta$   
→ iterative procedure rerunning Kalman fit with different  $\beta$  hypotheses

- **~10% of SMOG pHe**  
( $\sqrt{s_{NN}} = 110$  GeV) dataset
- **Background suppression:**  
 $\sigma(\beta) < 0.02$ ,  $\chi^2_{\text{OThits}}/\text{ndf} < 2$

**First deuteron candidates  
observed in pHe data!**



**LHCb-FIGURE-2023-017**



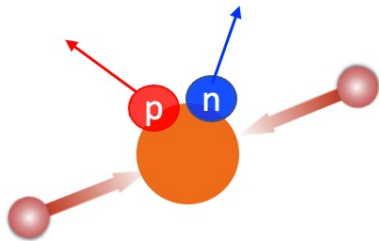
**LHCb-FIGURE-2023-017**

[https://cds.cern.ch/record/2881940/files/MPI23\\_v1.pdf](https://cds.cern.ch/record/2881940/files/MPI23_v1.pdf)



# Testing production models with hypertriton

- In small collision systems (as pp) size of system created in the collision is smaller or equal to that of the nucleus under study
- For small systems model **predictions are quite different**
- Coalescence is sensitive to the **interplay** between the **size of the collision system** and the spatial extension of the **nucleus wave function**



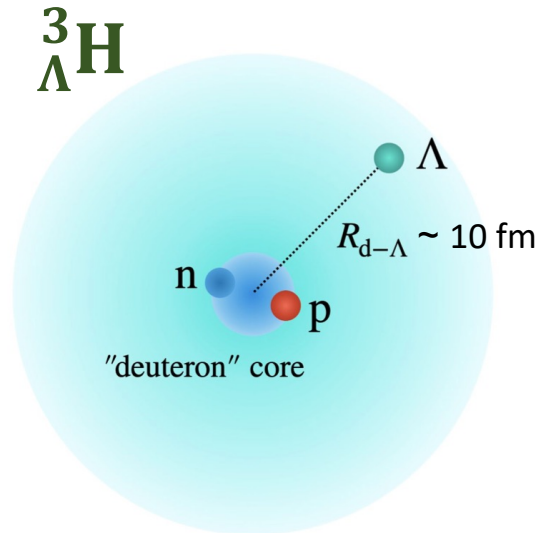
System size (pp, p—Pb): 1–1.5 fm

$r_d$ : 1.96 fm

$r_{3\text{He}}$ : 1.76 fm

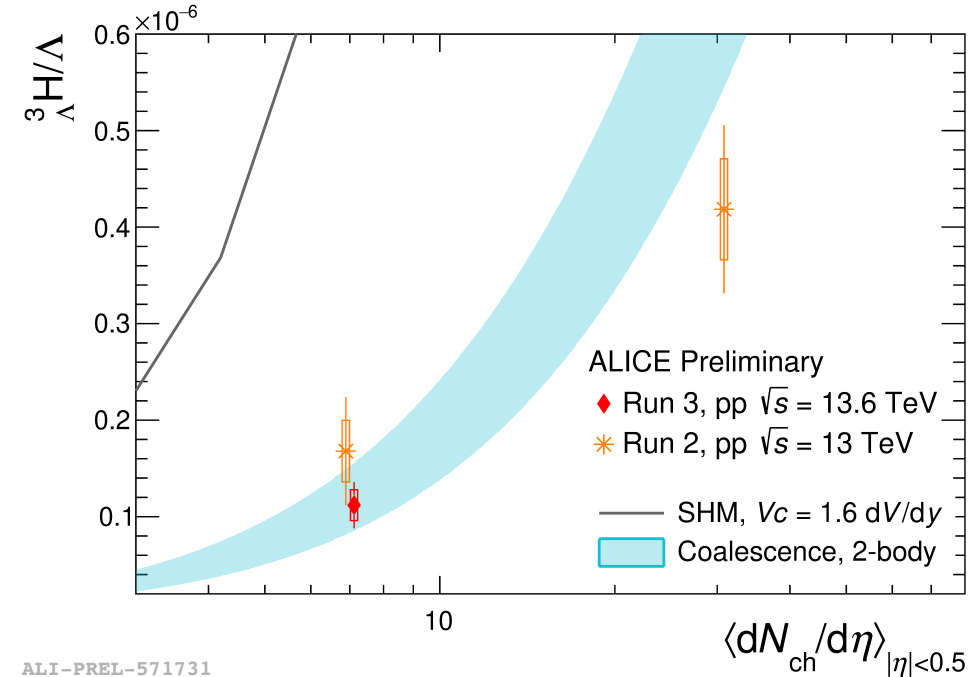
$r_{\Lambda\text{H}}^{3\text{H}(np\Lambda)}$ : 4.9 fm ( $B_\Lambda = 2.35$  MeV)

$r_{\Lambda\text{H}}^{3\text{H}(d\Lambda)}$ : 10 fm ( $B_\Lambda \sim 0.13$  MeV)



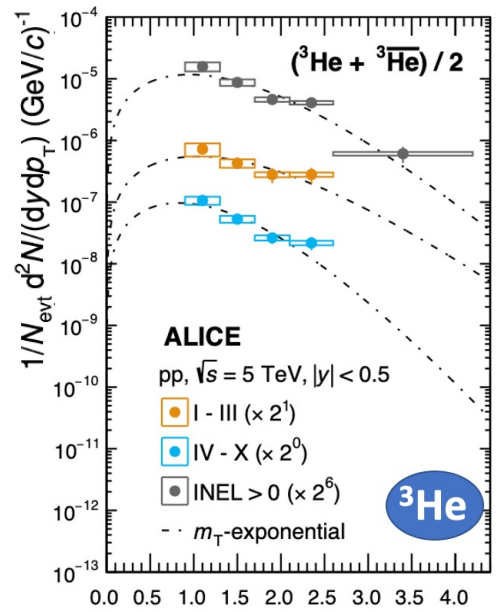
powerful probe for investigating the nucleon –  $\Lambda$  interaction

${}^3\text{H}/\Lambda$  ratio provides a powerful tool to investigate nuclear production mechanism

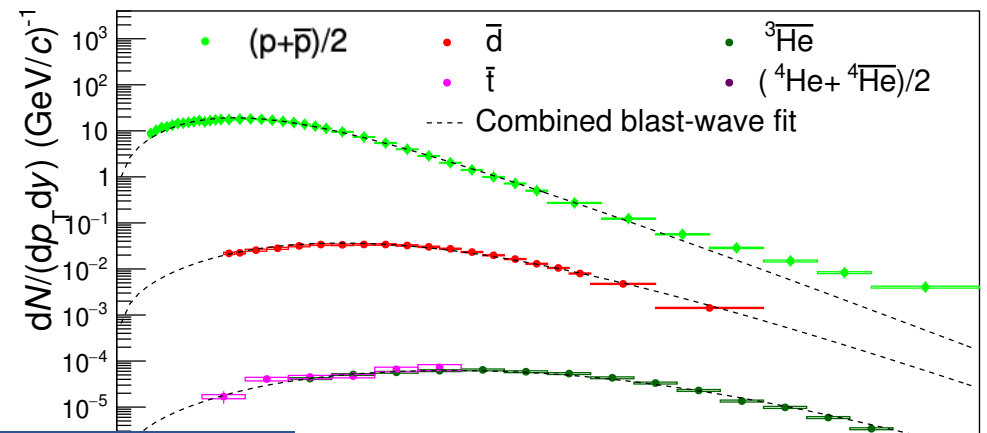
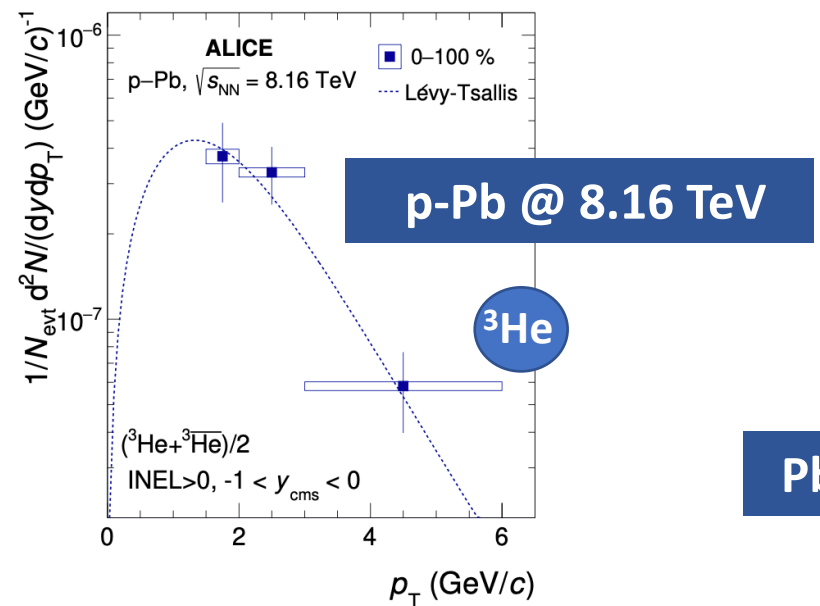


ALI-PREL-571731

# Measurement of (anti)nuclei with A=3

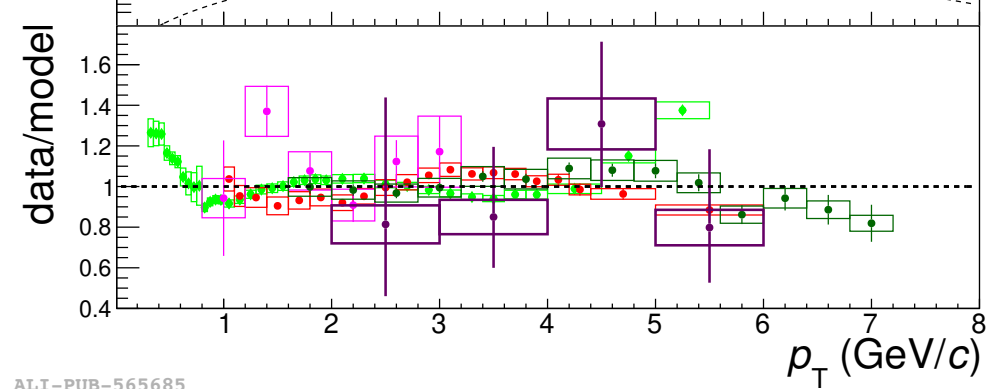
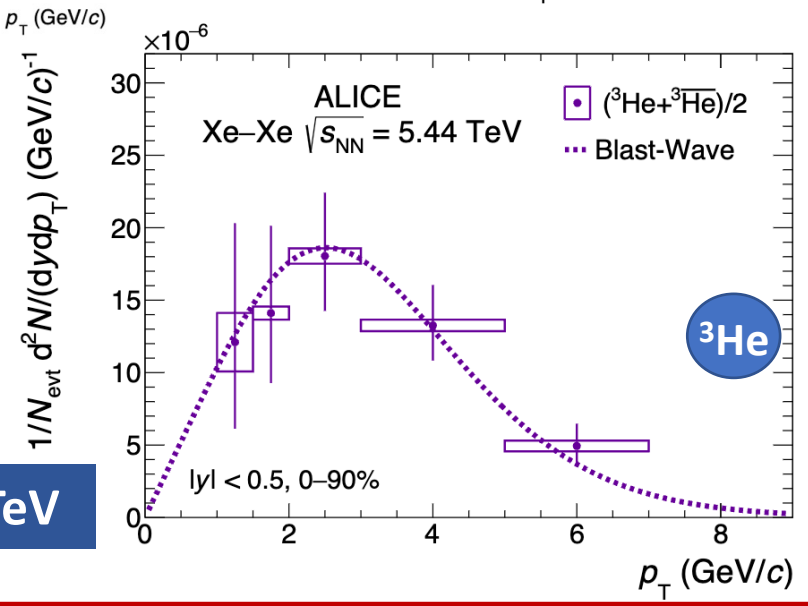


**pp @ 5.02 TeV**



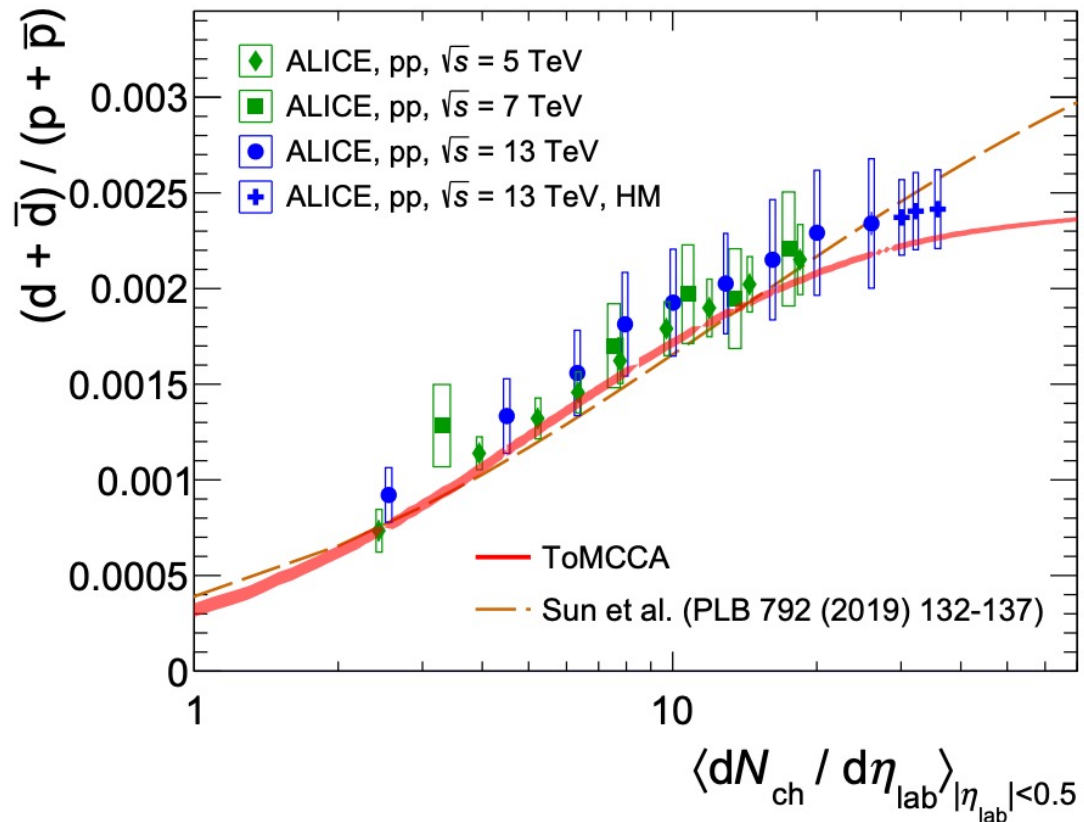
**Pb-Pb @ 5.02 TeV**

**Xe-Xe @ 5.44 TeV**



ALI-PUB-565685

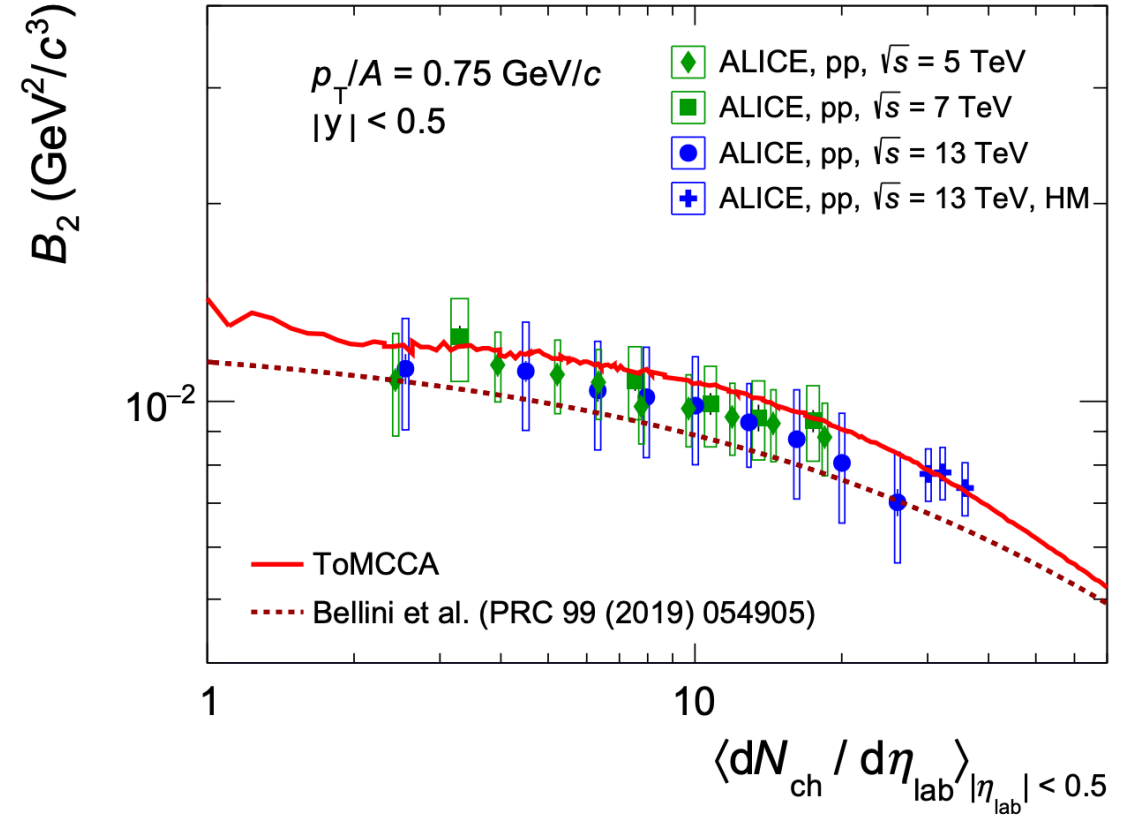
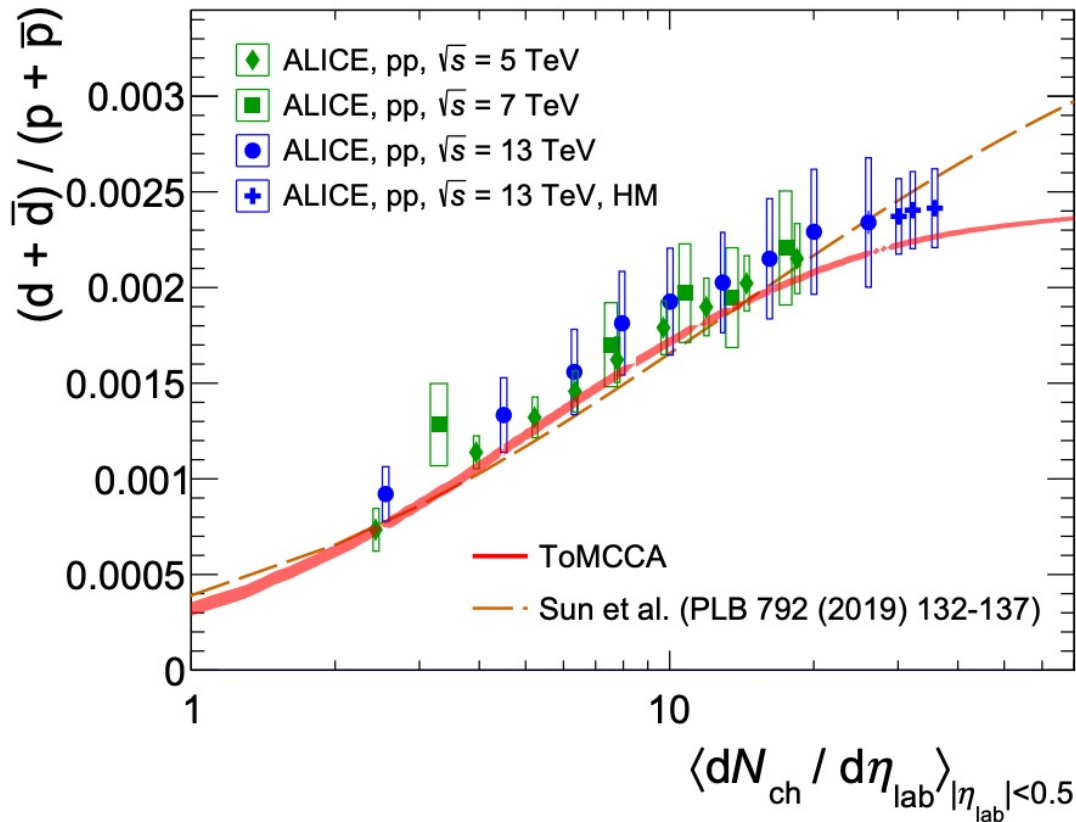
- pp: ALICE Collaboration, EPJC (2022) 82:289
- p-Pb: ALICE Collaboration, PLB 846 (2023) 137795
- Xe-Xe: ALICE Collaboration, arXiv:2405.
- Pb-Pb: ALICE Collaboration, arXiv:2311.11758



Predictions available only for the pp multiplicity range (1-70)

- **Coalescence** predictions of ToMCCA using Wigner function formalism & multiplicity-dependent input (momentum distributions of nucleons, source size and multiplicity distributions) reproduce all data points within 1sigma
- No  $^3\text{He}$  coalescence predictions yet

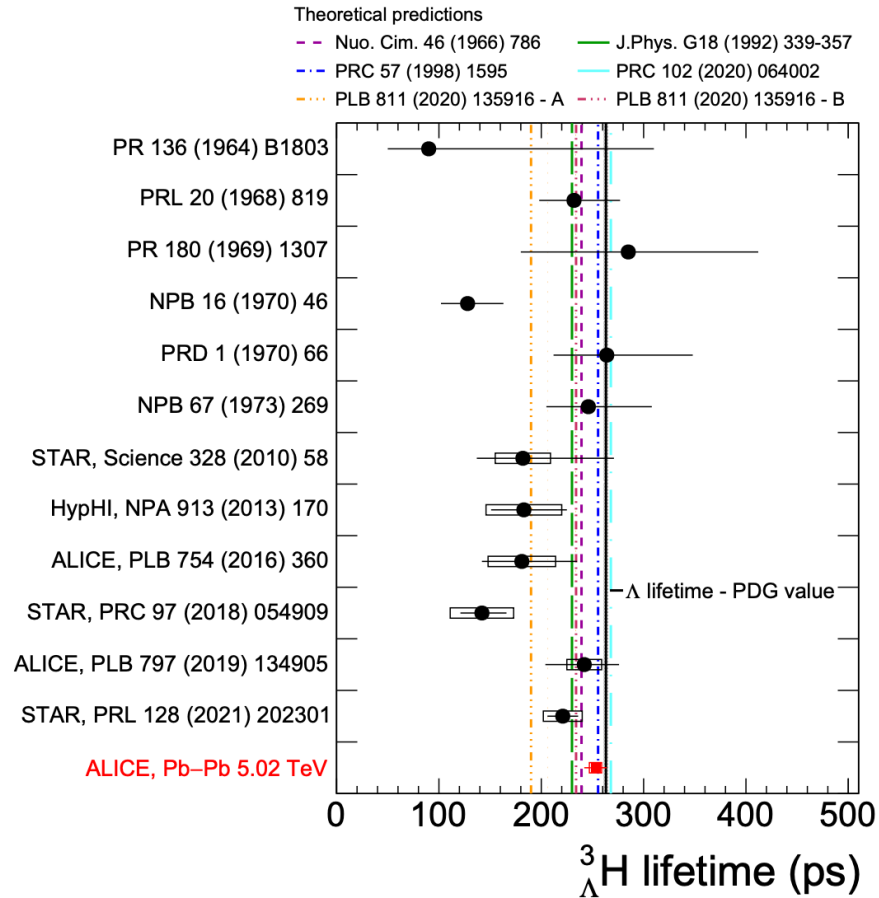
# Testing production models (focus at low multiplicity)



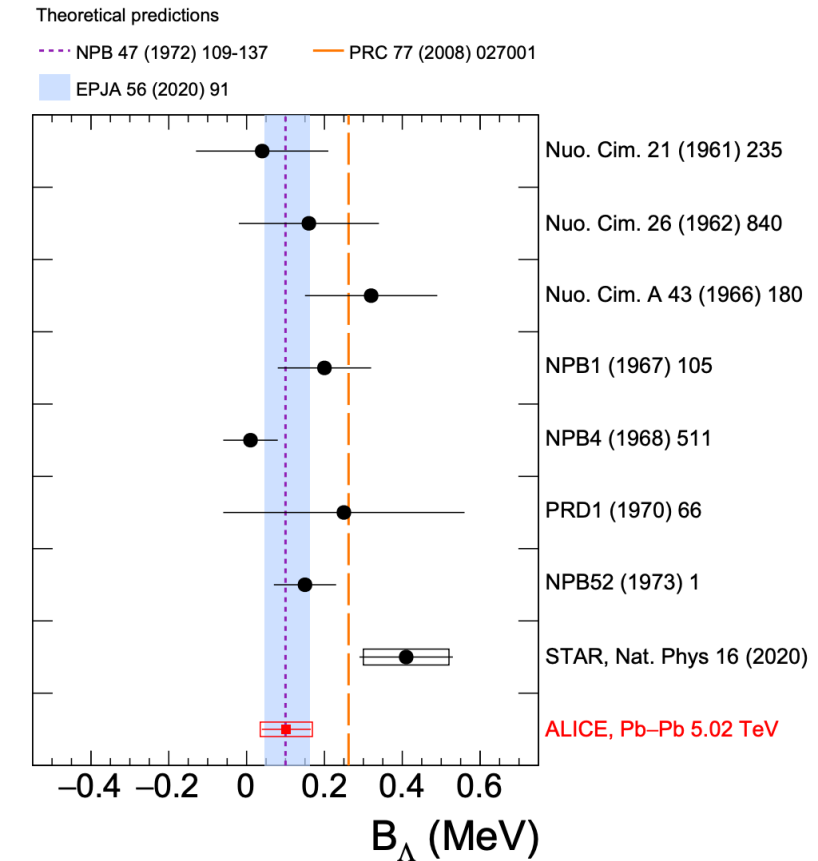
- **Coalescence** predictions of ToMCCA using Wigner function formalism & multiplicity-dependent input (momentum distributions of nucleons, source size and multiplicity distributions) reproduce all data points within 1sigma
- No <sup>3</sup>He coalescence predictions yet
- Also coalescence parameter  $B_2$  vs multiplicity is well reproduced by ToMCCA

# Hypertriton lifetime & binding energy (Pb–Pb collisions)

$$\tau = [253 \pm 11 \text{ (stat.)} \pm 6 \text{ (syst.)}] \text{ ps}$$



$$B_{\Lambda} = [102 \pm 63 \text{ (stat.)} \pm 67 \text{ (syst.)}] \text{ keV}$$



- Models predicting a lifetime close to the [free  \$\Lambda\$](#)  one are favoured
- Strong hint that hypertriton is weakly bound

- $B_{\Lambda}$  compatible with zero  $\rightarrow$  Weakly bound nature of  ${}^3_{\Lambda}\text{H}$  is confirmed

Phys. Rev. Lett. 131 (2023) 102302

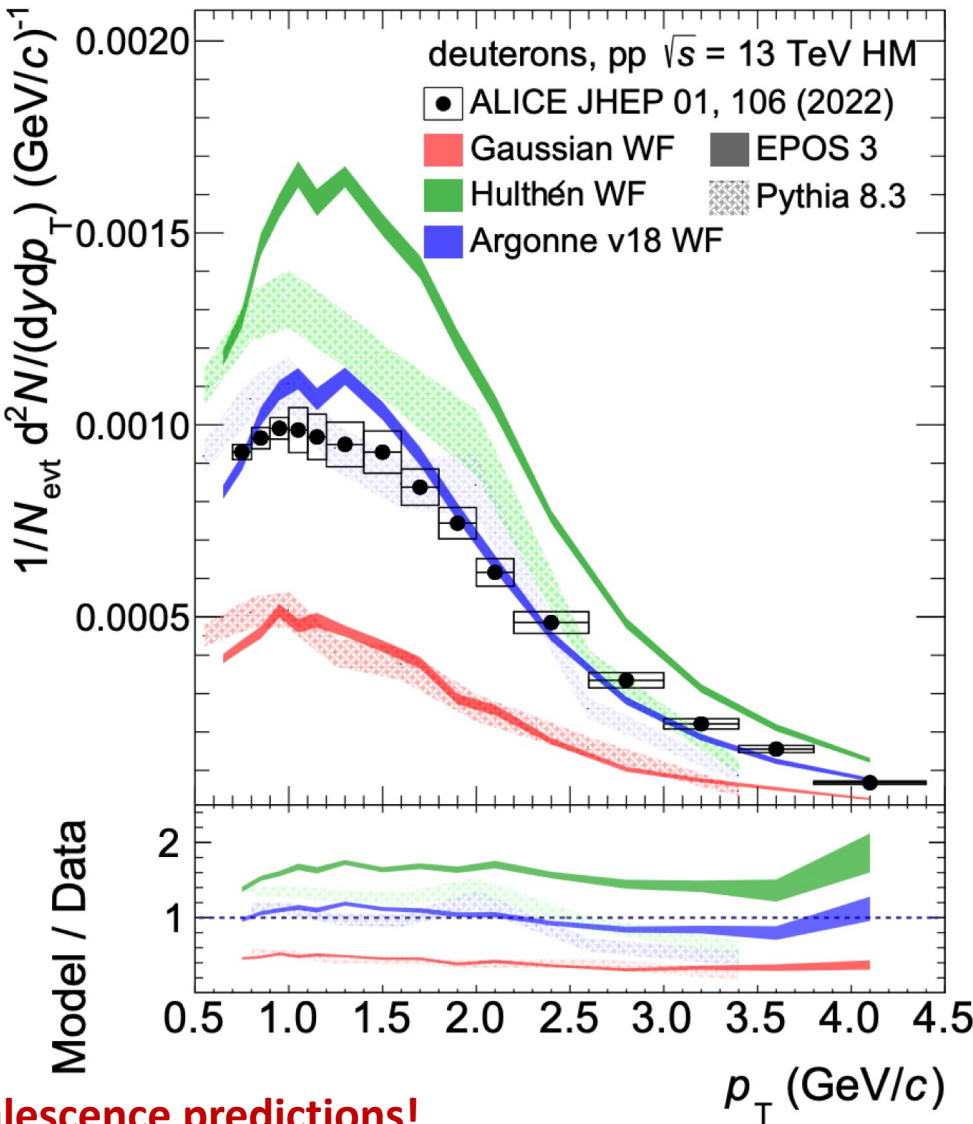
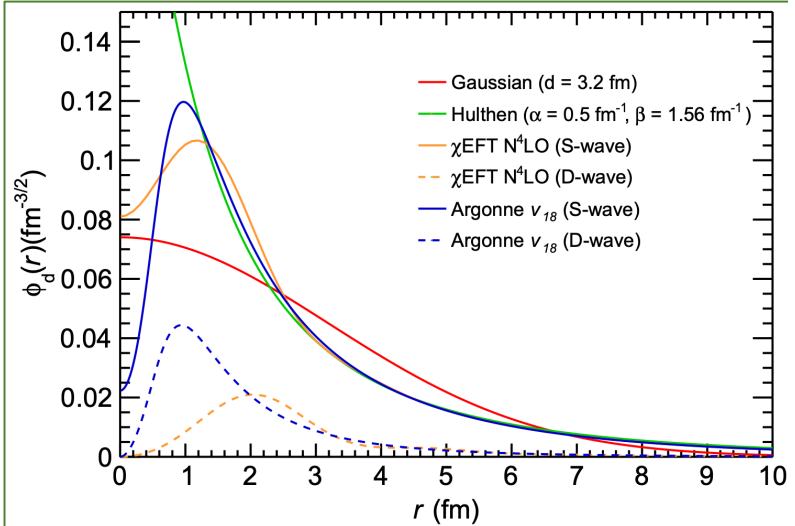
# State-of-the-art coalescence model

Coalescence afterburner based on Wigner function formalism

- Use event generators (PYTHIA 8.3 & EPOS 3)
- Emulate experimental multiplicity trigger
- Calibrate (anti)nucleon momentum distribution
- Take resonance cocktail from SHM
- **Tune emission source**
- **Employ realistic wavefunction**



- **Hulthén:** Favoured by low energy scattering experiments
- **Gaussian:** easiest WF calculation
- **Two Gaussians:** Approximates Hulthén, easy to use in calculations
- **$\chi$ EFT:** Favoured by modern nuclear interaction experiments (e.g. Femtoscopy)
- **Argonne v18** phenomenological potential constrained to p-n scattering



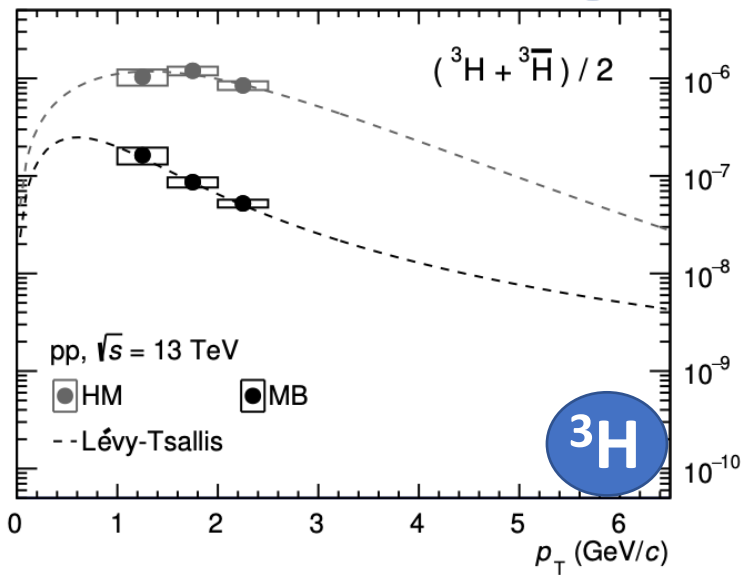
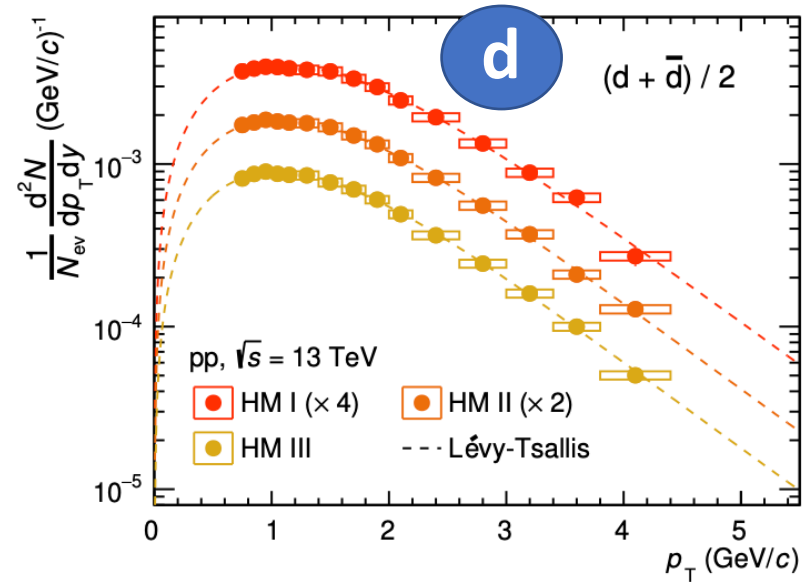
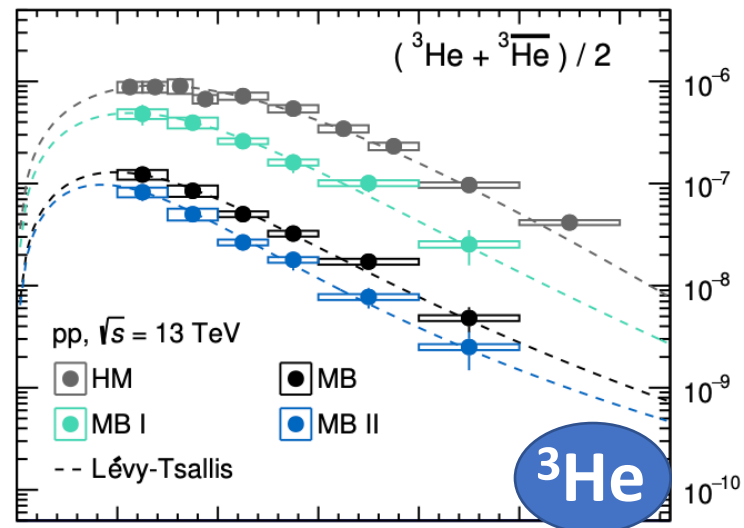
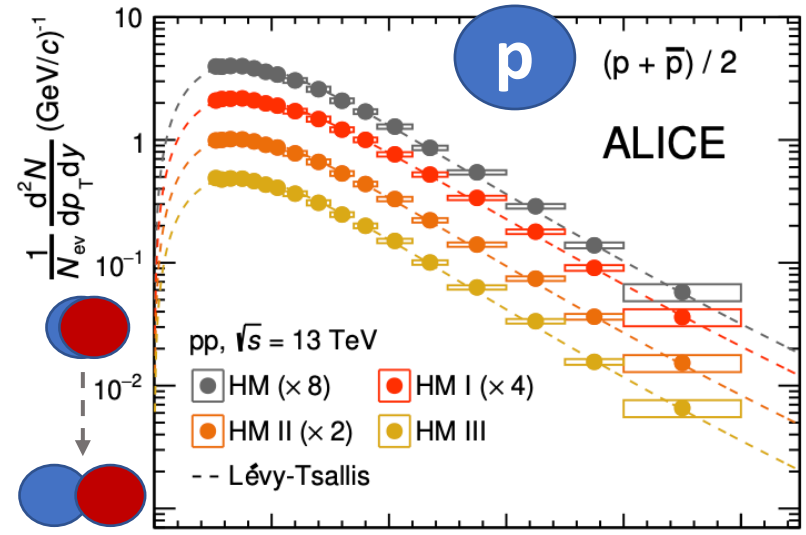
**Realistic wavefunction is key for coalescence predictions!**

Mahlein et al., EPJC 83 (2023) 9, 804



# Measurement of light (anti)nuclei with ALICE

ALICE Collaboration, JHEP 01 (2022) 106

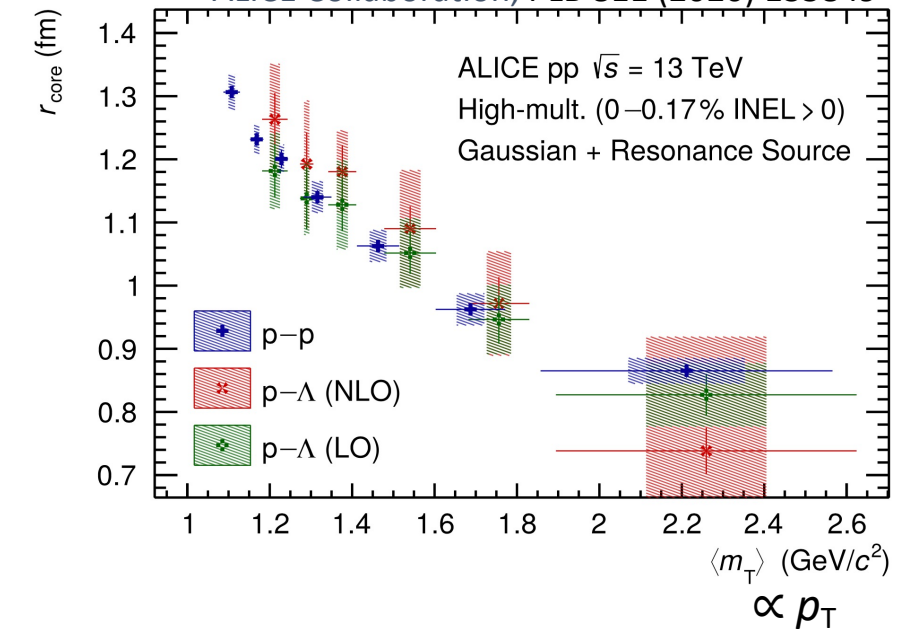


## HM pp @ 13 TeV

- Focus on the HM data sample → narrow multiplicity interval covered (0-0.1%)
- Precise measurement of the emission source size  $r_{core}$  using femtoscopy is available

→ crucial to test the coalescence model

ALICE Collaboration, PLB 811 (2020) 135849



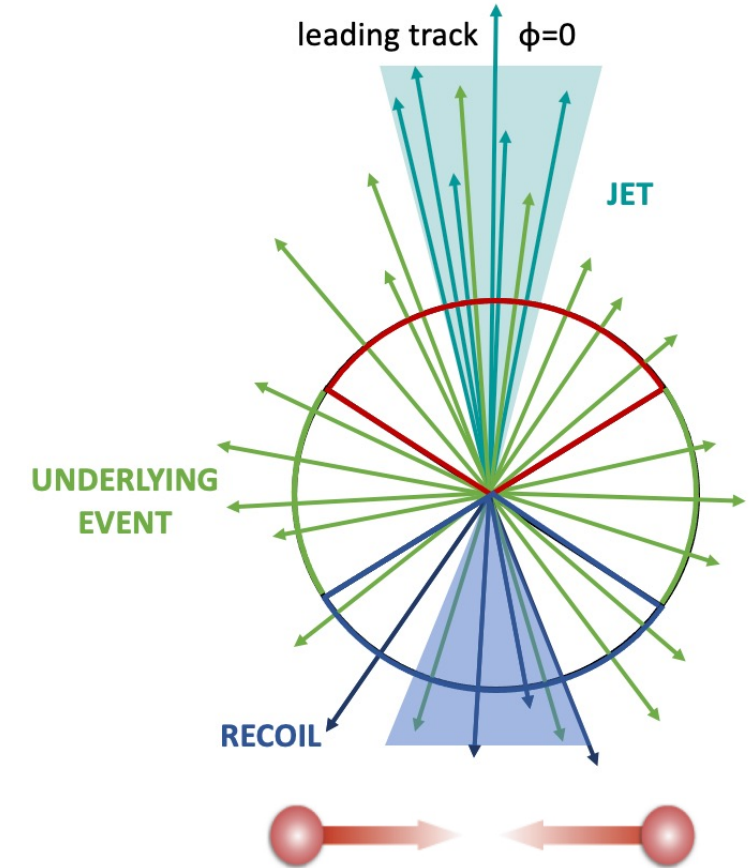


# Nuclear production in and out of jets

- Powerful tool to investigate coalescence mechanism is the study of nuclear production in and out of jets
- In jets nucleons have strong phase-space constraint

→ **Study  $B_2$  in and out of jets:** jets obtained simply by subtracting the **UE** from the **Toward** region (**Jet** + **UE**)

- Studying the antideuteron production in jets in small systems (pp, pA) is important to understand and model nuclear production
- Implications for cosmic ray physics
- Antideuteron in the Galaxy is produced in interactions of cosmic rays (p,  $^4\text{He}$ ) with kinetic energies of  $\sim 300$  GeV

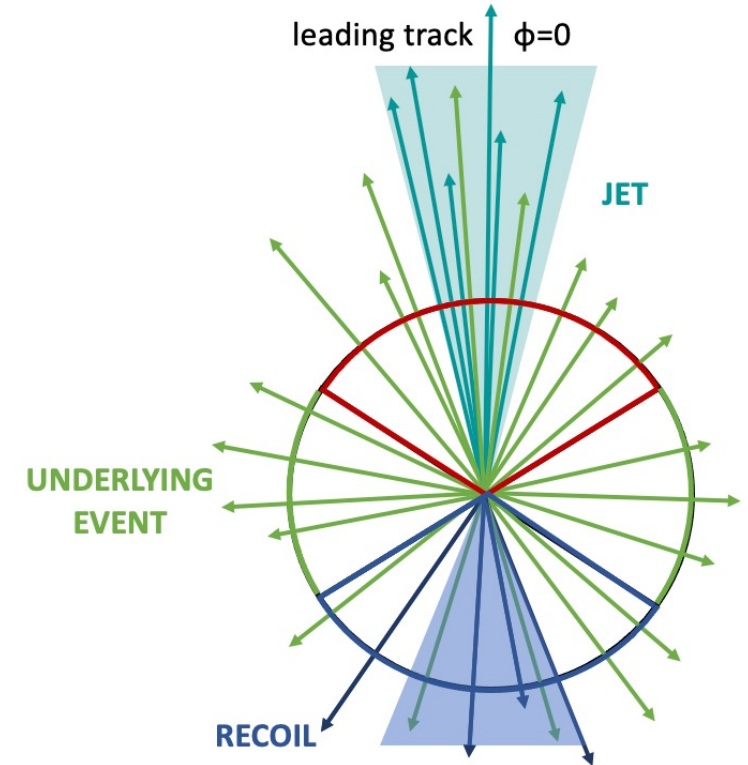
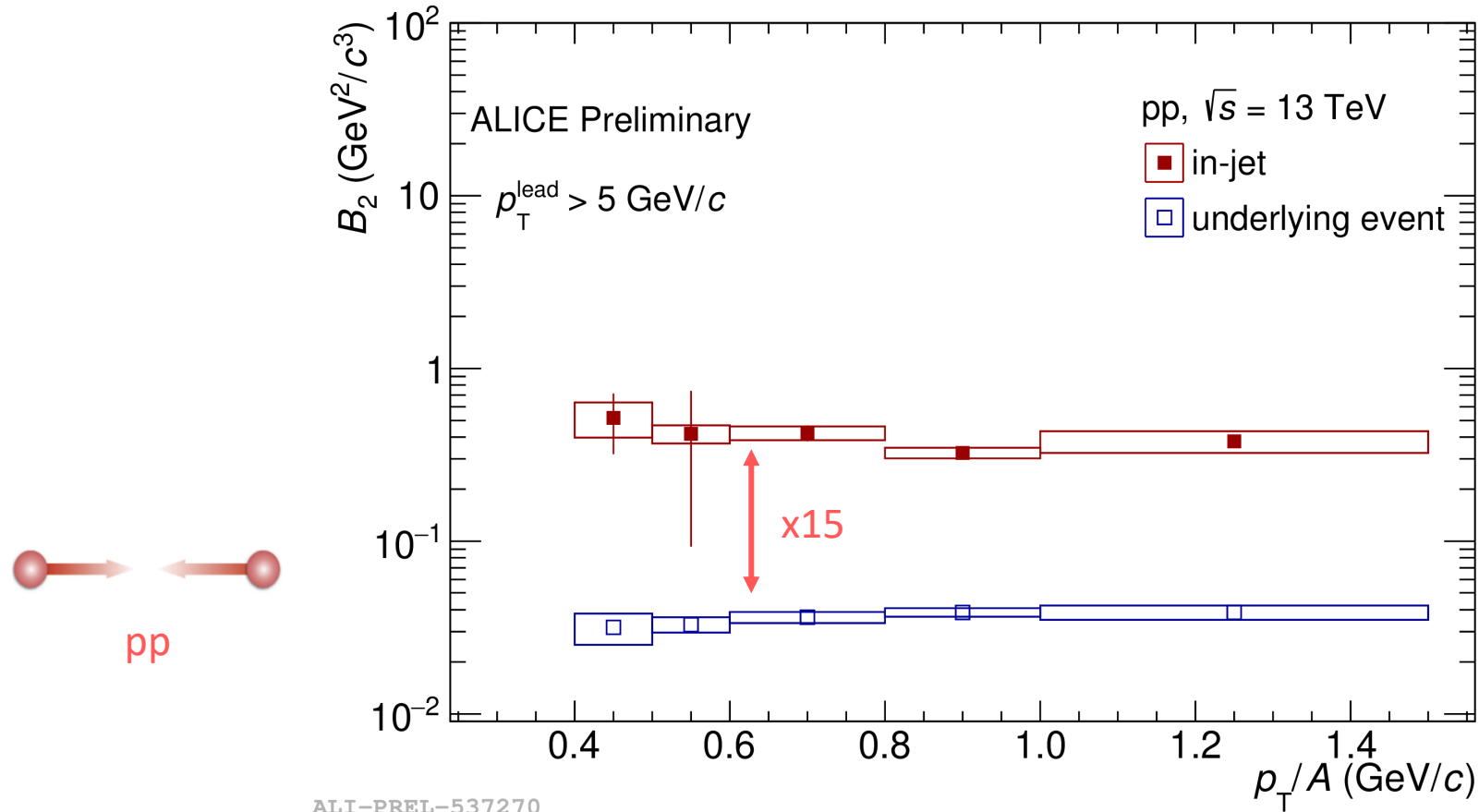


**Toward:**  $|\Delta\phi| < 60^\circ$

**Transverse:**  $60^\circ < |\Delta\phi| < 120^\circ$

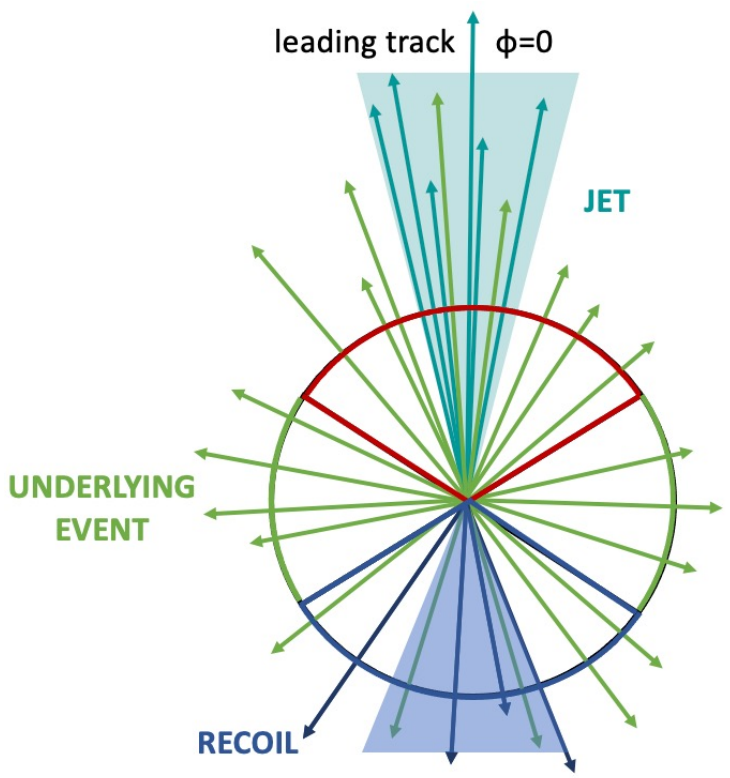
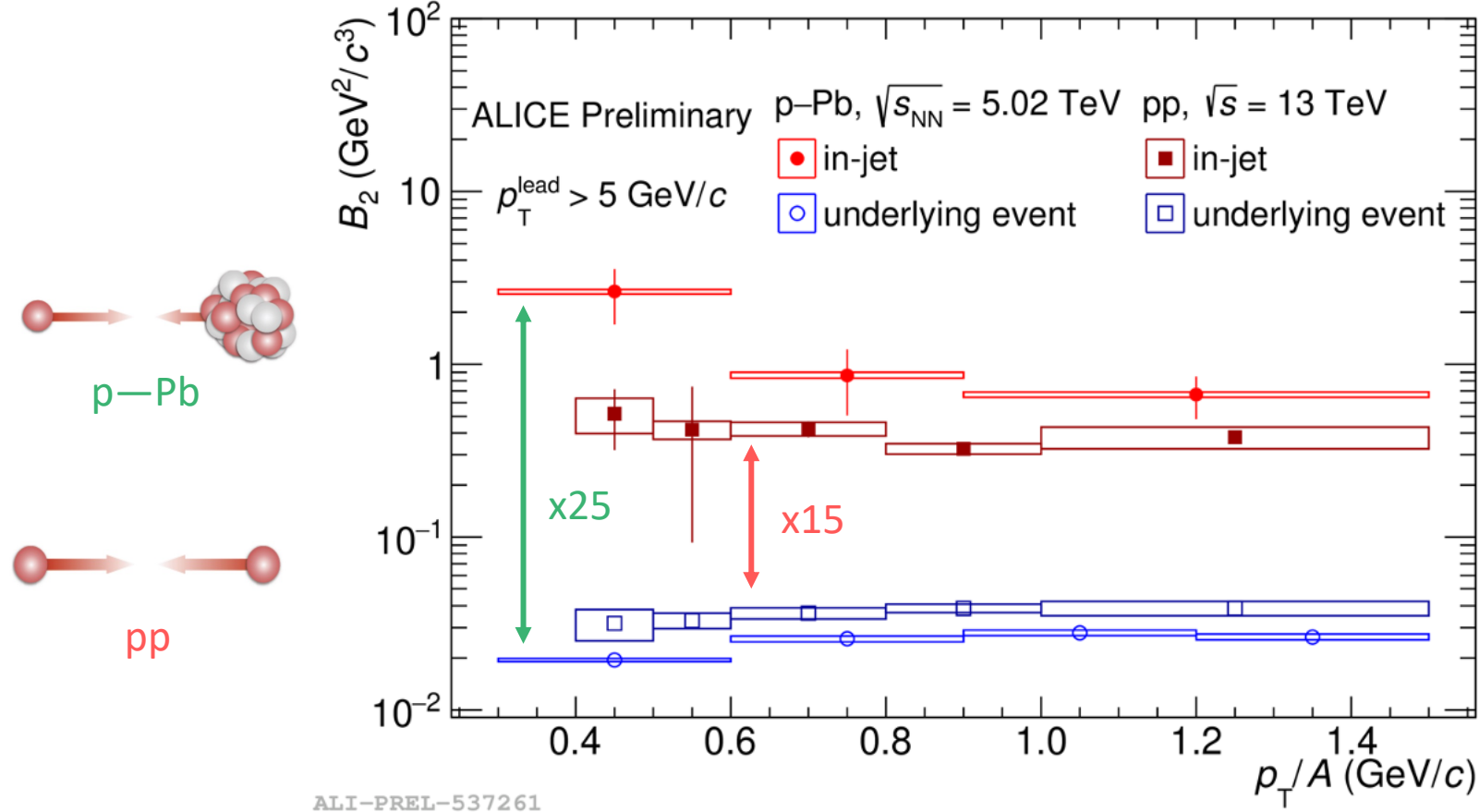
**Away:**  $|\Delta\phi| > 120^\circ$

# Coalescence parameters in and out of jets



- Enhanced deuteron coalescence probability in jets wrt UE is observed for the first time in pp collisions
- Due to the reduced distance in phase space of hadrons in jets compared to those out of jets  $\rightarrow$  favors coalescence picture

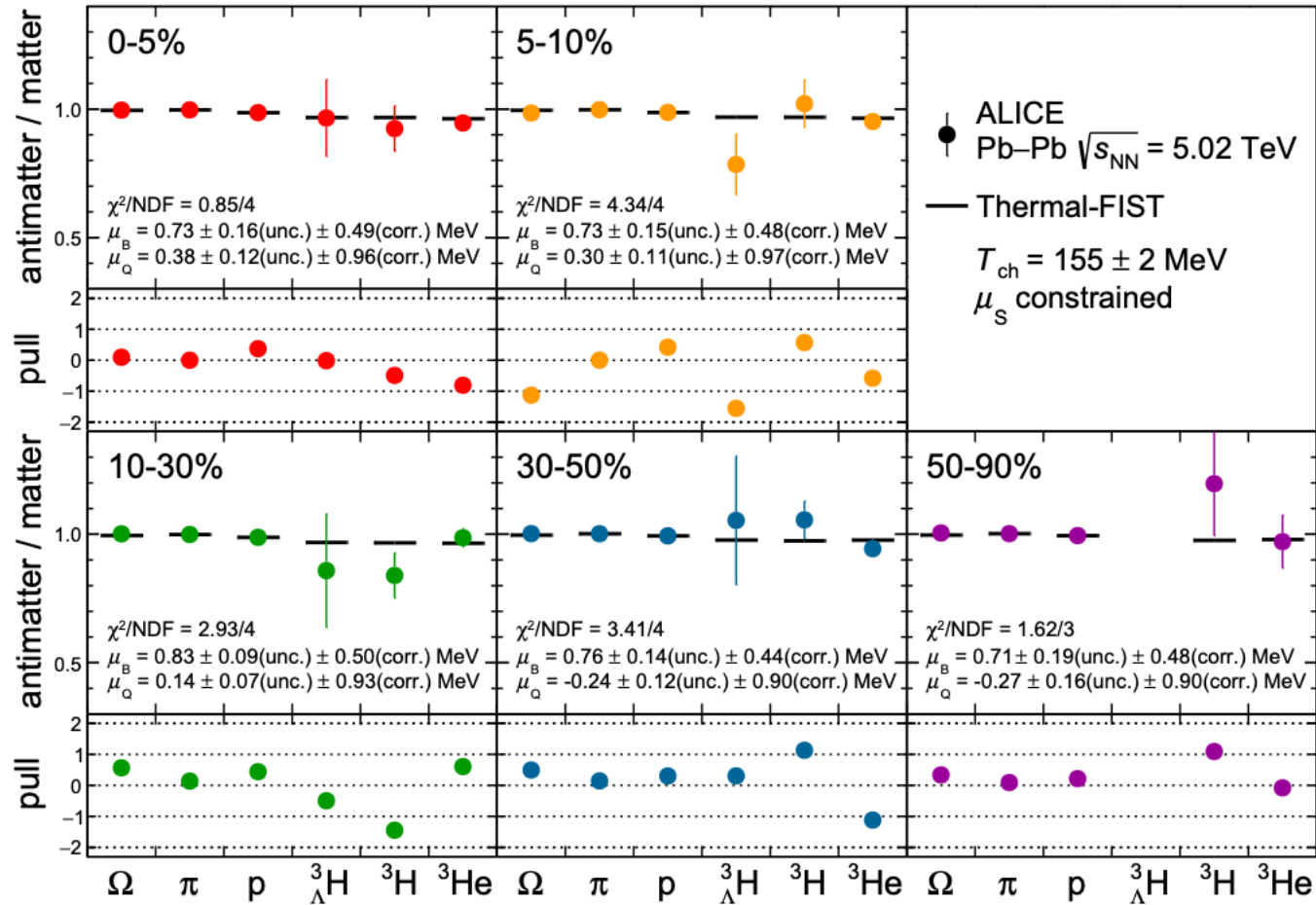
# Coalescence parameters in and out of jets



- $B_2$  in-jet in p-Pb is larger than  $B_2$  in-jet in pp  
 → could be related to the different particle composition of jets in pp and p-Pb → to be further investigated
- $B_2$  in UE in p-Pb is smaller than  $B_2$  in UE in pp due to the larger source size in p-Pb  
 (pp<sup>(1)</sup>:  $r_0 \sim 1$  fm, p-Pb<sup>(2)</sup>:  $r_0 \sim 1.5$  fm)

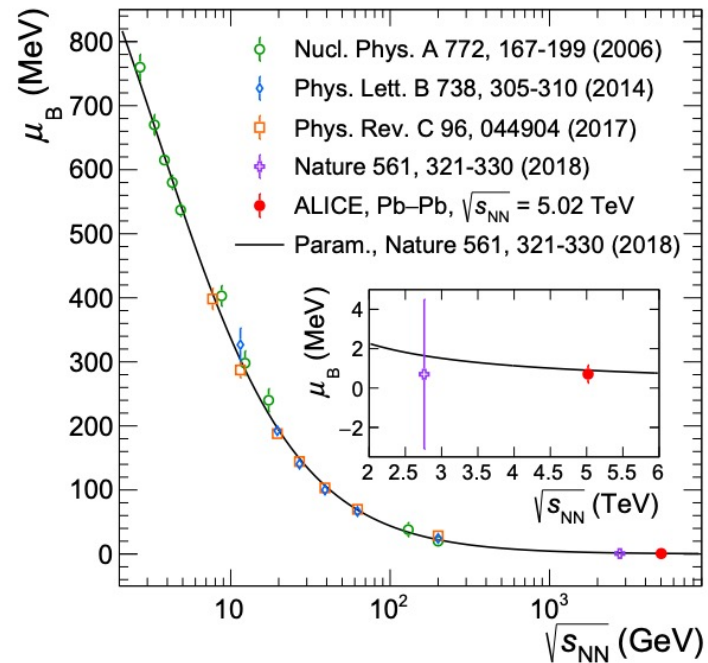
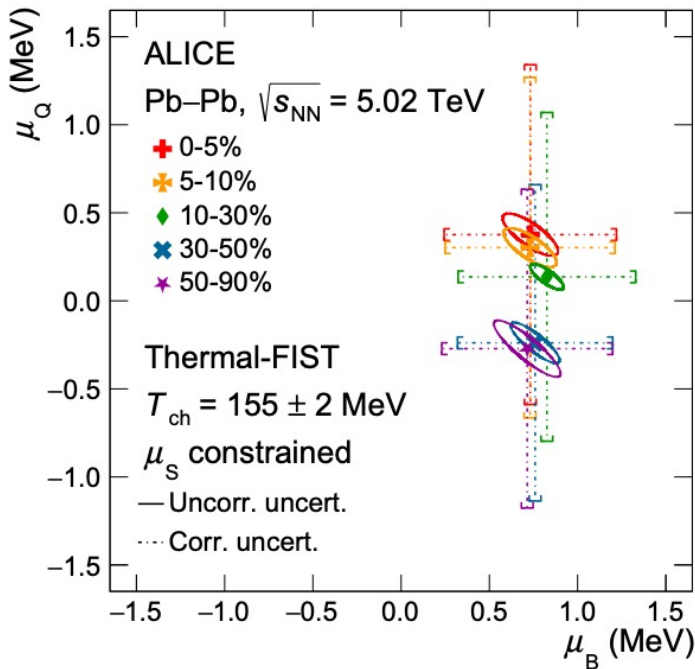
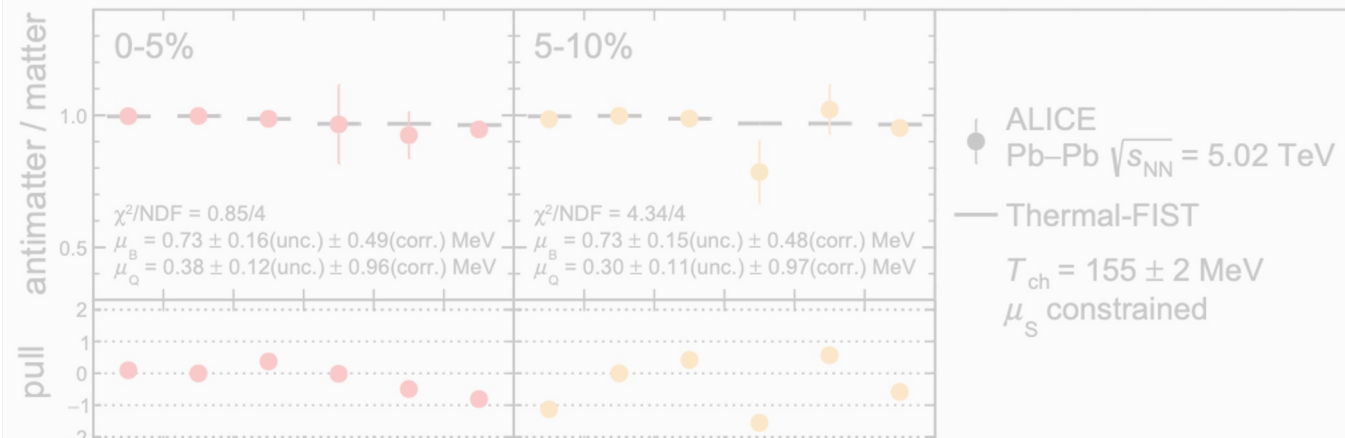
<sup>1</sup> Phys.Rev.C 99 (2019) 024001  
<sup>2</sup> Phys.Rev.Lett. 123 (2019) 112002  
 Phys.Rev.Lett. 131 (2023) 4, 042301

# Chemical potential at the LHC



- $\mu_B$  and  $\mu_Q$  are extracted fitting the antiparticle-to-particle yield ratios with the predictions of the grand-canonical SHM using the Thermal-FIST code

# Chemical potential at the LHC

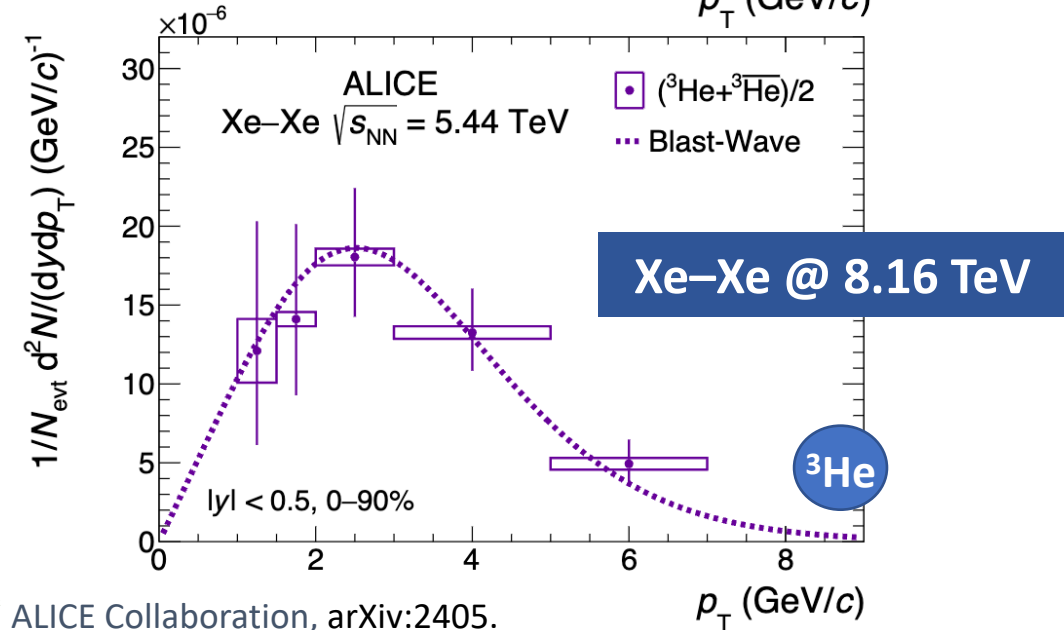
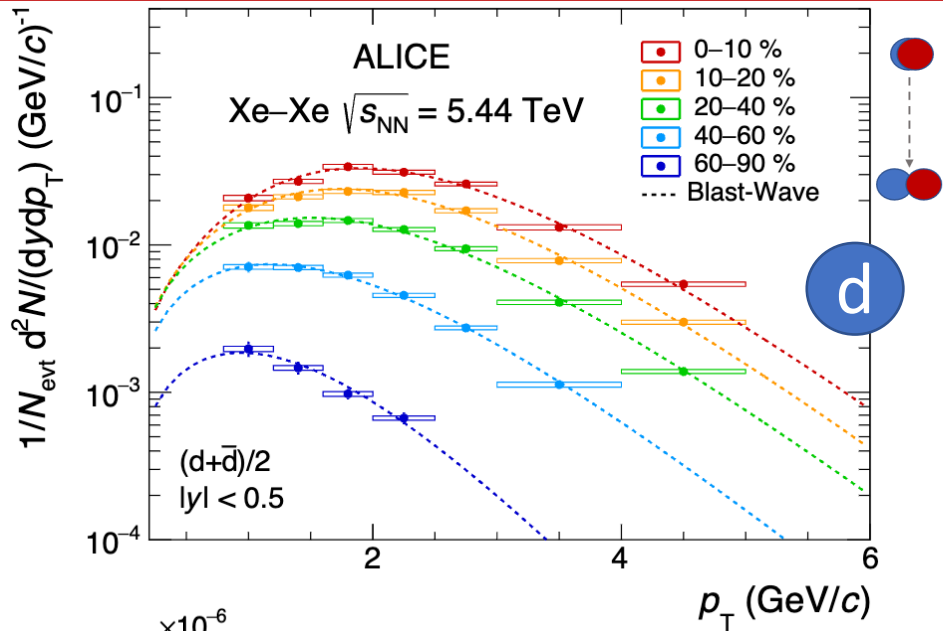


- $\mu_B$  and  $\mu_Q$  are extracted fitting the antiparticle-to-particle yield ratios with the predictions of the grand-canonical SHM using the Thermal-FIST code
- $\mu_Q = -0.18 \pm 0.90 \text{ MeV}$
- $\mu_B = 0.71 \pm 0.45 \text{ MeV}$  (~8 times more precise than previous measurement)
- Nuclear transparency regime** is reached ( $\rightarrow$  baryon transport from the colliding ions to the interaction region is negligible)
- No centrality dependence**  $\rightarrow$  nuclear transparency also in central Pb-Pb (despite  $\mu_B > 0$  could be expected from a more significant baryon number transport at midrapidity)

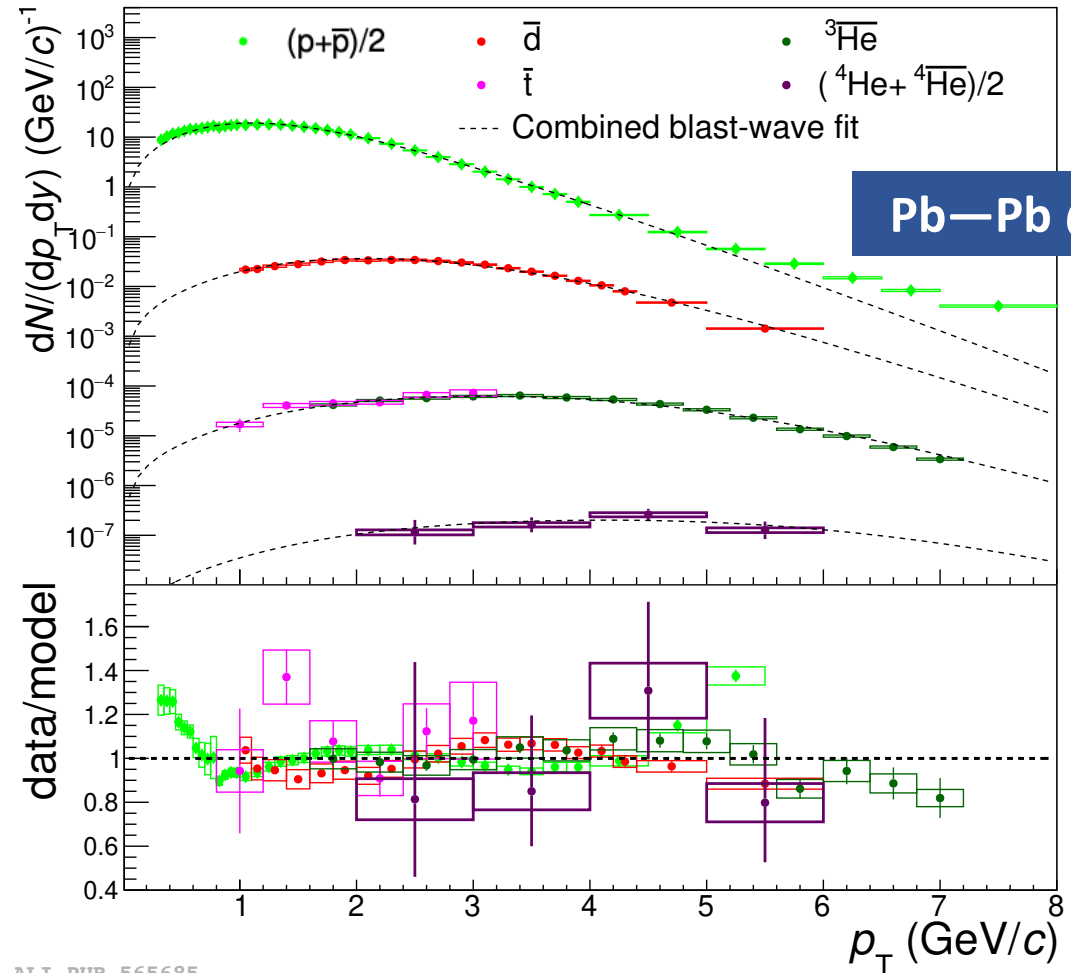
**The system created in Pb-Pb collisions at the LHC is on average baryon-free and electrically neutral at midrapidity  $\rightarrow$  approaching the early Universe more than any other experimental facility**



# Light (anti)nuclei with ALICE: large systems



- Recently measured d and  $^3\text{He}$  in Xe—Xe collisions
- In Pb—Pb collisions (anti)nuclei up to  $^4\text{He}$  are measured

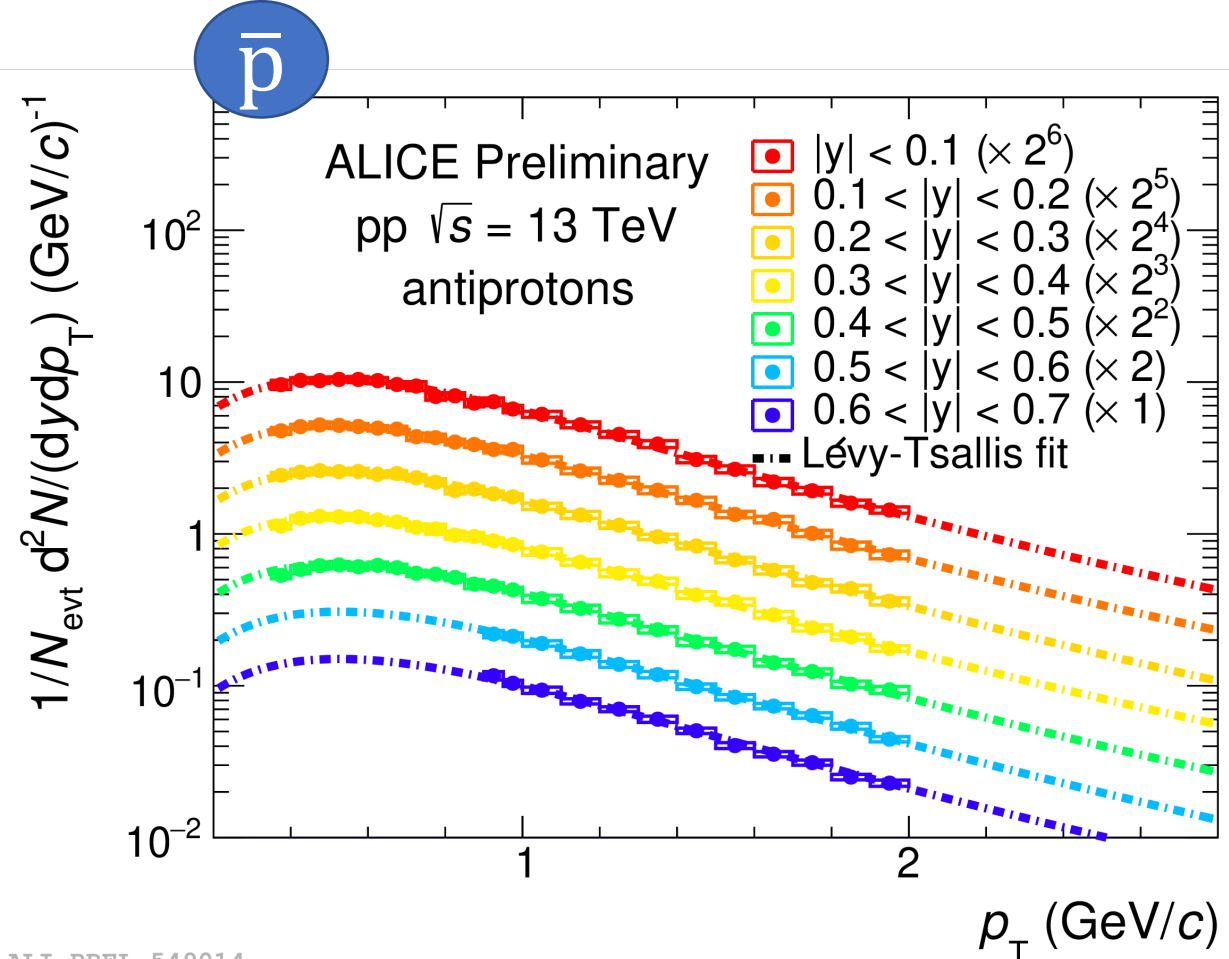
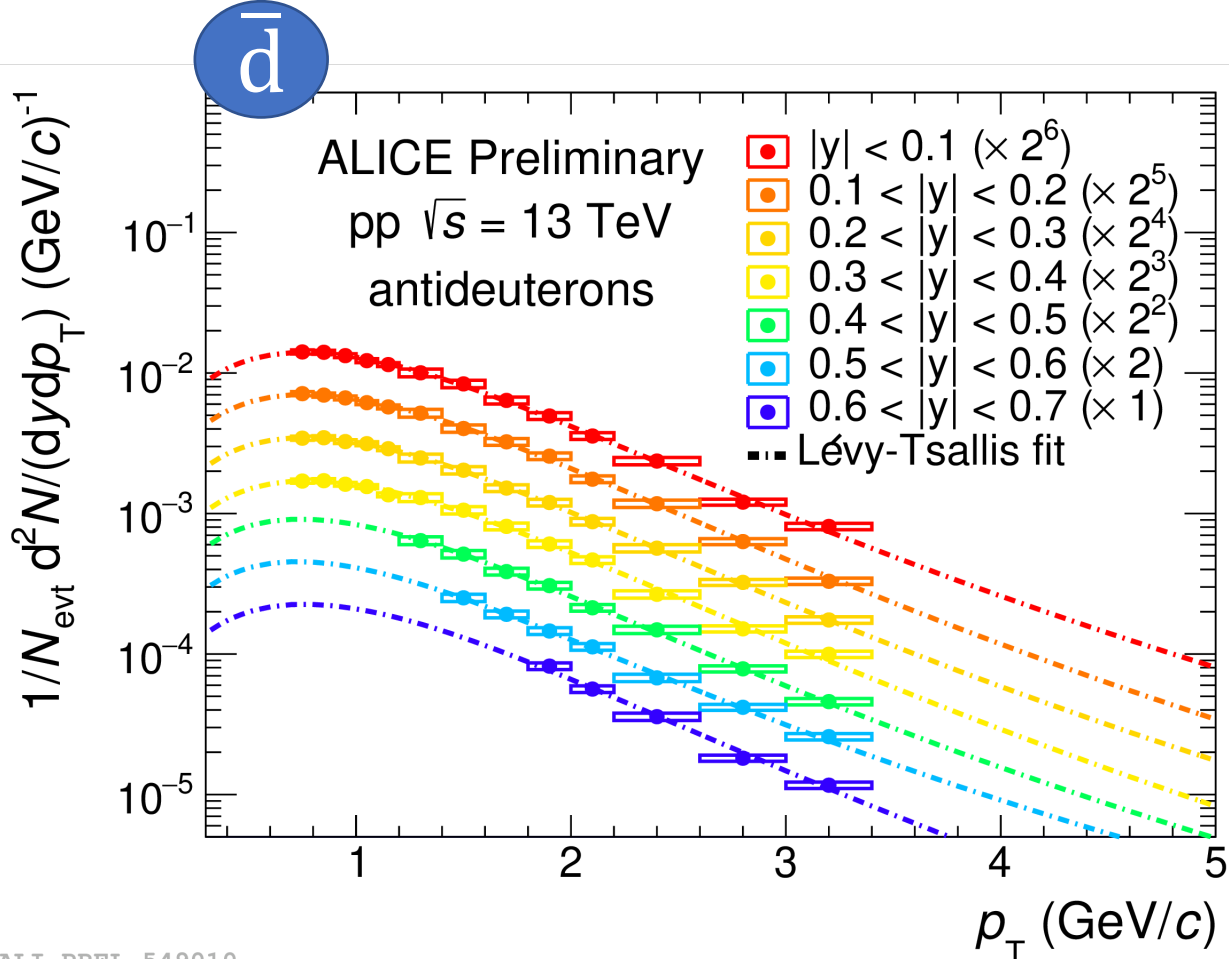


ALI-PUB-565685

ALICE Collaboration, arXiv:2311.11758



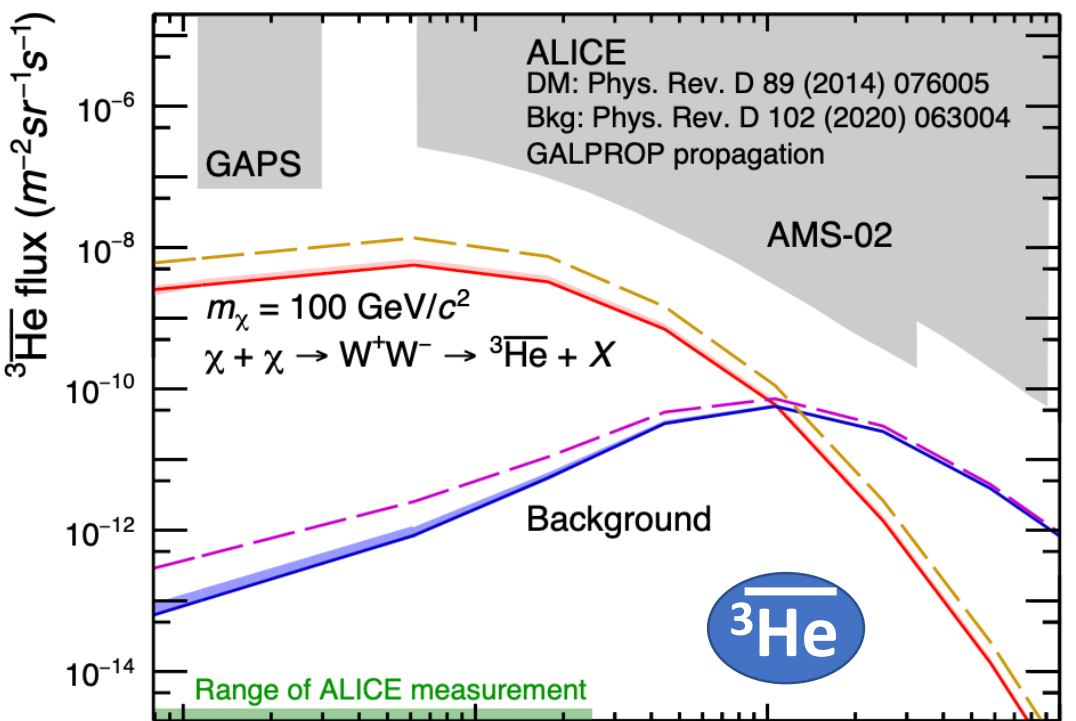
# Spectra as a function of rapidity



- Current acceptance of ALICE detector allows to extend the measurement of antinuclei up to  $y = 0.7$
- All rapidity classes show a common trend with  $y$ , for both species (ratio to  $|y| < 0.1$  is  $\sim 1$ )

# Transparency of Galaxy to anti<sup>3</sup>He

Solar modulated flux

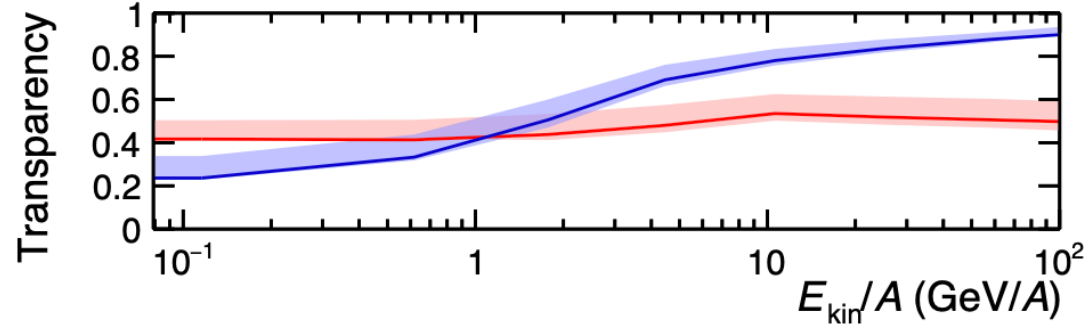


$$\text{Transparency} = \frac{\text{flux with annihilation}}{\text{flux without annihilation}} = \frac{\sigma_{\text{inel}}^{\text{ALICE}}}{\sigma_{\text{inel}}^{\text{GEANT4}}} \left( \frac{\sigma_{\text{inel}}^{\text{ALICE}}}{\sigma_{\text{inel}}^{\text{GEANT4}}} \right) \text{ for bkg (DM)}$$

- $\sigma_{\text{inel}}^{\text{GEANT4}}$  DM
- $\sigma_{\text{inel}}^{\text{GEANT4}}$  bkg
- $\sigma_{\text{inel}}^{\text{ALICE}}$  DM
- $\sigma_{\text{inel}}^{\text{ALICE}}$  bkg
- - -  $\sigma_{\text{inel}} = 0$  DM
- - -  $\sigma_{\text{inel}} = 0$  bkg

Fluxes are model dependent

- **Our Galaxy is rather constantly transparent to <sup>3</sup>He passage**
- Data are in good agreement with Geant4 predictions
- Uncertainties on Transparency only due to absorption measurements (10-20%)

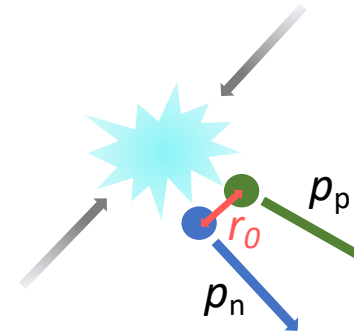


anti<sup>3</sup>He: Nature Phys. (2023) 19, 61–71

# Testing coalescence model using $B_2$

- Important observable in accelerator measurements: coalescence parameter  $B_A$

$$B_A(p_T^p) = \frac{1}{2\pi p_T^A} \frac{d^2 N_A}{dy dp_T^A} \bigg/ \left( \frac{1}{2\pi p_T^p} \frac{d^2 N_p}{dy dp_T^p} \right)^A$$



- Comparison to model predictions based on Wigner formalism

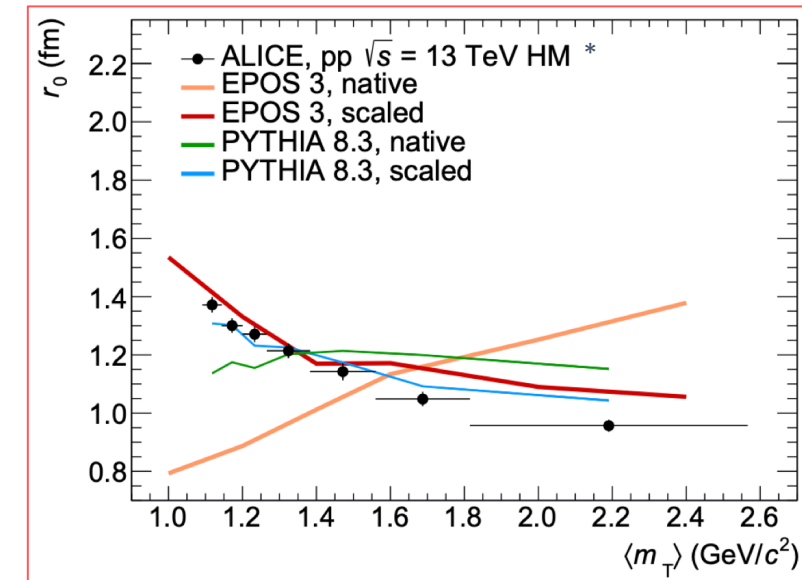
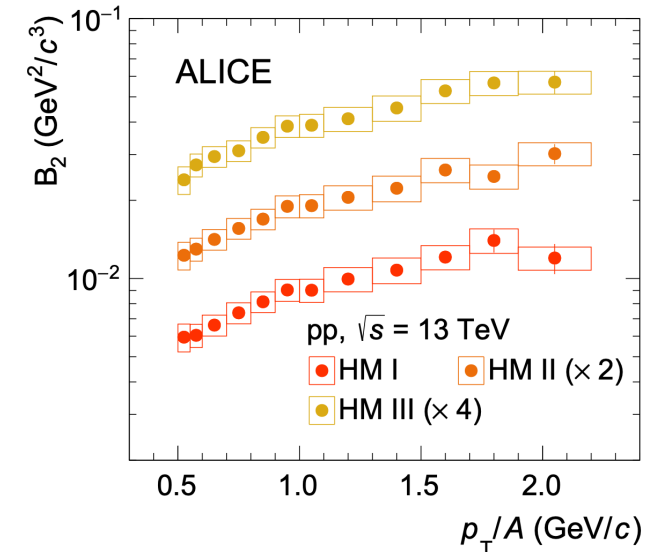
- Using event generators (PYTHIA 8.3 & EPOS 3)
- Calibrating (anti)nucleon momentum distribution & multiplicity distributions to measurements
- Obtaining deuteron  $p$  distributions according to the probability:

$$\mathcal{P}(r_0, q) = \int d^3 r_d \int d^3 r H_{pn}(\vec{r}, \vec{r}_d; r_0) \mathcal{D}(\vec{q}, \vec{r})$$

*emission source size*  
→ tuned to data

$$\mathcal{D}(\vec{q}, \vec{r}) = \int d^3 r |\phi_d(\vec{r})|^2 e^{-i\vec{q}\cdot\vec{r}}$$

*deuteron wave function*  
→ testing different ones



\* ALICE Collaboration, PLB 811 (2020) 135849  
ALICE Collaboration, JHEP 01 (2022) 106

Kachelrieß et al., EPJA 56 1 (2020) 4  
Kachelrieß et al., EPJA 57 5 (2021) 167

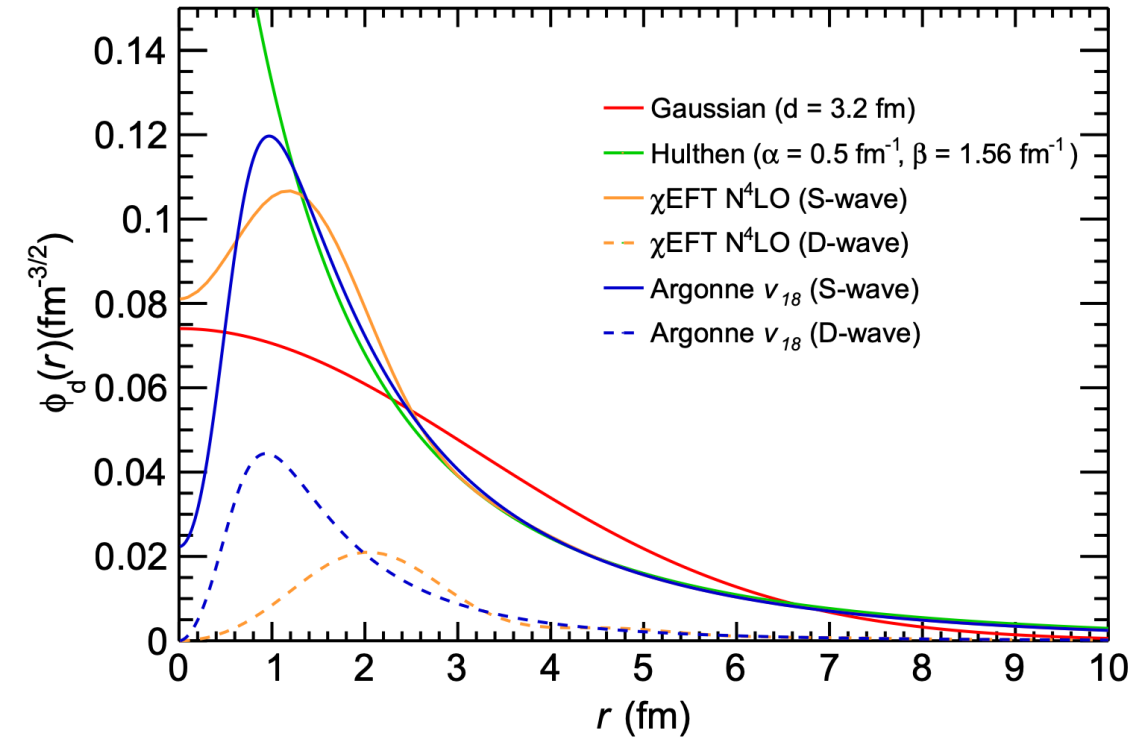
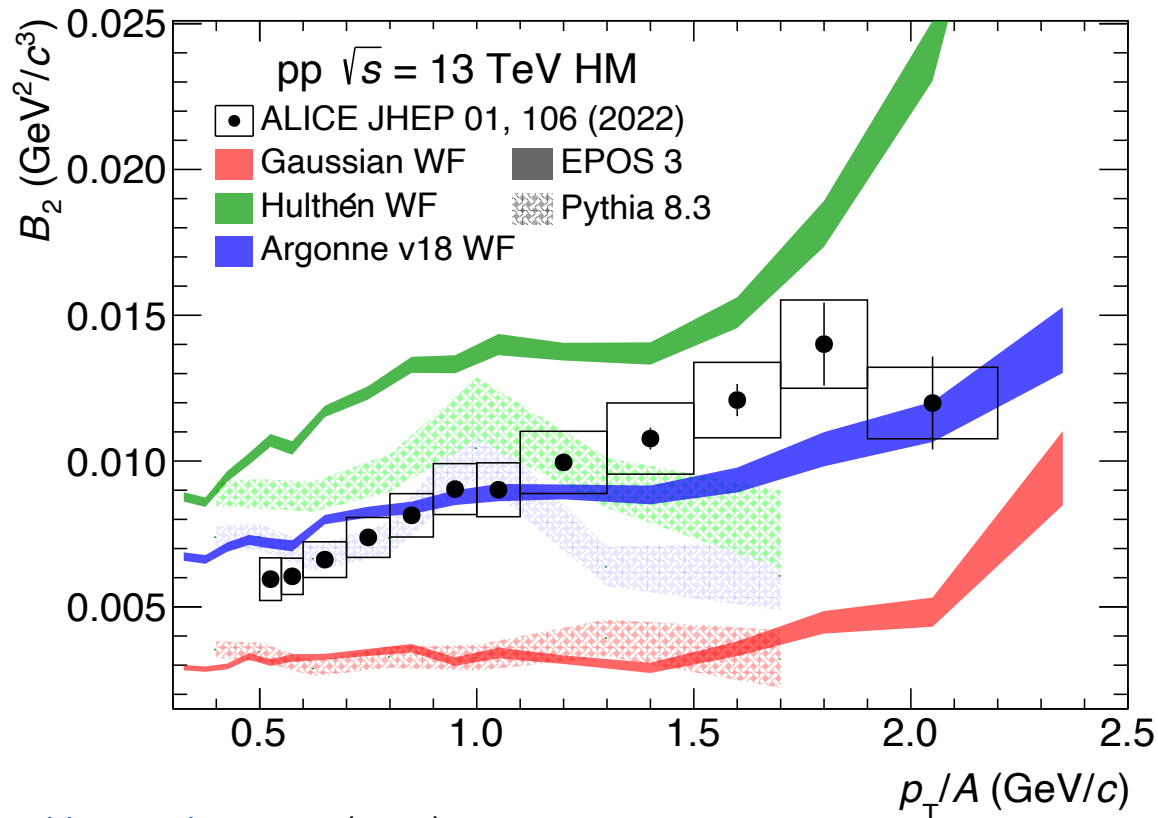
Mahlein et al., EPJC 83 (2023) 9, 804

# Testing coalescence model using $B_2$

State-of-the-art coalescence model describes deuteron momentum distributions and coalescence parameter!



Production measurements can be used to constrain the nuclear wavefunction!



- **Hulthén\***: Favoured by low energy scattering experiments
- **Argonne  $v_{18}$ \*\***: phenomenological potential constrained to p-n scattering
- **$\chi\text{EFT}$** : Favoured by modern nuclear interaction experiments (e.g. Femtoscopy)

\* Scheibl et al., PRC 59 (1999) 1585-1602

\*\* Wiringa et al., PRC 51 (1995) 38-51

\*\*\* D. R. Entem et al., PRC 96 2 (2017) 024004